THE INFLUENCE OF POLYMERIC CHARGE AND STRUCTURE, MOLECULAR WEIGHT AND IONIC CONDITIONS ON DEPRESSANT ABILITY TO REDUCE THE NATURAL FLOATABILITY OF TALC

Paul Graham Shortridge

September 2002

University of Cape Town

The copyright of this thesis vests in the author. No quotation from it or information derived from it is to be published without full acknowledgement of the source. The thesis is to be used for private study or non-commercial research purposes only.

Published by the University of Cape Town (UCT) in terms of the non-exclusive license granted to UCT by the author.

University of Cape Town

ACKNOWLEDGEMENTS

The author wishes to thank the following people and companies for their invaluable support in the completion of this project. Without a doubt, without their support and encouragement, this thesis would never have been completed.

To begin with, my Creator and Saviour, without whom there would be nothing at all.

To my thesis supervisors, Peter Harris and Dee Bradshaw, not only for their excellent supervision, but also for their consistent and patient support and encouragement.

To my colleagues in the Depressant Research Facility and the Chemical Engineering Department of the University of Cape Town for their input to the thesis as well as their friendship and support.

To the Foundation for Research and Development (FRD) whose financial assistance made the completion of this project possible. Also to Impala Platinum Mines and Scotia Mines who kindly donated the minerals used in this work.

Last, but not least, to my lovely wife Shannon, whose selfless and uncomplaining support made it possible for me to complete this work.

SYNOPSIS

Talc is a naturally floatable gangue material common in South African platinum bearing (PGM) ore bodies. Long chain polysaccharide depressants are effective in depressing talc flotation and improving the grade of the concentrates of those ores with talc as a gangue constituent.

This thesis describes an investigation into the surface interactions of two types of long chain polysaccharide depressants (carboxymethylcellulose and guar gum) with pure talc and with Merensky PGM ore (which is known to contain talc as a gangue constituent). Specifically, the objectives of this thesis were as follows:

1. To characterize the differences in the depressants selected.
2. To examine the effects that polymeric structure and molecular weight of the depressant have on the hydrophobicity of talc.
3. To extrapolate the findings from highly controlled laboratory conditions to batch flotation tests with Merensky PGM ore.

During the course of the experiments, it became clear that ionic conditions were an important factor in this system and they were therefore incorporated into the work done.

Overall, the molecular weight of the depressants was not seen to be an important factor in their ability to depress talc. The molecular structure did appear to impact depressant efficiency, but only under conditions of low ionic strength in the microflotation system.

Ionic conditions were found to be a pivotal factor in the performance of the CMC depressants in reducing the flotation of talc. It was also found that the ions adsorbed onto the talc surface in the absence of depressants – leading to a reduction in talc floatability. Divalent cations were more effective than monovalent cations in enhancing the effectiveness of the CMC depressants – suggesting stronger adsorption under these conditions. Guar depressants appeared to be unaffected by varying ionic conditions.

The batch flotation tests, and the microflotation tests at the higher ionic strengths, showed that similar depressing ability was obtained for the CMCs and the guars. However, the batch floats indicated that increasing dosage led to improved depressant performance while the microflotation tests indicated that a maximum level of depression was achieved at fairly low dosages (<40 mg/l). These differences were attributed to the differences in cell hydrodynamics, pulp density and depressant interactions with the other components of the ore. At high dosages, the largest guar appeared to depress the nickel sulphides in the system while the smallest guar and CMC depressants appeared to perform a cleaning function on the nickel and copper sulphide minerals as well as a froth stabilisation function.

It is recommended that this work be extended to examine lower depressant dosages than those studied in the microflotation tests in this investigation – in order to simulate the depressant equilibrium concentrations experienced in the batch flotation system. It is also recommended that the interaction of these depressants with non-talc materials such as the copper and nickel sulphides and gangue materials common in Merensky ore be investigated and that the batch work be extended.

LIST OF PUBLICATIONS

Shortridge P. G., Harris P. J. & Bradshaw D. B., "The influence of ions on the effectiveness of polysaccharide depressants in the flotation of talc", *in "Polymers in the mineral processing industry"*, Laskowski J. S. Ed., MetSoc, Canada, (1999)

Shortridge P. G., Harris P. J., Bradshaw D. B. & Koopal L. K., "The effect of chemical composition and molecular weight of polysaccharide depressants on the flotation of talc", *International Journal of Mineral Processing*, **59**, 215-224, (2000)

TABLE OF CONTENTS

LIST OF FIGURES

LIST OF TABLES

GLOSSARY

B.E.T. isotherms – Brunauer Emmet Teller isotherms

$Ca(NO_3)_2$ – calcium nitrate

Ca^{2+} - calcium cation

$Ca(OH)_2$ – calcium hydroxide

CMC – carboxymethylcellulose

$CuSO_4$ – copper sulphate

DLVO theory – Derjaguin Landau & Verwey Overbeek theory

FF10, FF30, FF150, FF300 – CMC reagents from the Finnfix series by Trohall

ΔG^0 – Gibbs free energy

HCL – hydrochloric acid

$HClO_4$ – perchloric acid

HF – hydrofluoric acid

HNO_3 – nitric acid

k – flotation rate constant

K^+ - potassium cation

KNO_3 - potassium nitrate

$Mg(NO_3)_2$ – magnesium nitrate

Mg^{2+} - magnesium cation

$Mg(OH)_2$ – magnesium hydroxide

M_n – number average molecular weight

M_w – mass average molecular weight

$[\eta]$ – intrinsic viscosity

η_{red} – reduced viscosity

p.z.c. – point of zero charge

PGM – Platinum Group Mineral

R_{10min} – cumulative mass percent flotation recovery after 10 minutes

SIBX – sodium isobutyl xanthate

SM4060, IMP4, SM4560 – guar reagents from the Acrol series by Trohall

XRD – X-Ray Diffraction

XRF – X-Ray Flouresence

1 Introduction

In South Africa, the froth flotation process is used for the separation of platinum bearing minerals (PGM's) from platinum ore. The mechanism that is relied on in the application of flotation is one of differential surface properties whereby certain chemicals (referred to as collectors) are applied to a mineral pulp which selectively cause the desired minerals to become hydrophobic, thereby attaching to air bubbles passing upward through the pulp. Certain undesirable gangue minerals in the flotation system are hydrophobic and therefore float along with the valuable minerals, reducing the quality of the concentrate being recovered. Chemicals (referred to as depressants) are added to the pulp in order to reduce the hydrophobicity of these minerals.

This thesis describes an investigation into the interaction between depressants and talc (a hydrophobic gangue mineral common in PGM Merensky ore). Two types of long chain polysaccharides depressants (carboxymethylcellulose (CMC) and guar), which are known to be effective in improving concentrate grade in ores where talc is present, were used.

A number of techniques were used to investigate the talc-depressant system.

- X-Ray Diffraction (to determine minerals present), X-ray Flouresence (to determine the ions and impurities present) and B.E.T isotherms (to determine surface area) were used to characterise the talc

- Column exclusion chromatography and viscometry were used to characterise the depressants

- Microflotation and batch flotation tests were used to investigate the effect of the different depressants and ionic conditions on the depression of talc

Initially, a comprehensive literature review of the system is presented, followed by a discussion of the experimental techniques used. Thereafter, the results are presented and discussed and some key conclusions drawn.

2 Literature survey

This section describes the theoretical background upon which this investigation was based. Initially, flotation and hydrophobicity will be discussed, followed by a review of the talc and polymers used. Hereafter, a short review of the characterisation methods, including viscometry is included. Finally, interactions between talc and the polymers and its environment are presented.

Flotation is a physico-chemical process used to separate out valuable minerals from an ore body. It is a technique used in the separation of the valuable platinum group minerals from the PGM Merensky ore body in South Africa. Flotation involves crushing the ore, adding plant water (which is generally of a high and varied ionic content) and then passing the resultant pulp into a series of flotation cells. In these cells, reagents (collectors, activators, depressants and frothers) are added to the ore and air is bubbled through the pulp. The purpose of the collectors is to render the valuable mineral hydrophobic – thereby causing it to attach to the air bubbles and move to the concentrate. The role of depressants is to render the gangue material hydrophilic – causing it to move to the tails. Frothers are added to improve the quality and stability of the froth and activators are added to improve the effectiveness of the collectors or depressants. A more detailed description of the flotation process can be found in Wills (1988). This study is focussed on the area of depressants, and in particular, the interactions of certain depressants with talc. Therefore, depressants will be discussed in more detail further along in this literature review.

Hydrophobicity and hydrophilicity are concepts upon which the entire mechanism of separation of minerals via flotation hinges. These concepts are explored and discussed in more detail below.

2.1 Hydrophobicity and hydrophilicity

The factor that makes water unique is the existence of the hydrogen bond. This bond causes water to have exceptionally high melting and boiling points compared to other substances of similar molecular structure. Israelichvili (1992) gives the following characteristics of the hydrogen bond:

1. It is orientation dependant
2. It is stronger than normal Van der Waals forces but weaker than covalent or ionic bonds
3. It is an electrostatic interaction
4. This bond exists in varying degrees where hydrogen atoms are in contact with strongly electronegative atoms such as O, N, F and Cl
5. It can occur both intermolecularly and intramolecularly
6. The O-HO bond is generally linear but can form a bond of angle 120°. This linearity means that the preferred structure of a network of hydrogen-bonded atoms is tetrahedral – as is the case for ice

Figure 1 schematically depicts the three dimensional structure of ice (Israelachvili, 1992).

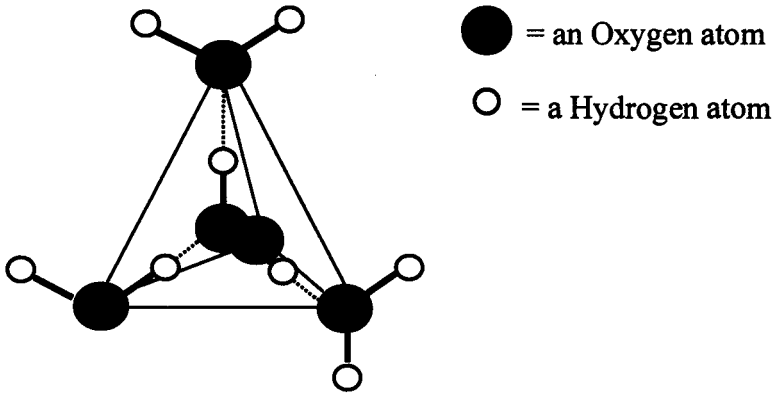

Figure 1: The three dimensional structure of ice

When ice melts, the structure breaks down and the number of molecules adjacent to each other increases from four. This is seen in the phenomenon whereby the density of ice drops as it moves from solid to liquid form – to a minimum density at 4 °C.

Free films of liquids are always unstable, but a solid surface can acquire a stable liquid film. If the liquid is water, such a surface is hydrophilic. When the aqueous film on a solid surface is unstable, that surface is hydrophobic (Rao, 1974).

Generally, hydrophobicity refers to the degree to which a molecule is repelled by water.

In analysing what makes a particle hydrophobic, Laskowski (1996) compares the work of cohesion of water to the work of adhesion of the solid particle to the water. If a particle is to be hydrophilic, its work of adhesion must exceed the work of cohesion of water. However, the work of cohesion of water is known to be extremely high (due to the hydrogen bonding properties of water molecules as discussed previously). The work of

adhesion must therefore be correspondingly high if there is to be hydrophilicity. The work of adhesion is made up of three components: that due to dispersion forces, that due to electrical forces and that due to hydrogen bonding forces (whereby the solid particle has sites available for hydrogen bonding to the water molecules). Dispersion forces have been established to be too weak to ever overcome the work of cohesion of water alone and therefore, a particle with no charge (i.e. no electrical forces) and no hydrogen bonding groups (thereby no hydrogen bonding forces) will always be hydrophobic. Scatena et al. (2001) indicate that a hydrophobic surface alters the interfacial water structure.

A hydrophobic particle within water affects the system as follows. In order to minimise the amount of contact that the water molecules have with a hydrophobic particle, the water structures itself in a more tetrahedral type structure around the solid particle. This leads to a more structured (and thus entropically unfavourable) system – resulting in a highly unfavourable free energy of solubilisation for the particle (Israelichvili, 1992).

When there are two hydrophobic substances within an aqueous medium, the most entropically favourable state for the system is that where there is a minimum amount of contact between the water molecules and the solid particles. Thus, a force termed "hydrophobic bonding" arises whereby in order to minimise the total contact area between the water and the hydrophobic particles, the particles agglomerate, reducing the total surface area in contact with the water. It has been reported that for hydrophobic particles, their attraction within an aqueous environment is greater than their attraction outside of it.

Air is a relatively inert substance. Therefore, in a flotation system, it is energetically favourable for hydrophobic particles to attach to the air bubbles through hydrophobic bonding as they pass through the pulp. As a result, hydrophobic particles are naturally floatable.

2.2 The structure and properties of talc

Talc is a hydrophobic gangue material commonly found in the PGM ores of the Bushveld complex in South Africa (Steenberg, 1982). This work is focussed on the interactions between two types of depressants (CMCs and guars – at different chain lengths) and talc. Therefore, a review of the properties of talc is appropriate.

2.2.1 The structure of talc

Talc is a layer silicate of the clay mineral class of phyllosilicates. Figure 2 shows the overall position of talc within the silicate mineral class (Morris, 1996).

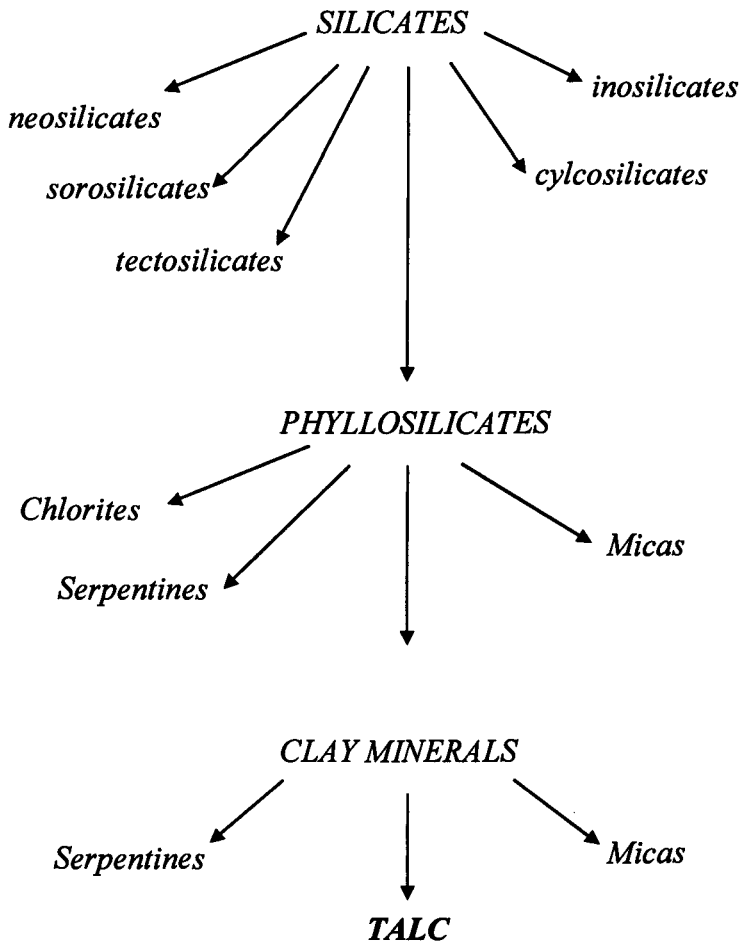

Figure 2: The position of talc within the silicate mineral class

Grimshaw (1971) described the structure of talc as a layer silicate material, which consists of a trioctahedral brucite sheet sandwiched between two hexagonal silica sheets. The brucite is formed from the six-fold co-ordination of Mg^{2+} with oxygen and hydroxyl groups. The silica layer is formed from the tetrahedral co-ordination of silica and oxygen

atoms. The silicate and brucite sheets are linked together with ionic bonds (Laskowski, 1996). Roberts et al. (Morris, 1996) give a unit structure for talc of $Mg_3(Si_2O_5)_2(OH)_2$.

Figure 3 is a schematic depiction of the structure of talc (Morris, 1996)

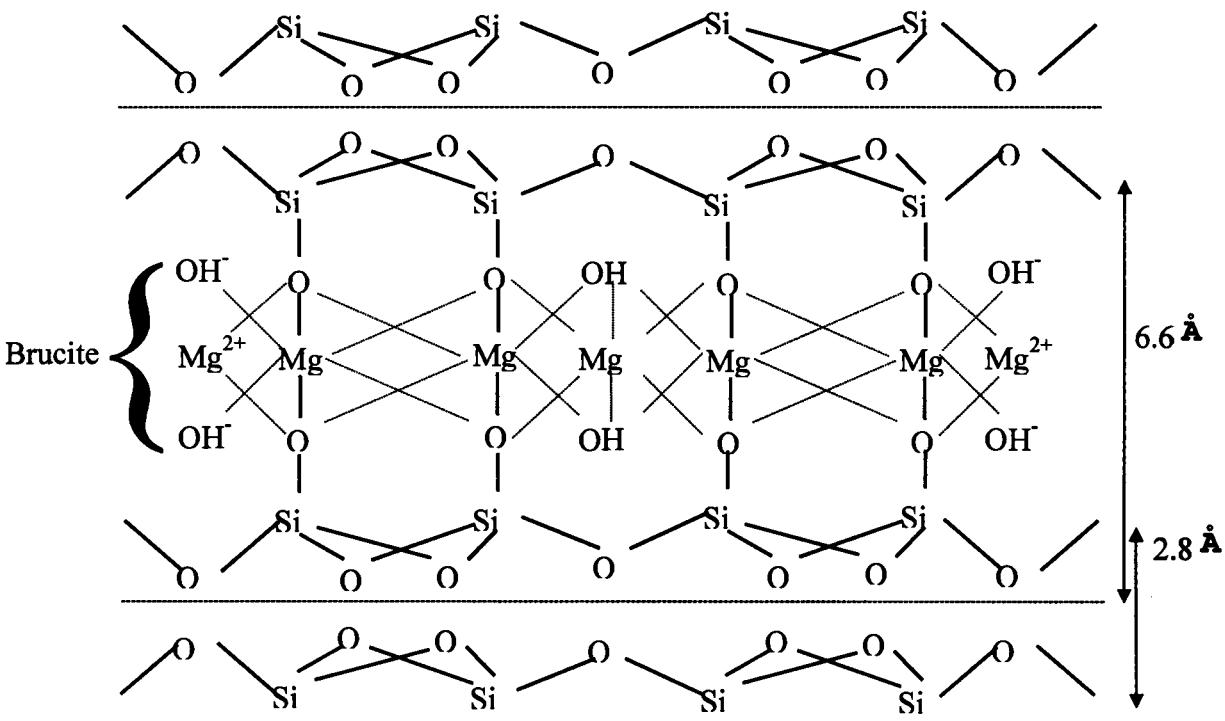

Figure 3: A schematic diagram of the talc structure

Talc has a hardness of 1 on the Moh scale and a perfect cleavage plane in the {001} plane (Morris, 1996). This indicates that the intermolecular forces binding adjacent talc molecules together between the silicon oxide planes are relatively weak – especially in comparison to the forces binding the edges of the talc (Grimshaw, 1971 and Morris, 1996). It is likely that the weak attractive forces between the silica oxide sheets arise from the partially ionic nature of the Si-O bond – which is strong enough to create

permanent weak dipoles on the planar surface. The edges of the talc are bonded together with ionic forces between the positively charged magnesium ions and the negatively charged hydroxyl ions (Grimshaw, 1971; Fuerstenau, 1988) as well as covalent bonds between the silica tetrahedral and magnesium octahedral due to satisfied oxygen atoms.

This difference in bonding mechanisms within the talc structure leads to the formation of two very distinct types of surface when talc is broken. If the breakage occurs along the silica – oxide plane, a neutral planar surface of silica and oxygen atoms is formed. In water, because of the neutral nature of this surface, it will exhibit hydrophobic properties.

If the breakage occurs through the rupturing of the ionic bonds at the edges, a charged surface composed of oxygen, magnesium, hydroxyl and silica ions is formed. Conventionally, the uncharged surfaces are called planes and the charged surface are termed edges. These charged surfaces are likely to be hydrophilic.

Ionic exchange can occur within the crystal lattice of talc. Magnesium can be replaced by zinc, aluminium or iron (Pask and Warner, 1954; Steenberg, 1982). The silica ions can be replaced by aluminium ions (Steenberg, 1982). These substitutions will alter the ions present and therefore the surface characteristics of talc.

2.2.2 Surface properties of talc

2.2.2.1 Surface Charge

A number of workers have reported electrophoresis measurements for talc. Figure 4 shows some of the zeta potential curves reported by various workers. A number of different talc sources were used and it appears that the same trends were observed overall – namely that talc has a very low point of zero charge (between pH of 1 and 3) and a

negative zeta potential over most of the pH range (Steenberg, 1982; Fuerstenau, 1988; Morris, 1996; Rath et al., 1995; Dalvie, 2001). Included in Figure 4 is a set of zeta potential measurements reported by Dalvie (2001). This was done on the same talc sample that was used in the experiments in this investigation. The same trends are seen as reported by the other workers.

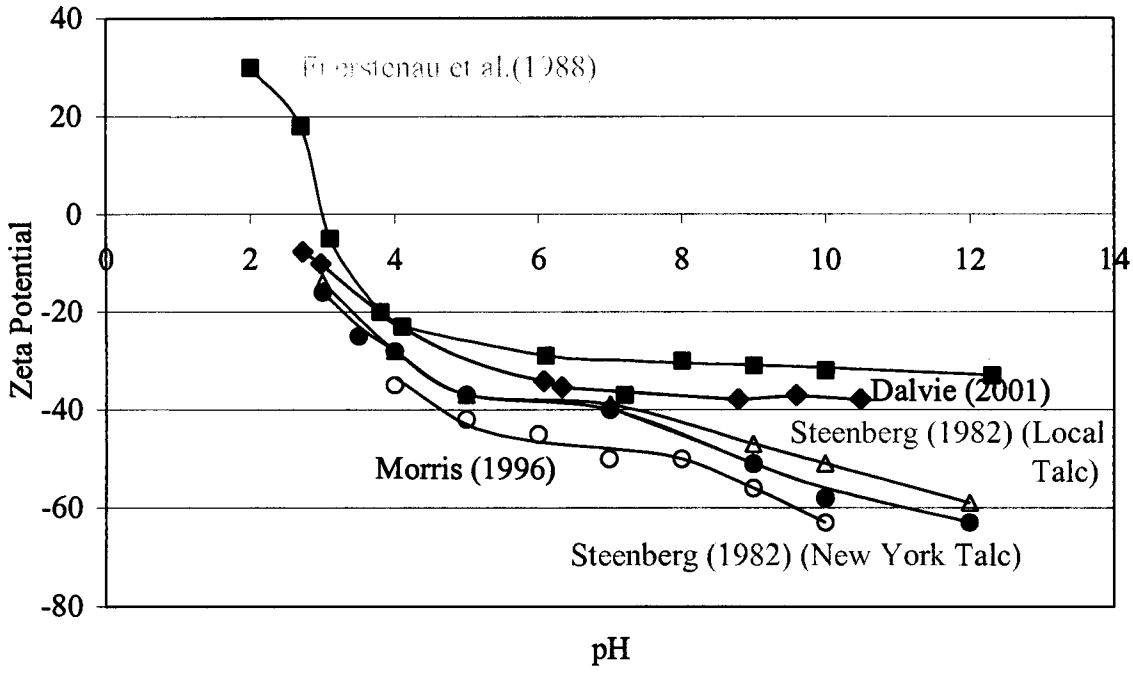

Figure 4: Zeta potential measurements of talc done by a number of workers

It is worth noting that around a pH of 9, the zeta potential remains fairly constant for the talc used in this investigation.

The differences reported between the curves in Figure 4 can be attributed to differences in talc source and mineral structure (Steenberg, 1982).

As mentioned earlier, the planes and edges of talc are different from a structural point of view and therefore, the curves in Figure 4, which report an average charge over the entire surface, will be affected by the ratio of planar to edge surface. This is confirmed by Chander et al. (1975) who found that for anisotropic minerals of this sort, the zeta potential is affected by the plane to edge ratio. Table 1 gives some plane to edge ratios and zeta potential measurements reported by workers in this field. p-Nitrophenol adsorption (Steenberg, 1982) was used to determine plan-edge surface area ratio.

Table 1: Plane to edge surface area ratios and electrophoresis measurements reported in the literature

Plane : Edge	Point of Zero Charge	Zeta Potential at pH = 7	Source
89 % : 11 %	2.5	-50 mV	Morris (1996)
71 % : 29 %	1	-40 mV	Steenberg (1982) New York Talc
31 % : 69 %	2	-38 mV	Steenberg (1982) Local Talc

As Table 1 shows, the ratio of the plane to edge surface of talc can vary considerably depending on the talc source. This is due to the macroscopic crystal structures that the talc assumes. Figure 5 shows microphotographs of the two talc samples used by Steenberg (1982)

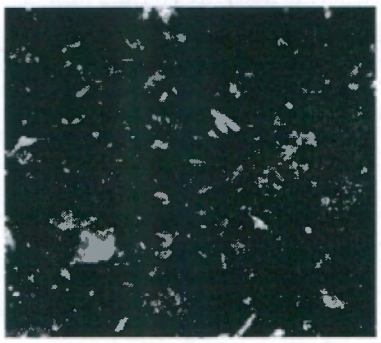

New York Talc

(71:29 plane:edge)

Local Talc

(31:69 plane:edge)

Figure 5: Microphotographs of local and New York talc

These pictures show that the New York talc (with a high plane to edge ratio) contains a number of particles with a needle-like structure (high plane to edge ratios), while the local talc appears to have a lower plane to edge ratios overall.

In order to establish why such a highly negative zeta potential is observed for talc, the two types of surfaces of talc need to be considered separately.

2.2.2.1.1 Charge on the planes

The talc planes consist of bonded oxygen and silica atoms and thus have a neutral surface charge (with very weak dipoles formed as a result of the weak polarisation of the Si-O groups). This neutrality results in the planes being hydrophobic and as such their behaviour can be deduced from considering other similar types of surfaces. Oils are other electrically neutral structures and are known to have a negative zeta potential when

placed in water. Arbiter et al. (Steenberg, 1982) propose that for a hydrophobic solid, the electrical double layer on the hydrophobic surface could be very ill developed and exist entirely on the water - side of the interface. Therefore, the charge on the talc planes is likely to be negative over the entire pH range.

Ionic substitution can also change the surface charge characteristics on the talc planes. Van Olphen (1977) mentions that a clay may exchange an adsorbed, intercalated or structural ion with one of lower valency, producing a negatively charged surface. For example, Al may replace Si in the surface, tetrahedral layer of a clay.

Figure 4 shows that the talc examined by Fuerstenau et al. (1988) exhibited a p.z.c. at a pH of around 3. This corresponds to the p.z.c. of α - quartz (SiO_2). The talc examined by Steenberg (1982), however, had a zeta potential of around –20 mV at pH=3 and when the curves were extrapolated, they appeared to exhibit a lower p.z.c. of around 1. This indicates that the talc examined by Steenberg (1982) had a different SiO_2 arrangement compared to the talc examined by Fuerstenau et al. (1988).

2.2.2.1.2 Charge on the edges

The edges of clay minerals behave like simple oxides (Laskowski, 1996). Thus the charge at these edges is ascribed to the protonation / deprotonation of the surface hydroxyls by Equation 1, Equation 2 and Equation 3 (Laskowski, 1996):

Equation 1

$-MOH + H^+ = MOH_2^+$ at low pH values

Equation 2

$-MOH + OH^- = -MO^- + H_2O$ at high pH values

Equation 3

At the p.z.c: $[-MOH_2^+] = [-MO^-]$

Magnesium forms strong ionic bonds with oxygen (Grimshaw, 1971). Magnesium hydroxides and magnesium oxides are easily dissolved in water under acidic conditions. Rath et al. (1995) have observed that under acidic conditions, magnesium dissolution from talc occurred - at a rate that increased as the pH was lowered. It is not established whether this dissolution of magnesium ions occurs to a significant enough degree to influence the surface characteristics of talc.

The atoms that make up talc are joined together in a crystal lattice structure. The anions dominate the surface properties in this type of structure (Grimshaw, 1971). In the case of talc, the main anion in talc is oxygen. The edges of talc are composed of magnesium, oxygen, hydroxyl and silicon atoms. The magnesium ions undergo hydrolysis at low pH conditions and form magnesium oxides at very high pH conditions.

It is unclear as to how the magnesium sites affect the zeta potential characteristics of talc. The overall zeta potential could be a influenced by:

1. The magnesium sites – either from magnesium oxides and hydroxides formed above the critical pH of precipitation for Mg(II) or as a result of the O and OH sites left by the magnesium when it dissolves off the talc at low pH values.

2. The silica groups. This would be a negative contribution either from pH = 1 or pH = 3 depending on the form that these oxides take on the talc edges.

3. The hydrophobic groups. This is caused by the reorientation of the water molecules at the talc surface creating a charged double layer. Morris et al. (1999) report that after silane modification of talc (i.e. neutralisation of the talc edges) the zeta potential does become slightly less negative. This confirms that the hydrophobic zeta potential contribution and the edge contributions are both negative.

4. The system impurities such as other oxide groups substituted in the place of the Mg or Si ions.

It is not known to what extent each of these terms contribute to the zeta potential of the talc. Work by Fuerstenau et al. (1988) showed that the adsorption of trivalent cations on the talc edges caused a complete charge reversal in the zeta potential – without affecting the floatability (hydrophobicity) of the talc.

2.2.2.2 Hydrophobicity of talc

A number of workers have reported flotation results for talc. Some of these are shown in Figure 6 (Steenberg, 1982; Fuerstenau, 1988; Morris, 1996, Rath et al., 1995).

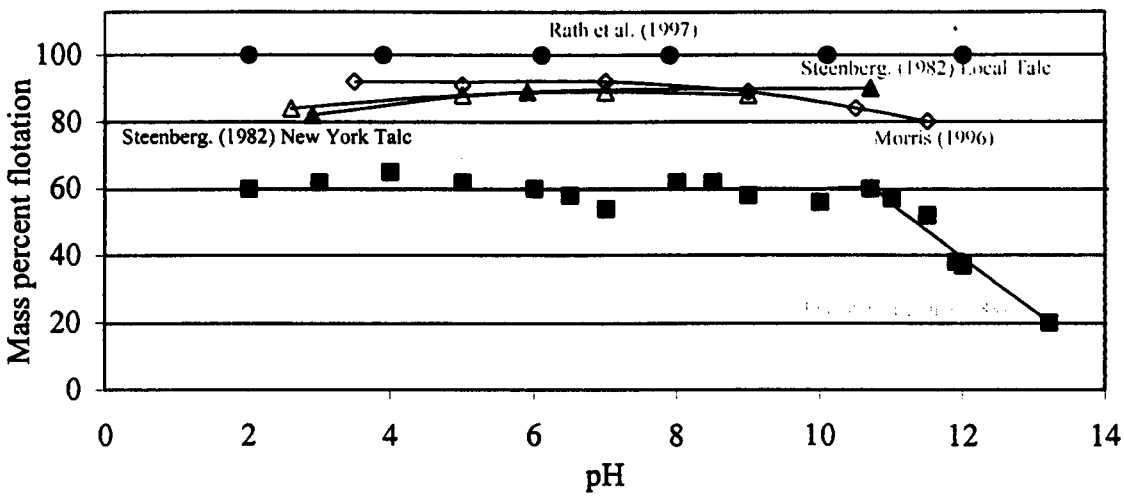

Figure 6: Flotation results of talc from other workers

Although different techniques and talc samples were used, these studies consistently show that talc has a very high degree of natural floatability. It is believed that the hydrophobic planes determine the hydrophobicity of talc and thus the independence observed in floatability with pH indicates that the planar regions do not undergo hydrolysis.

Talc also consists of a charged edge surface that undergoes hydrolysis (Fuerstenau et al., 1988). However, even in the case where 69% of the talc surface was edge rather than planar, Steenberg (1982) found flotation independent with pH and very similar to the flotation results of the talc with a 29 % edge surface. This indicates that as long as there

is enough hydrophobic surface area available for an air bubble to attach to the talc particle, it will be naturally floatable. This is significant when one considers the question of talc depression. In order to reduce the flotation of talc, the hydrophobicity of the planar surface area must be reduced below a critical value.

A study by Ouyang et al. (1995) of the dispersion stability of fine talc particles in aqueous solution showed that classical DLVO theory is invalid for explaining the aggregation of hydrophobic particles in aqueous solution. They suggest that the total energy of the system is the summation of the potential energy of the Van der Waals and electrical double layer interactions between talc particles as well as a further term for the hydrophobic interaction between particles. They reported that for naturally hydrophobic minerals, such as talc, the aggregation of fine talc particles in aqueous solution is dominated by the hydrophobic interaction between the particles.

2.2.2.3 The effect of ions on talc

It has been found that in an aqueous solution, ions have a strong effect on both the surface charge and floatability of talc (Fuerstenau, 1988).

The nature and degree of hydrolysis of ionic species is strongly dependent in many cases on the pH of the system. pH_s (or critical pH of solubility) is the solubility limit (C_s) of the hydrated species in solution. Above this limit, the hydrated species precipitates out of solution as the solid species. This is the pH at which the cationic species form metal hydroxides, which precipitate either into solution or out of solution as solid hydroxides. Fuerstenau et al. (1988) showed that this point of precipitation has a strong effect on the zeta potential and the floatability of talc.

Fuerstenau et al. (1988) added the trivalent cation Cr(III) to a talc system and tested the zeta potential and floatability of that system. They found that at pH values below the pH_s – or point of precipitation of the Cr(III) species that the zeta potential of the talc increases when Cr(III) is added. The flotation results for talc in the presence of this ion indicated that the flotation of the talc did not decrease before the point of hydroxide precipitation. But after this point, the flotation of the talc was drastically reduced. Fuerstenau et al.'s (1988) interpretation of this data was "This shift in zeta potential must arise from specific adsorption of the metal hydroxy complex on sites at the polar edges of the talc molecules".

2.3 The structure and properties of long chain polysaccharide depressants

Polysaccharides have been found to be effective depressants in flotation and there is a wide range of polysaccharide depressants commercially available. Two types of polysaccharide depressants selected for this investigation – CMCs and guars – have found widespread use in the processing of Platinum Group Mineral (PGM) ores in the Bushveld complex in South Africa. In some cases, these depressants constitute the largest plant reagent cost.

Polysaccharides are polymeric molecules built up of sugar monomers. These molecules can take up a variety of shapes, sizes and physical and chemical properties.

Polysaccharides have an element of hydrophobicity associated with them due to the fact that they have CH_2 groups along the chain. King (1982) defines the Gibbs free energy of adsorption of an organic molecules as consisting of electrostatic, chemical and "water" Gibbs free energy contributions. The water contribution is broken down into hydrophobic and hydrogen bonding components. The hydrophobic bonding component consists of the amount of free energy required for the removal of one mole of CH_2 from solution through hydrophobic association. The value for this is –1.0 R.T or 2.5 $kJ.mol^{-1}$ (King, 1982). This energy contribution is small but its contribution becomes more and more considerable as the length of a polysaccharide chain increases. The hydrogen bonding contribution also has a fairly low energy associated with it (about 20 $kJ.mol^{-1}$ (Morris, 1996)) but again its contribution becomes greater as the number of unsubstituted OH groups along the polysaccharide chain is increased (through increased chain length or increased degrees of substitution).

Two types of polysaccharides are investigated in this thesis: carboxymethylcellulose - which is a cellulose derivative and guar gum, which is a polysaccharide of the galactomannan group.

2.3.1 Solvation properties of polysaccharides

All polysaccharides have abundant hydrogen bonding groups along their chains that rapidly absorb water molecules when placed in solution. Thus, when polysaccharides are placed in water, the water molecules penetrate the amorphous regions, which have unsatisfied hydrogen - bonding positions, and bond to these positions. This causes a swelling and consequent rupturing of intermolecular hydrogen bonds between the polysaccharide molecules leading to their complete solvation and solubilisation (Whistler, 1973).

However, perfectly linear neutral polysaccharides - like cellulose are capable of fitting snugly together through hydrogen bonding, creating an almost crystalline intermolecular structure. These structures do not absorb water and are not solvated when placed in aqueous solution.

This effect may be overcome in these molecules in two ways.

Introducing charged groups along the chain will cause the chains to repel as they approach each other and thus prevent the hydrogen bonded crystalline structures being formed. These groups are substituted onto the chain in the place of hydroxyl groups on the monomer rings. The extent to which these groups are introduced is known as the degree of substitution of a molecule. A degree of substitution of one means that one charged group is substituted for each monomer on the polysaccharide chain. The amount

of charged groups scattered over the chain must be distributed over the whole molecule and there must be enough charge to prevent segments of the chain from joining together. In the case of carboxymethylcellulose - which is cellulose with carboxylic groups introduced along the chain, the minimum number of groups that will prevent precipitation is 4 for every 10 monomeric units (which is a degree of substitution of 0.4) (Whistler, 1973).

Secondly, groups with branched structures prevent intermolecular coagulation of chains through steric hindrance and thus these molecules are soluble in aqueous solutions. This is clearly seen in the fact that amylose – a linear component of starch molecules - is insoluble in water, while amylopectin a branched component of starch molecules is readily soluble (Aspinall, 1970). It also accounts for the solubility of guar molecules.

2.3.2 Carboxymethylcellulose

Cellulose is a linear structure built up from the 1,4 linkage of D-glucose monomers. Celluloses are generally insoluble in water, and are of colloidal dimensions (Colloidal dimensions are in the region of about 0,005 μm to 0,2 μm (Grimshaw, 1971)).

A study of the kinetics of the hydrolysis of cellulose shows that 99 % of the bonds in the structure are of the same type (Aspinall, 1970). Therefore, cellulose is termed a homopolysaccharide. Figure 7 shows the structure of a carboxymethylcellulose building block (Steenberg, 1982).

Carboxymethylcellulose is formed by steeping cellulose in sodium hydroxide solution and then etherifying the alkali cellulose with sodium monochloroacetate to form sodium carboxymethylcellulose, sodium chloride and sodium glycolate (Whistler, 1973). The

source of the cellulose and the modification conditions affect the nature of the product used in industrial applications. Equation 4 describes this reaction.

Equation 4

$$R_{cellulose}(OH)_3 + ClCH_2COONa$$

$$= NaOH\ (\ R_{cellulose}(OH)_2(OCH_2COONa) + NaCl + H_2O + NaC_2H_4O_3$$

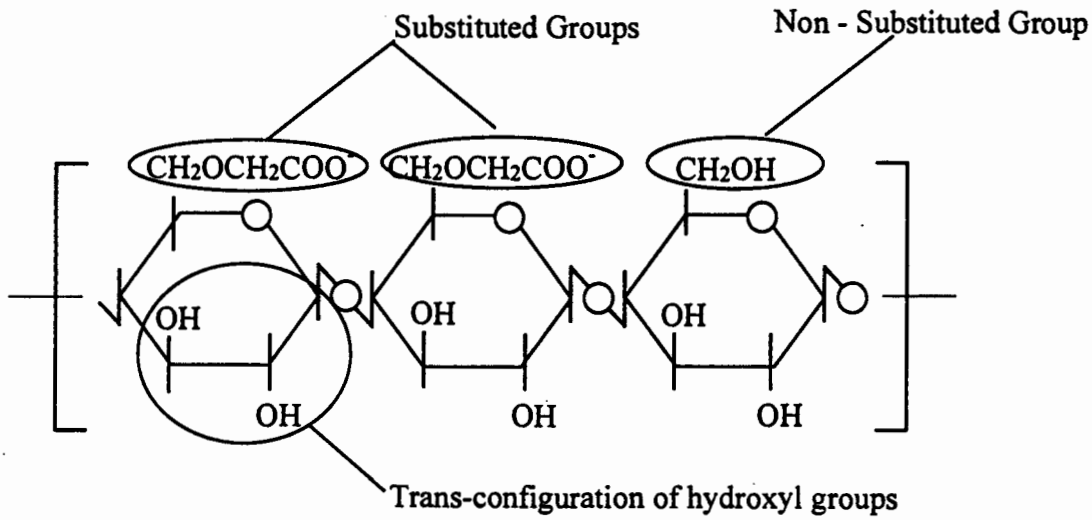

Figure 7: The structure of a carboxymethylcellulose building block

An important point to note about this makeup procedure is that the industrially used CMC's have sodium ions included both along the CMC chain and through the NaCl by-product. The CMC is an ionic molecule and therefore the ionic strength and the ions present in solution do have an effect on its characteristics and behaviour.

CMC's used in industry generally have a degree of substitution of about 0.8 (Whistler, 1973). As discussed, this degree of substitution allows for solvation of the polysaccharide in water.

Polysaccharide molecules with carboxyl groups substituted along the chain have the following special characteristics (Whistler, 1973):

1. Alkali salts of these molecules are highly ionised in solution and the distribution of ionic charge along the molecule creates columbic repulsion effects, which increases the stability of the polymer in solution and causes the molecule to adopt an extended conformation. These extended polymers produce highly viscous solutions

2. Cationic species, like calcium or copper, can create salt bridges between the polysaccharide molecules both intra- and intermolecularly. The cross-linking of these polysaccharides leads to gel formation and, if extensive, to precipitation

2.3.3 Guar gum

The galactomannan group of polysaccharides is formed from the combination of D-mannose with D-galactose monomers attached by 1-6 linkages. D-mannose is different to D-glucose in that the 1 and 2 hydroxyl groups are arranged in a cis-configuration as opposed to the trans-configuration of the glucose groups. This is clearly seen in the schematic representations of carboxymethylcellulose (Figure 7) - with a trans-configuration and guar gum (Figure 8) - which has a cis-configuration.

Guar gum is defined by Whistler (1973) as a non-ionic polysaccharide with linear chains of (1-4)-D-mannopyranosyl units with D-galactopyranosyl units attached by 1-6 linkages. The ratio of galactose units to mannose units is 1:2 (Aspinall, 1970). There is no chemical evidence that the galactopyranosyl side chains are attached regularly to alternate mannopyranosyl units in the main chain. However, regularity of substitution is indicated by the formation of crystalline fibres, which give x-ray diffraction diagrams (Aspinall, 1970).

Figure 8 shows a schematic of the structure of a guar gum molecule (Steenberg, 1982).

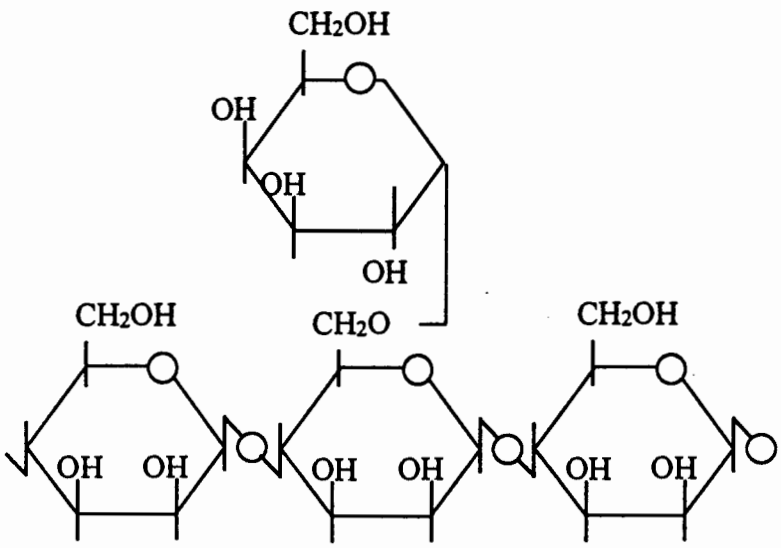

Figure 8: The structure of a guar gum derivative building block

Natural guar gums are modified for use in flotation, predominately by varying the molecular weight but in some cases through introducing charge substitutions along the polymer chain.

2.3.4 Viscometry

The viscosity of a polymer is indicative of the hydrodynamic volume that the polymer occupies in solution. The relation between viscosity and polymer solution concentration used in viscosity analysis is given by Equation 5, the Einstein equation (Hiemenz and Rajagopalan, 1997):

Equation 5: The Einstein equation

$$\frac{\eta}{\eta_0} = 1 + 2.5\phi + k_1\phi^2 + \ldots$$

Where: η = the viscosity of the polymer solution, η_0 = the viscosity of the bulk solution (i.e. in the absence of polymer), ϕ = the volume fraction of polymer in solution and k_1 is a constant. The equation can be rearranged as shown in Equation 6:

Equation 6

$$\frac{(\eta/\eta_0 - 1)}{\phi} = 2.5 + k_1\phi + \ldots$$

The term on the left - hand side of Equation 6 is known as the reduced viscosity (η_{red}). The intrinsic viscosity [η] of a polymer in a given system can be found using Equation 7:

Equation 7

$$[\eta] = \lim_{\phi \to 0}(\eta_{red})$$

This intrinsic viscosity can be related to the average molecular weight of a polydisperse polymer by Equation 8, the Mark–Houwink–Sakurada equation (Brandrup and Immergut, 1989).

Equation 8: Mark–Houwink–Sakurada

$$[\eta] = kM^{\alpha}$$

Where: M = the average molecular weight of the polymer (viscometrically measured), k is a constant which depends on the polymer chemical composition, α is a constant which depends on polymer–solvent interactions. Ideally, k and α are independent of polymer molecular weight and concentration (Frisch and Simha, 1956). However, in practice, the values of k for calculating a number average molecular weight or a mass average molecular weight are greatly influenced by the polydispersity of the sample, with the former being affected the most (Brandrup and Immergut, 1989). Polydispersity is the ratio of the number average molecular weight (M_n) to the weight average molecular weight (M_w). If the polydispersity is equal to 1, then M_n equals M_w and the polymer is said to be monodisperse. In reality, polymers are never monodisperse, the polydispersity will always be greater than 1.

When a mass average molecular weight (M_w) is used in Equation 8, the constant k is represented as k_w. For the mass average molecular weight, the error associated with the calculated k_w is decreased as α is increased. Kurata and Tsunashima (Brandrup and Immergut, 1989) report that for a polydispersity of 30, k_w/k is 0.89 at $\alpha = 0.5$, but k_w/k is 1 at $\alpha = 1.0$. k_w/k is given as 0.963 at $\alpha = 0.9$ (k_w represents the value of k when a mass average molecular weight is used). This value (k_w/k) was used to correct the k value in Table 2 and determine a corrected molecular weight for the sample under investigation.

Table 2: The values for α, k and kw for sodium carboxymethylcellulose (CMC) with a degree of substitution of 0.62 – 0.74 at differing salt concentrations and at 25 °C (Kurata and Tsunashima, 1989)

Salt concentration (NaCl)	α	k (ml/g)	k_w (ml/g)
0.001M	1.40	1.00×10^{-4}	1.00×10^{-4}
0.01M	1.20	6.46×10^{-4}	6.46×10^{-4}
0.1M	0.91	1.23×10^{-2}	1.16×10^{-2}

Therefore, for a given series of polymers in a given solvent, one can deduce that a polymer with a high intrinsic viscosity has a larger molecular weight than one with a low intrinsic viscosity. Table 2 gives the constants k and α for the CMC reported by Kurata and Tsunashima (Brandrup and Immergut, 1989). These constants were calculated using sedimentation diffusion techniques at a temperature of 25 °C. The value for k has been corrected for polydispersity assuming a polydispersity of 30 (Brandrup and Immergut, 1989). The author is unaware of any values for k and α for the guars.

2.4 Interactions between talc and polymeric depressants

1. Interactions between polymers and talc have been studied by a number of authors (Wie and Fuerstenau, (1974), Huang et al (1978), Steenberg (1982), Morris (1996) Rath et al. (1995), Dalvie (2001)) but a number of key questions remained unanswered.

The adsorption of molecules onto a surface is governed by the Gibbs free energy of adsorption, which is dependent on electrostatic, chemical and hydrophobic interactions (King, 1982). Equation 9 describes this relation:

Equation 9

$$\Delta G^{o}_{ads} = \Delta G^{o}_{elec} + \Delta G^{o}_{water} + \Delta G^{o}_{chem}$$

Where: ΔG^{o}_{ads} = The free energy of adsorption. This must be negative for spontaneous adsorption to occur

ΔG^{o}_{elec} = The free energy contribution to adsorption through electrostatic forces. It is also defined in King (1982) as

$$\Delta G^{o}_{elec} = z.F.\varphi_{\delta}$$

Where: z = the valency

F = Faraday's constant

φ_{δ} = The Zeta potential at the stern plane

$$\Delta G^{o}_{water} = \Delta G^{o}_{hydrophobic} + \Delta G^{o}_{hydrogen}$$

$$\Delta G^{o}_{hydrophobic} = n\phi$$

Where : ϕ = the amount of free energy required for the removal of one mole of CH_2 from solution through hydrophobic association. It has been found that ϕ = -1,0.R.T or 2,5 kJ/mol (King,1982). However, this is for the reduction in free energy due to the naturally hydrophobic hydrocarbon chains associating with each other. In the interactions between depressant and talc, this free energy would arise from the depressant associating with the

surface of the talc. Thus this figure may not apply. What is certain is that the energies associated with this are small.

n = the number of CH_2 groups in the molecule.

$\Delta G^{\circ}_{hydrogen}$ is the energy associated with the formation of hydrogen bonds. The specific energy associated a hydrogen bond is low (about 20 $kJ.mol^{-1}$ (Morris, 1996))

ΔG°_{chem} = The free energy contribution when chemical bonds are formed

The difference between the nature of the talc planes and edges results in the interactions between the polymers on the talc edges differing from those between the polymer and the talc plane.

It is likely that hydrophobic bonding will be insignificant compared to electrostatic and chemical bonding effects when polymers adsorb onto the talc edges.

Bonding on the talc planes will occur either due to hydrophobic attraction (a reduction in entropy due to CH_2 groups moving onto the hydrophobic talc surface) or by hydrogen bonding between the hydroxyl groups on the polymer and the silica-oxygen dipoles along the surface of the talc plane. Both of these mechanisms have extremely small energies associated with them, but the summation of a large number of links can lead to significant energies of adsorption. Steenberg (1984) postulated that the adsorption of anionic polymers (like CMC) onto the talc surface could be due to Van der Waals forces based on an attraction between the charged polymers and a slightly polar talc planar surface caused by the electronegativity difference between the oxygen and silica ions. Gong et al. (1999)

report that hydrophobic interaction is the main mechanism that drives the adsorption of polyacrilamides onto talc – with the most effective depression resulting from those polyacrilamides which had OH groups capable of hydrogen bonding to the aqueous environment. Jenkins and Ralston (1997) also report that hydrophobic interactions dominate the adsorption of depressants onto talc, reporting that hydrogen bonding made a small contribution and chemical adsorption mechanisms were absent.

Liu and Laskowski (1999) discuss the adsorption mechanism of CMC onto mineral surfaces. They conclude that metallic adsorption centres play a significant role in the CMC (a charged polysaccharide) adsorption. They also conclude that the substituted functional groups on CMC's influence the adsorption and that solution pH will significantly affect matters. Oliviera and Gomes (1995) report that the preparation of controlled types of CMC seems to be fundamental to the efficiency of their use as a depressant. They refer to a model by Salmi et al. (1994), which calculate the distribution of mono-, di- and tri-substituted units as a function of degree of substitution. Oliviera and Gomes (1995) also report that for CMC, a lower degree of substitution results in a higher effectiveness in talc depression. This is ascribed to be due to a lower electrostatic repulsive force between the CMC and the negatively charged talc surface. This allows the formation of hydrogen (OH polarised to the Si-O dipoles along the planes) and hydrophobic bonds (CH_2 groups condensing on the planes to reduce the entropy of the system). In their investigation into the depression of certain sulphide minerals using long chain depressants, Liu and Laskowski (1999) report that depressants have differing affinity for differing metal hydroxy species. This could be a basis used for promoting selective depression of minerals. Mao et al. (1999) report that when guar gum is adsorbed

strongly onto ilmenite and rutile, it can prevent adsorption of collector, allowing for separation of these minerals from zircon using guar depressants.

Rath et al. (1995) showed that the adsorption of guar gum on talc was almost independent of pH and the adsorption isotherm followed Langmurian behaviour. Morris (1996) reports that the adsorption of a CMC (FF300) on talc follows Langmurian adsorption of the high affinity type.

Rath et al. (1999) reported a dependence of adsorption on talc particle size. It was found that the adsorption of guar gum on talc decreased as the particle size was reduced. Rath et al. (1999) attribute this to a reduction in the ratio of face to edge ratio of talc as it is ground down further but unfortunately do not provide evidence that such a change in ratio does in fact occur. Their assumption is that guar gum tends to adsorb onto the talc plane preferably to the talc edge. However, if one considers the findings of Steenberg (1982), it seems that the guar gum packs itself more thickly onto the talc edges than the talc planes. Therefore if there was an increase in the ratio of edge to plane, perhaps one should rather expect an increase in guar gum adsorption onto the talc.

The polysaccharide depressants used in industry are generally very long molecules, with a few thousand monomeric links in the chain. The conformation of these chains onto the talc surface could be an important factor in determining how they influence the behaviour. Figure 9 depicts the conformation of a polymeric molecule onto a surface:

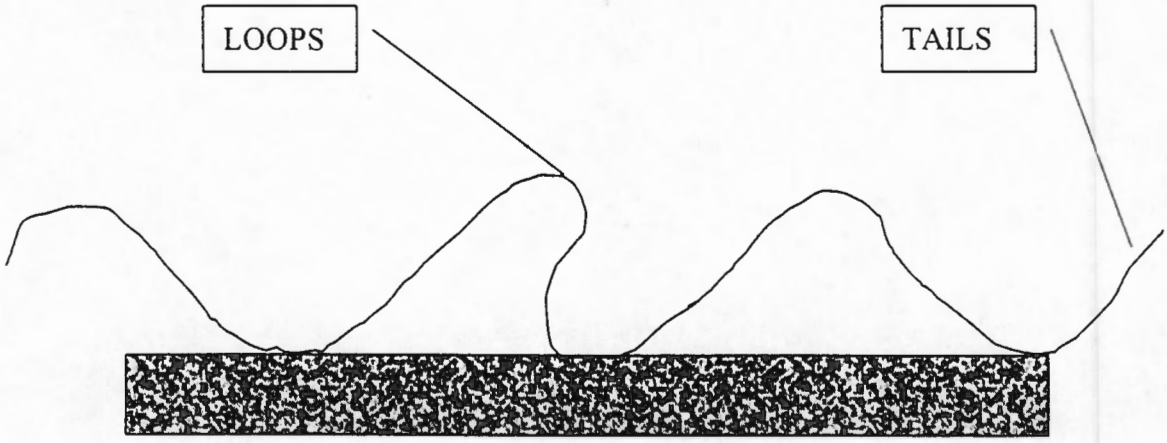

Figure 9: A schematic diagram of the adsorption of a polymer onto a mineral surface

The points at which the polymer touches the surface are termed trains, the ends of the polymer, which stick out into solution, are termed tails and the segments between the trains are termed loops.

Steenberg (1984) reports that both guars and CMC's adsorb onto the talc surface. It was found that a greater quantity of guar adsorbed onto the talc than CMC's, but the planar surface area covered by a single guar molecule was much lower than that covered by a CMC molecule. This could be due to the branched nature of the guar molecules. Jenkins and Ralston (1997) reported that guar gum adsorbed onto the talc planes in a flat conformation with 75% of the polysaccharide present in trains along the surface. They also reported that the mannose backbone adsorbed on the surface with the galactose units protruding into the bulk solution.

It was also reported by Steenberg (1984) that the area covered by a single CMC on the edge of talc was smaller than that occupied on the plane, indicating a less extended conformation on the edges. The guar also occupied a smaller surface area on the talc edge than on the plane.

Morris (1996) found a direct correlation between the adsorption of CMC onto talc and the depression of talc. Higher adsorption densities of CMC onto talc led to greater depression. Steenberg also found that CMC and guar depressed talc. Rath et al. (1995) also report that guar gum is an effective depressant of talc.

Oliviera and Gomes (1995) discuss the forces that hinder the capture of a talc particle by an air bubble once the particle has a hydrophilic macromolecular coating. He reports that the total interaction made up of three contributions – that due to Van der Waals forces, that due to the electrical double layer and that due to a hydration force. Steric hindrances were disregarded as not significant in this situation – this may indicate that the conformation of the polymer on the talc surface may not be as significant as suggested by Steenberg (1996).

Ions can significantly affect the interactions between talc and the depressants. The ions can reduce the charge on the depressants and talc, thus reducing electrostatic repulsion effects between them. This was shown by Gomes and Oliviera (Morris, 1996) who reported enhanced CMC adsorption onto talc in the presence of metal cations. Divalent cations like copper can create salt linkages (Steenberg, 1982). Ions can also affect the conformation of depressants adsorbed on to talc. CMC's were found to adsorb with greater surface area (or flatter on the surface) when in a higher ionic strength solution

(Morris, 1996). Fuerstenau showed that ions can significantly change the surface characteristics of talc – both electrostatically and hydrophobically. Rath et al. (1995) report that guar gum – magnesium complexes form in the bulk solution when magnesium was leached from the talc surface.

Both CMC's and guars can act as flocculants (Steenberg, 1982). Flocculation through polysaccharide adsorption is postulated to occur through bridging mechanisms (Steenberg, 1982). Harris et al. (1999) reported that larger guar depressants led to increased pulp coagulation. Kato and Nakai (1980) from the biological sciences report that the emulsifying activity of a protein increases as the protein's hydrophobicity increases.

CMC's are also reported to act as dispersants (Steenberg, 1982). This is postulated to occur through the CMC creating a more negative charge on the particle thus increasing electrical repulsion effects (Steenberg, 1982).

3 Research objectives

The purpose of this thesis is to examine the effect that a set of different molecular weight and molecular type polymeric depressants have on the hydrophobicity of talc and the flotation performance of PGM Merensky ore. In addition, the effect that the ionic environment has on the talc-depressant interactions is examined. The following key questions are addressed in this thesis:

- How do the solution ionic conditions affect the conformation of the polysaccharide depressants as measured by viscometry?
- How does the polymeric nature of a depressant impact its effectiveness on talc floatability as measured by microflotation?
- How do CMC (charged linear polymers) compare to guars (uncharged branched polymers) with respect to their ability to depress talc?
- How do the molecular weights of the depressants impact on their effectiveness in reducing talc hydrophobicity and are the trends similar between the guars and CMC's studied?
- How do ionic conditions affect the floatability characteristics of talc without depressants?
- How do ionic conditions affect the depressant-talc interactions?
- How similar is the impact of ionic strength on the two types of depressants (guar and CMC)?

- Can findings in a highly controlled microflotation system with pure talc and no other factors such as collector and activator influence be extrapolated to the results of a batch flotation experiment with PGM Merensky ore?

4 Experimental details

4.1 Minerals, chemicals and equipment used

4.1.1 Mineral samples

Natural talc from Scotia Mines, Barberton, South Africa, was wet screened into the size fractions +38 μm –45 μm, +45 μm –53 μm, +53 μm –75 μm, +75 μm –106 μm and +106 μm –150 μm. Repeated ultrasounding and decantation was used to eliminate ultrafines. The talc size fraction +75 μm –106 μm was split into 2 gram portions and used for microflotation.

Merensky ore was obtained from Impala Platinum Mines. The ore was crushed to -2 mm and then split into 1 kg samples. These samples were wet milled in a rod mill to obtain a size classification of 60% passing 75 μm and used in batch flotation tests.

X-Ray Diffraction (XRD) analyses on the talc (done by the Council for Mineral Technology (MINTEK)) showed that the only major impurity in the sample was magnesite. This analysis is attached in Appendix 1.

X-Ray Flouresence (XRF) analyses (done by the Department of Geology, University of Cape Town) of the size fractions +38 μm –45 μm, +45 μm –53 μm, +53 μm –75 μm, +75 μm –106 μm and +106 μm –150 μm showed no variation in the silicon–magnesium peak ratios with talc size. This implies that the magnesite is intimately associated with the talc structure and is not liberated by grinding. Sample analyses for three size fractions +38 μm –45 μm, +45 μm –53 μm, and +106 μm –150 μm are included in Appendix 2.

The talc surface area was determined using the B.E.T. nitrogen adsorption. The B.E.T. summary reports are included in Appendix 3. Table 3 shows the values found for surface area for the talc at two different size fractions.

Table 3: Surface area of talc at two different size fractions

Talc Source	Talc size fraction	Surface Area
Scotia Mines, Barbeton	-38 μm	3.6285 m^2/g
Scotia Mines, Barbeton	-106 +75 μm	1.5125 m^2/g

The mineralogical composition of the Merensky ore used is shown in Table 4 (Dalvie, 2001).

Table 4: Mineralogy of Merensky ore

Mineral	Abundance (%)
Talc	0.5
Feldspar	40
Pyroxene	52
Chromite	3-4
Sulphides	<1
Other	2-3

4.1.2 Polysaccharide depressants

The carboxymethylcellulose (CMC) depressants used were FF10, FF30, FF150 and FF300, provided by Trohall. The abbreviation FF indicates that they belong to the Finnfix reagent series. The numbers indicate the relative viscosity of the reagents, which increase in the order FF10 < FF30 < FF150 < FF300.

For the CMC's used, the average number of glucose hydroxyl groups substituted by $CH_2COO^- Na^+$ per glucose monomer is approximately 0.8 (degree of substitution). This indicates that the CMC molecules are highly charged.

The guar depressants used in this study were SM4060, IMP4 and SM4560. These were also provided by Trohall and belong to the Acrol reagent series. The viscosity of the reagents increases in order SM4060 < IMP4 < SM4560.

For the guars used, the average number of glucose hydroxyl groups anionically substituted is approximately 0.1 (degree of substitution). This indicates that these guars have a very low charge.

The solid polymer samples were dried overnight in the oven at a temperature between 60°C and 80°C and cooled in a vacuum desiccator in order to remove excess moisture. The polymer solutions were prepared by weighing out a 4-gram portion of polymer and adding this slowly to an agitated vessel containing deionised water. The solutions were stirred for 30 minutes. The solution was made up to the required volume by adding deionised water and left to equilibrate overnight. Fresh solutions were prepared every four days.

4.1.3 Ionic conditions

When required, analytical grade potassium nitrate (KNO_3), magnesium nitrate ($Mg(NO_3)_2.6H_2O$) and calcium nitrate($Ca(NO_3)_2.4H_2O$) were used to adjust the ionic strength of solution. Analytical grade sodium hydroxide (NaOH) was used to adjust the pH to 9.

Deionised water was used in all tests.

4.2 Viscometric test procedure

A Brookfield digital viscometer (model LVTDV-II) was used to measure the viscosity of the polymer solutions. The viscosity of each polymer was measured at various concentrations ranging from 0.2 % to 5.0 % by mass at two different ionic strengths (10^{-2} M KNO_3 and 10^{-1} M KNO_3). The temperature was maintained at 25°C ± 0.03°C. The pH values of the solutions varied between 6.3 and 7.6. Discussion of the equations and calculations used in the viscometry work is given in the literature survey portion of this report (section 2.3.4).

4.3 Microflotation test procedure

Microflotation experiments were carried out to test the depressing ability of the polymers on talc. These tests were performed using the U.C.T. flow-through microflotation cell (Bradshaw and O'Connor, 1996). Figure 10 schematically depicts the microflotation cell used.

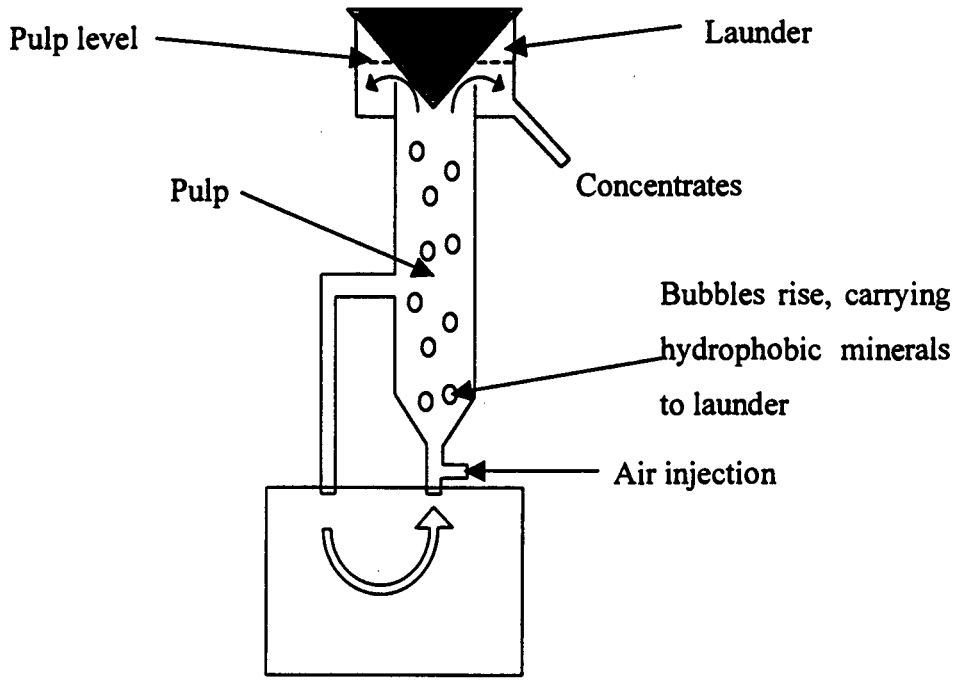

Figure 10: A schematic diagram of a U.C.T. flow-through microflotation cell

The pH was set at 9 for all the tests and the concentrations of the polymers were varied between 4 and 400 mg/l. The ionic strength of solution was set according to Equation 10:

Equation 10

$$u = \frac{1}{2}\sum c_i . z_i^2$$

Where: u = ionic strength, c_i = concentration of ion i and z_i = valency

Table 5 reports the concentrations of salts used to set the ionic strength of solution.

Table 5: The concentrations of the salts used to set the ionic strength in the microflotation experiments

Salt	Molar Concentration	Ionic Strength
KNO_3	10^{-3} mol/dm^3 10^{-2} mol/dm^3	10^{-3} 10^{-2}
$Mg(NO_3)_2.6H_2O$	3.33×10^{-4} mol/dm^3 3.33×10^{-3} mol/dm^3	10^{-3} 10^{-2}
$Ca(NO_3)_2.4H_2O$	3.33×10^{-4} mol/ dm^3 3.33×10^{-3} mol/ dm^3	10^{-3} 10^{-2}

The following conditioning procedure was used for all microflotation tests. A 2-gram talc sample (size +75 μm –106 μm) was chosen representatively and ultrasounded for 5 minutes in 50 ml deionised water – after which the fines were decanted. The sample was then placed in a conditioning beaker and the level was raised to 250 ml with the polymer solution at the required concentration and ionic strength and a pH of 9. This suspension was conditioned for 20 minutes. After conditioning, the pulp was transferred to the microflotation cell and the cell was filled to the required level with the same polymer solution at the given concentration, ionic strength and pH. The air was turned on to commence flotation and concentrates were taken at 30 seconds, 1 minute, 2 minutes, 5 minutes and 10 minutes.

In removing the concentrate from the system during flotation, solution was drained from the launder of the cell. Fresh polymer solution of the same concentration, ionic strength and pH as that specified for the talc – depressant system, was used to refill this section of the cell after each concentrate removal. Concentrates were dried overnight and weighed. Three repeats of each condition investigated were done.

The results are expressed as the cumulative mass percent floated after 10 minutes (R_{10min}) and as the first order rate constant (k), calculated using Equation 11.

Equation 11: First Order Rate Equation (assuming 100% conversion)

$R_t = 1\text{-}e^{-kt}$

Where: t = time

R_t = the recovery at time t.

k = the flotation rate constant

It was found that when the polymer concentration in solution was diluted during the microflotation test by adding deionised water to the launder instead of polymer solution, the flotation results of the talc were significantly different with respect to the guar, and fairly similar with respect to the CMC (see section 5.2.1).

Appendix 5.1 shows an example of the microflotation test sheet used. Appendix 5.2 shows a sample of the microflotation test results.

4.4 Batch flotation test procedure

Batch flotation tests were performed on Merensky ore obtained from Impala Platinum Mines. This ore was split representatively into approximately 1 kg samples using a mechanical revolving sampler. These samples were milled in a laboratory rod mill with stainless steel rods and at 600 ml tap water per 1 kg ore. The samples were milled to obtain a size classification of 60% passing 75 μm.

Flotation was performed in a 3 l modified Leeds cell (Bacus, 2000; Dalvie, 2001).

The following flotation process was followed:

1. Immediately after milling, the pulp was transferred to the modified Leeds cell and the level set by adding tap water. The impeller was set to 1200 rpm

2. Sodium isobutyl xanthate (SIBX – the collector) was added at 45 g/ton

3. After 5 minutes of conditioning, copper sulphate ($CuSO_4$ – an activator) was added at 30 g/ton

4. After a further 2 minutes, the depressant was added

5. A minute later the frother was added. DOW200 frother was used in all tests

6. A minute hereafter the air feed was turned on at 6 l/min and the float timer set to zero

7. Concentrates were collected by scraping the froth every 15 seconds. Concentrates were collected at 1 minute, 4 minutes, 13 minutes and 25 minutes

8. Copper and nickel assaying were done using an acid digestion technique. This technique is based on the principle that the ore is dissolved in aqua regia with the addition of hydrofluoric and perchloric acid, after which the sample is made up to a known volume, filtered and read on an AA spectrometer. The method is as follows:

Reagents used: 40 % Hydroflouric acid, 60 % Nitric acid, Concentrated Perchloric acid, 30 % Hydrochloric acid, Mix 4 parts HCl to 1 part HF per volume, Sample should be finely ground

1. The sample is weighed out according to the type (concentrates 0.1g, Feeds 0.5g), into a 250 ml wide mouthed Erlenmeyer flask as follows:

   - Add 10 ml of the HCL/HF mixture to the sample and heat to boiling
   - Add 10 ml $HN0_3$ to the flask and boil until the sample volume is approximately 2 ml
   - Add 5 ml $HClO_4$ to the flask and boil until the sample volume is approximately 2 ml (A white cloud will form and rise once the reaction has taken place)

2. Make up to volume and filter:

   - Transfer the sample quantitatively to a 100 ml volumetric flask and make up to 100 ml with distilled H_2O.
   - Filter this through Whatman no. 1 into a sample bottle.
   - Read the filtrate on the AA spectrometer, store the sample in a fridge if reading is delayed

The detailed batch flotation test results are included in Appendix 6.

5 Results and discussion

5.1 Depressant Characterisation

5.1.1 Depressant Research Facility characterisation

The depressant sample used in this study were submitted to the Depressant Research Facility, University of Cape Town and the following characteristics were measured: moisture, purity, degree of substitution, pH, percent insoluble material and molecular mass (measured using column exclusion chromatography). The methodology used by the depressant research facility is detailed in Appendix 7.

Table 6 shows the results of this study.

Table 6: Depressant characteristics

Characteristic	FF10	FF30	FF150	FF300	SM4060	IMP4	SM4560
Moisture (%)	6.4	5.7	5.1	5.8	9.3	10.4	10.1
Purity (%)	97.3	98.5	98.2	95.4	89.1	94.6	89.4
Degree of Substitution	0.61	0.62	0.71	0.70			
pH of a 1% Solution	5.90	6.72	6.22	6.46	3.35	6.17	5.42
% Insoluble Material	1.60	2.76	3	<1	5.85	5.42	3.86
Molecular Mass							
Weight Average	164100	323500	411400	575200	67920	180700	290800
Number Average	40800	47800	63100	52400	21500	37600	52600
Polydispersity	4.0	6.8	6.5	11.0	3.2	4.8	5.5

The primary purpose of investigating the molecular masses of the depressants was to determine whether the assumption with regard to the trend which they followed was correct (that is, that the weight average molecular masses of the modified guar depressants increase in the order SM4060 < IMP4 < SM4560 and the weight average molecular masses of the CMC polymers increase in the order FF10 < FF30 < FF150 <

FF300). Figure 11 shows the weight average molecular mass versus depressant type. It is clear that the trends expected are followed.

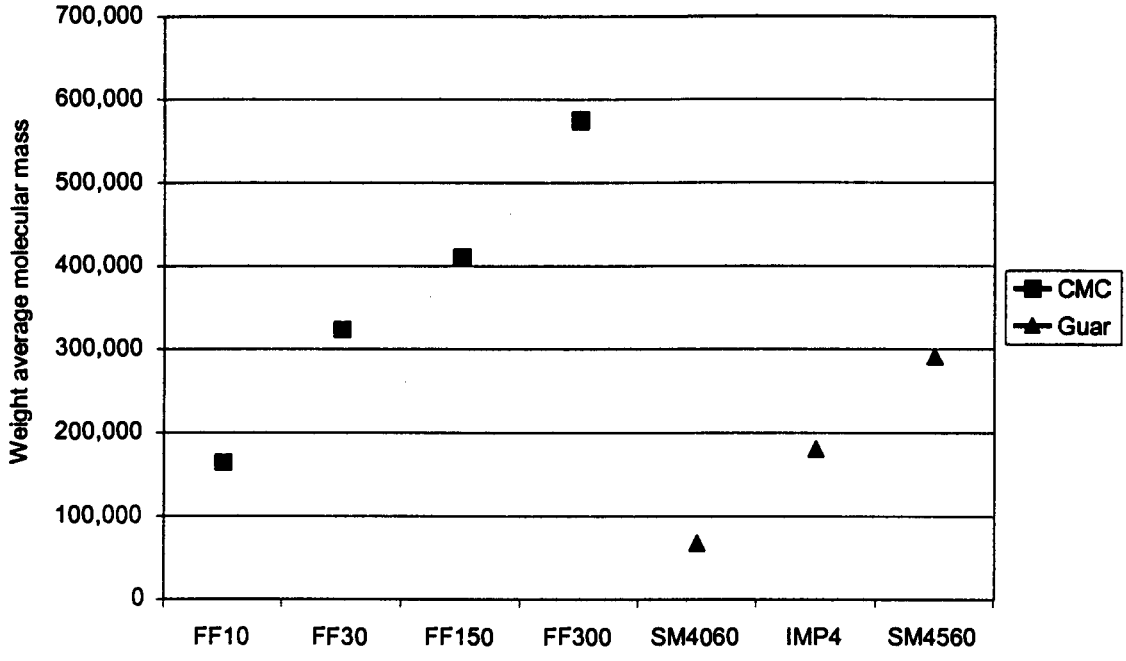

Figure 11: The weight average molecular mass versus depressant type.

5.1.2 Viscosity tests

As discussed in the literature review, the viscosity of a polymer is indicative of the hydrodynamic volume that the polymer occupies in solution.

Figure 12 shows the reduced viscosity measured for three guar depressants (SM4060, IMP4 and SM4560) plotted against the depressant solution concentration at two salt concentrations (10^{-2} M KNO_3 and 10^{-1} M KNO_3).

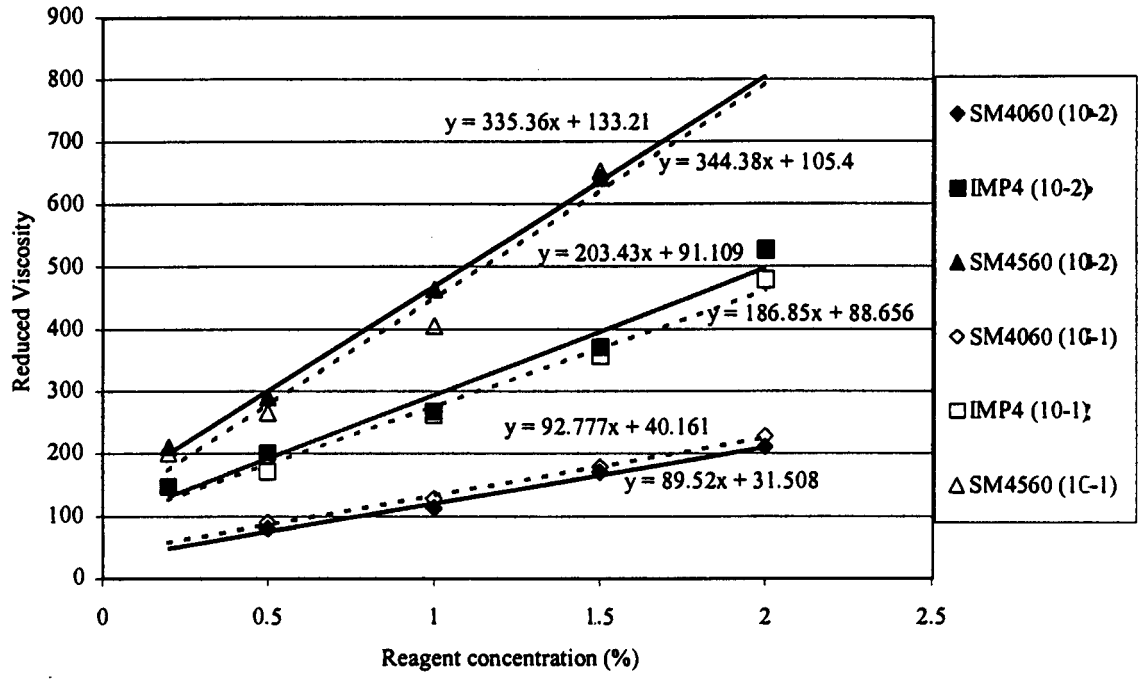

Figure 12: The reduced viscosity versus the solution concentration of the guars SM4060, IMP4 and SM4560 at 10^{-1} M KNO_3 and 10^{-2} M KNO_3

The chemical composition of these guars is similar and therefore an increase in viscosity corresponds to an increase in molecular weight. The results show that the molecular weights of the guar samples tested increase in the order SM4060 < IMP4 < SM4560. The average molecular weights could not be calculated from this viscosity data as k and α are unknown.

The reduced viscosity curves of the guars are not significantly affected by salt concentration. This indicates that an increase in the salt concentration from 10^{-2} M KNO_3 to 10^{-1} M KNO_3 did not affect the solvent – polymer and polymer – polymer interactions for the guar samples. This result indicates that the effect of the charge of the guar samples on their behaviour in solution is negligibly small. Alternatively, there could be compensating effects.

The manner in which the plot of η_{red} against polymer concentration increases with increasing concentration is an indication of solvent characteristics and the interactions of the polymeric molecules with each other in solution (Hiemenz and Rajagopalan, 1997). When the solvent quality does not influence the polymer and when inter-particular interactions are absent, the plot of η_{red} against polymer concentration should be a horizontal line intercepting the y – axis at the intrinsic viscosity. Hence, the increase in slopes of the lines plotted in Figure 12 shows that the interactions between the guar molecules increase as the molecular weight is increased.

Figure 13 shows the reduced viscosity measured for four CMC polymers (FF10 < FF30 < FF150 < FF300) plotted against the polymer solution concentration at two salt concentrations (10^{-2} M KNO_3 and 10^{-1} M KNO_3).

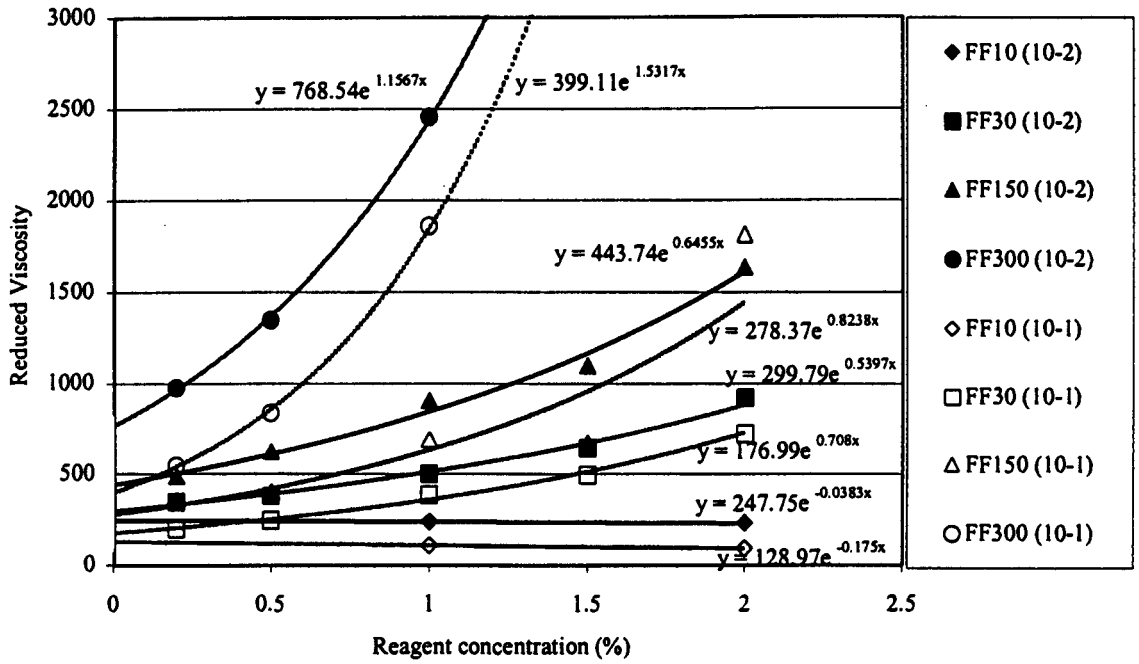

Figure 13: The reduced viscosity versus the solution concentration of the CMC's FF10, FF30 and FF150 at 10^{-1} M KNO_3 and 10^{-2} M KNO_3

The chemical compositions of these CMC's are similar. Therefore, the results extrapolated to zero polymer concentration show that the molecular weight of the CMC's increases in the order FF10 < FF30 < FF150 < FF300. The absolute magnitude of the average molecular weights for these samples can be calculated using the values for k and α given in Table 2 as the tests were done under conditions of similar ionic strength and temperature as the reported for these values. The average molecular weights for the CMC's calculated in this manner are shown in Table 7.

Table 7: The average molecular weights calculated for the CMC polymers used in this study, based on the values for k_w and α from Table 2

Depressant	KNO_3 Molarity	k_w	α	Intrinsic viscosity (cp)	Molecular mass
FF10	10^{-2}	6.46E-04	1.2	247.75	4.50E+04
	10^{-1}	1.16E-02	0.91	128.97	2.79E+04
FF30	10^{-2}	6.46E-04	1.2	299.79	5.27E+04
	10^{-1}	1.16E-02	0.91	176.99	3.96E+04
FF150	10^{-2}	6.46E-04	1.2	443.74	7.31E+04
	10^{-1}	1.16E-02	0.91	278.37	6.51E+04
FF300	10^{-2}	6.46E-04	1.2	768.54	1.16E+05
	10^{-1}	1.16E-02	0.91	399.11	9.67E+04
SM4060	10^{-2}			133.2	
	10^{-1}			105.4	
IMP4	10^{-2}			91.1	
	10^{-1}			88.7	
SM4560	10^{-2}			31.5	
	10^{-1}			40.2	

Figure 13 also shows that a high salt concentration results in lower viscosity readings for the CMC's. Due to the screening of the charges along the chain, the electrostatic repulsion is diminished. Therefore, at a high ionic strength, the CMC molecules are coiled more tightly than at a low ionic strength. These results show that in this case the hydrodynamic volume occupied by the CMC molecules decreases at increasing ionic strengths even though the molecular weight was not changed.

As with the guars, the intermolecular interactions of the CMC's increase with increasing molecular weight. Moreover, the slopes of the curves at high KNO_3 concentrations are steeper than the slopes at low KNO_3 concentrations. This indicates that the polymer-polymer interactions at a high KNO_3 concentration are greater than at a low KNO_3

concentration. This may be due to the charge screening effect, which lowers intermolecular electrostatic repulsion.

The constants k_w and α in Equation 8 are not known for the guars studied at the particular set of conditions studied and therefore, the exact molecular weight of the guar polymers could not be calculated quantitatively.

5.1.3 Key findings from depressant characterisation testwork

It should be noted that the molecular masses measured using column chromatography techniques are different from the molecular masses obtained from the viscometry tests. Light scattering data is likely to be the most accurate measure of absolute molecular weight, G. Morris (1996) used light scattering to measure the mass average molecular mass of FF300 and reported a result of 220,000. This lies somewhere between the estimate of 100,000 given by the viscometry tests and 575,200 given by the column exclusion chromatography tests. The differences in the results from the different measurement techniques can be attributed to the assumptions upon which each technique is based.

In this investigation, the purpose of examining the depressant molecular weights is for the purpose of examining the molecular weights of similar depressants relative to each other, therefore, the absolute molecular weight of each depressant examined is not relevant in this situation. At no stage in this investigation will CMCs and guars be compared directly with each other on the basis of similar molecular weights as it is recognised that the

that it is critical that the depressant concentration be maintained at a steady level throughout the flotation process, otherwise desorption would occur as the polymeric concentration in solution decreases steadily throughout the float. Figure 14 and Figure 15 show how the flotation of talc in the system is affected when the technique used is changed.

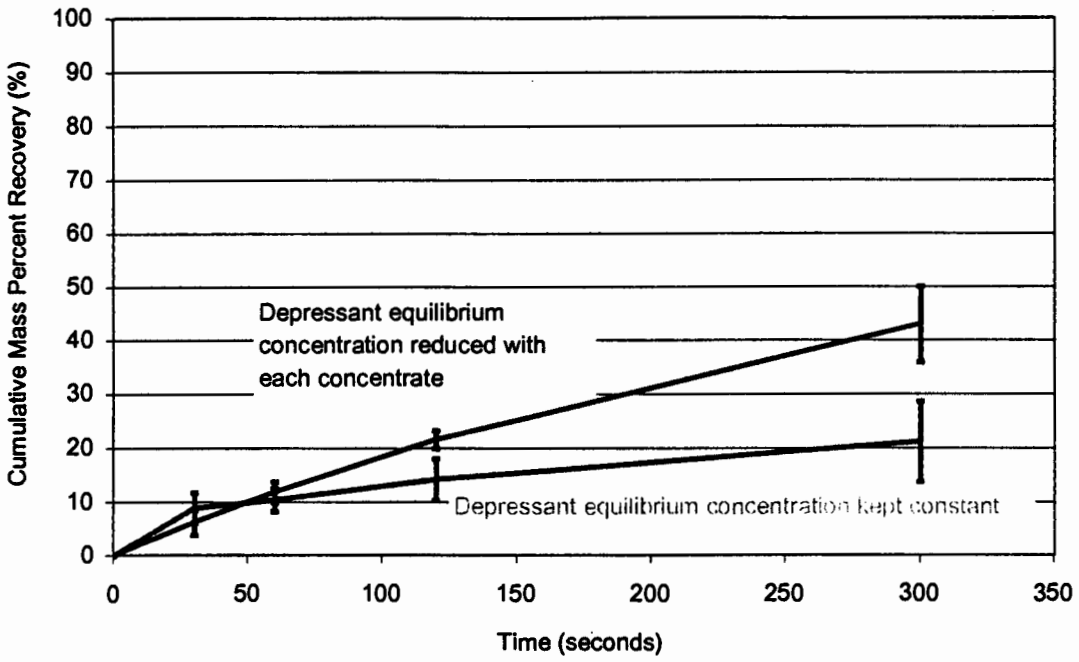

Figure 14: The difference in the flotation of talc with time when the depressant dosage technique was changed for IMP4 (a guar)

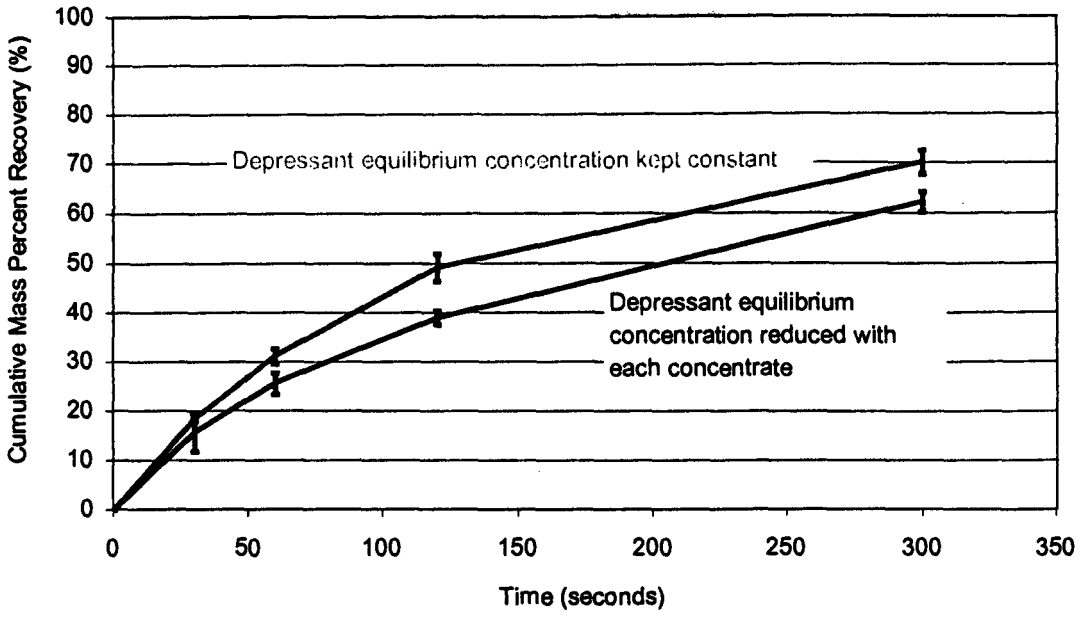

Figure 15: The difference in the flotation of talc with time when the depressant dosage technique was changed for FF150 (a CMC)

The fact that a clear difference in talc flotation is seen when the equilibrium conditions are kept constant as opposed to when the equilibrium conditions are allowed to reduce with each concentrate confirms that the adsorption of depressant onto talc is reversible and therefore led to the abovementioned refinement of the microflotation technique for the testwork for this investigation. It is also worth noting that the attainment of equilibrium appears to be rapid. The opposite effect obtained with the CMC's as opposed to the guars when the technique was changed is likely due to the lower depressing effect and cleansing action of CMCs.

5.2.2 Microflotation at low ionic strength

In this work, seven depressants were examined (FF10, FF30, FF150, FF300, SM4060, IMP4 and SM4560). The following dosages were used for each depressant: 0 mg/l, 4 mg/l, 20 mg/l (guar depressants only), 40 mg/l, 60 mg/l, 100 mg/l and 200 mg/l (CMC depressants only).

5.2.2.1 Reproducibility

In order to ensure good reproducibility of these results, each condition was repeated three times. All results in this section of work include the standard deviation around each point on the curve. The repeatability achieved on the float of natural talc flotation with time is shown in Figure 16. Table 8 shows the standard deviations for each point on the curve.

Table 8: Data points and standard deviations for Figure 16

Time (seconds)	Base 1	Base 2	Base 3	Base Average	Base Stdev
30	13.5	13.5	11.0	12.7	1.5
60	25.0	25.0	21.0	23.6	2.3
120	37.5	37.5	37.4	37.5	0.0
300	56.4	56.5	57.9	56.9	0.8
600	67.9	68.0	69.9	68.6	1.1
Time (seconds)	CMC 1	CMC 2	CMC 3	CMC Average	CMC Stdev
30	4.5	7.5	7.0	6.3	1.6
60	6.5	13.0	13.0	10.8	3.8
120	17.5	25.0	23.5	22.0	4.0
300	40.5	43.5	41.4	41.8	1.6
600	54.0	60.0	55.9	56.6	3.1
Time (seconds)	Guar 1	Guar 2	Guar 3	Guar Average	Guar Stdev
30	1.5	1.0	2.0	1.5	0.5
60	3.5	2.5	3.0	3.0	0.5
120	7.0	4.5	7.0	6.1	1.4
300	14.0	10.0	12.0	12.0	2.0
600	22.4	18.0	18.9	19.8	2.3

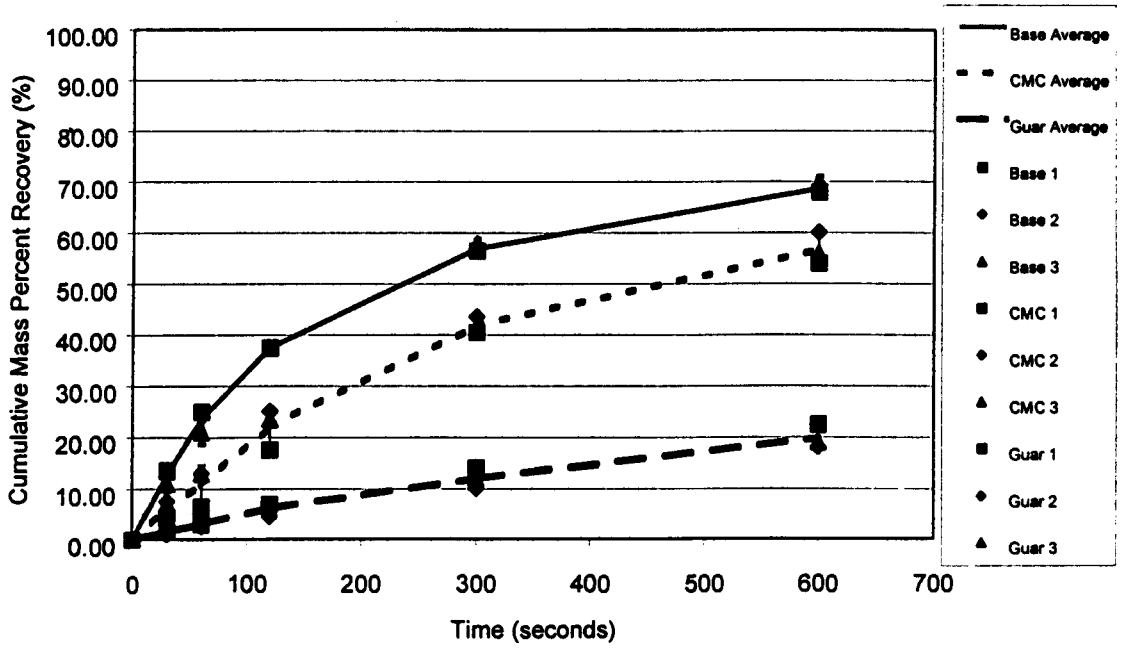

Figure 16: Example of flotation results to demonstrate reproducibility: the flotation of talc with time at low ionic conditions (10^{-3} M KNO_3): with no depressant addition, with a CMC (FF30 at 40 mg/l) and with a guar (SM4060 at 40 mg/l)

5.2.2.2 Microflotation results

Figure 17 depicts the cumulative mass percent recovery of talc after ten minutes.

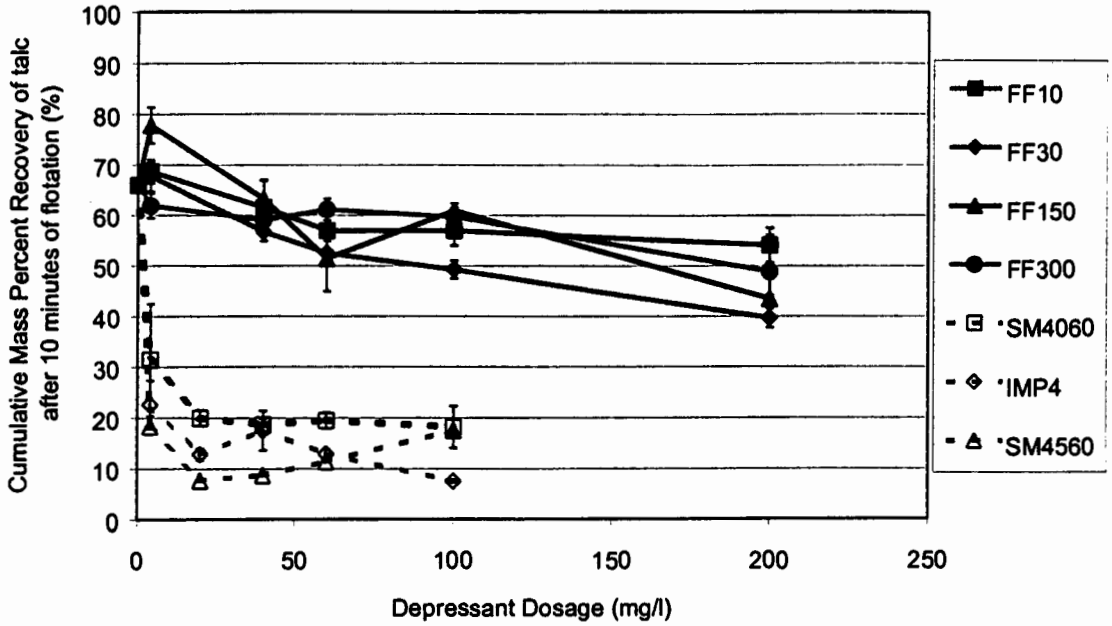

Figure 17: The cumulative mass percent recovery of talc after ten minutes with changing depressant dosage type and molecular mass

It is clear from Figure 17 that the guars act as strong depressants at a salt concentration of 10^{-3} M KNO_3.

The guars achieved a strong depressing action at low dosages (< 20mg/l), however at higher dosages no major increase in depression was observed. This indicates that sufficient surface area coverage of the guar on the talc to prevent particle-bubble attachment was achieved at 20 mg/l. This result is consistent with findings by Rath et al. (1997) who also showed that guar achieved a maximum level of depression at low dosages with no further depression being observed as the dosage was increased.

CMC's, on the other hand, showed poor depressing ability under the same solution conditions. Increased dosage of CMC lead to increased depression overall.

Adsorption results reported by Steenberg (1982) indicated that for an adsorption time of one hour and an ionic strength of 5×10^{-3}, considerably less CMC adsorbed onto the talc surface than guar. At low salt concentrations, the kinetics of CMC adsorption onto a negative surface may be slow as electrostatic repulsion is likely to occur between the surface and the polymer. On a plant scale, the conditioning time is relatively short (5 to 20 minutes), therefore, a conditioning step of 30 minutes was selected for this investigation.

Steenberg (1982) also found that the amount of surface area on the talc plane covered by a single CMC molecule could be up to 1000 times larger than that occupied by a guar molecule. Assuming that this also holds for the guar and CMC's samples used in this study, one can postulate that the considerable depressing ability of guar is due to the substantial adsorption of guar onto talc. The extended adsorbed layer of guar results in firm shielding of the talc surface from air bubbles. Jenkins and Ralston (1997) calculated that 75 % of the adsorbed guar polymers are in the form of trains on the talc surface. However, these calculations were based on an average uniform adsorbed layer thickness. The low depressing action of the CMC's could be indicative of low adsorption onto the talc.

In order to ascertain whether the molecular weight of the depressant affected its depressing action, the cumulative mass percent recovery of talc after ten minutes was

plotted against depressant molecular mass. Figure 18 shows the cumulative mass percent recovery of talc after ten minutes versus molecular weight.

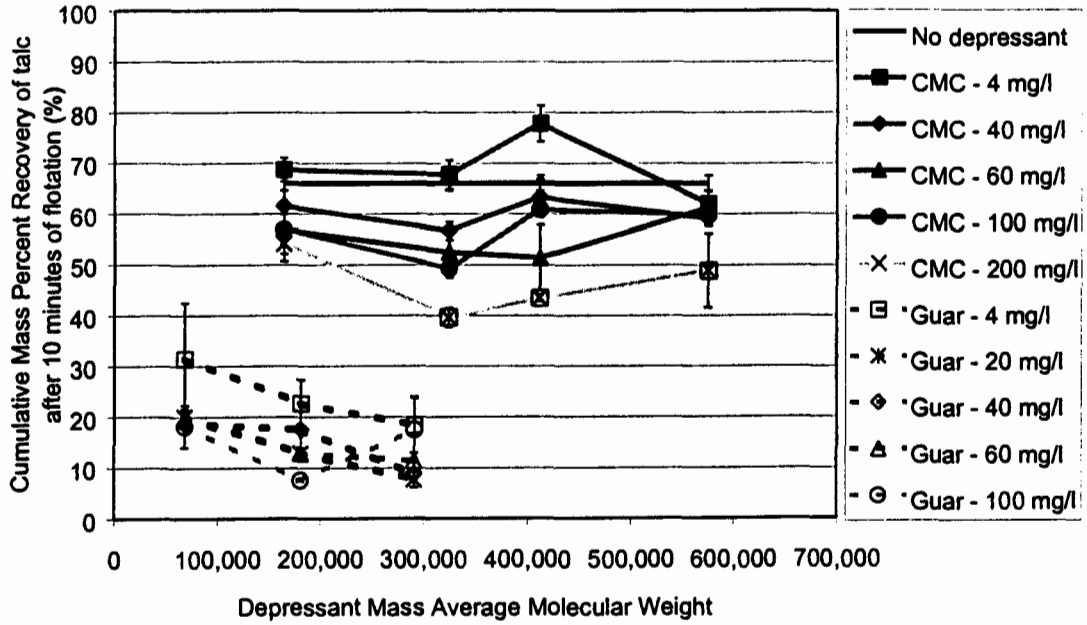

Figure 18: The cumulative mass percent recovery of talc after ten minutes versus molecular weight

Figure 18 shows that under conditions of a constant ionic strength 10^{-3} KNO_3, increasing the molecular weight of the CMC had no effect on its depressing behaviour.

Figure 18 shows that at low dosages (4 mg/l) the overall flotation of talc after 10 minutes was reduced as the molecular weight of the guar was increased. However, as the dosage was increased, the effect that molecular weight has on the overall talc depression diminished.

At the lowest dosage (4 mg/l) the overall recovery of talc after 10 minutes increased for all CMC depressants. This indicates that at very small dosages, the depressant could be exhibiting a cleaning action similar to that obtained when the equilibrium depressant

concentration was reduced as discussed in section 5.2.1. Dalvie (2001) showed that CMC depressants appear to adsorb onto talc even at extremely low dosages (4 mg/l). However, it is apparent that this adsorption does not lower the floatability of the talc – indicating that, at this low dosage, the adsorption may be occurring on the talc edges rather than the hydrophobic planes.

5.2.3 Microflotation at various ionic conditions

In section 5.1.2, it was shown that the ionic strength of solution has a strong effect on the viscosity characteristics of carboxymethylcellulose (CMC) polymers whereas guars were unaffected with regard to their viscosity characteristics when the ionic strength of the solution was changed. The microflotation tests of section 5.2.2 showed that under conditions of low ionic strength, the CMCs were ineffective depressants of talc – which is contrary to the experience of mineral processing plants. Guars were shown to be effective depressants of talc under these conditions. Morris (1996) showed that the use of magnesium ions at 3.33×10^{-4} M caused an increase in the depression of talc with FF300 (a CMC) at 100 mg/l, over the pH range 7 to 11.

It is therefore expected that at higher ionic strengths (as is common in most minerals processing plants) the CMCs would be more effective depressants of talc than at low ionic strengths, while the depressing ability of guars would not be changed.

The aim of this section was to investigate the influence of ionic strength and ionic type on the depressing ability of a modified guar gum (IMP4) and two CMCs (FF30 and FF300) of differing molecular weights.

The following dosages were used for each depressant: 0 mg/l, 4 mg/l and 40 mg/l for the IMP4 and 0 mg/l 20 mg/l 60 mg/l and 100 mg/l for the CMC depressants FF30 and FF300.

Three ion types were investigated - K^+, Mg^{2+} and Ca^{2+} - as described in section 4.1.3. Each ion was tested at an ionic strength of 10^{-3} and 10^{-2} as discussed in the experimental procedure section.

5.2.3.1 Reproducibility

In order to ensure good reproducibility of these results, each condition was repeated three times. All results will include the standard deviation around each point on the curve.

The repeatability achieved on the float of natural talc flotation with time is shown in Figure 19. Table 9 shows the standard deviations for each point on the curve.

Table 9: Data points and standard deviations for Figure 19

Time (seconds)	Base 1	Base 2	Base 3	Base Average	Base Stdev
30	4.2	6.5	10.3	7.0	3.1
60	7.9	11.4	18.0	12.4	5.2
120	15.8	21.1	27.3	21.4	5.8
300	31.1	37.3	44.9	37.7	6.9
600	45.8	53.5	59.8	53.0	7.0
Time (seconds)	FF30 1	FF30 2	FF30 3	FF30 Average	FF30 Stdev
30	2.8	0.0	0.5	1.1	1.5
60	5.0	6.7	2.5	4.7	2.1
120	7.2	8.6	5.5	7.1	1.5
300	12.8	13.4	9.6	11.9	2.1
600	20.6	20.6	17.1	19.4	2.0
Time (seconds)	FF300 1	FF300 2	FF300 3	FF300 Average	FF300 Stdev
30	1.0	0.0	3.7	1.6	1.9
60	2.6	0.5	7.3	3.5	3.5
120	4.2	1.1	8.9	4.7	3.9
300	7.3	5.4	13.6	8.8	4.3
600	11.4	10.8	19.4	13.9	4.8
Time (seconds)	IMP4 1	IMP4 2	IMP4 3	IMP4 Average	IMP4 Stdev
30	3.1	1.5	1.2	1.9	1.0
60	5.3	3.1	2.3	3.6	1.6
120	6.9	6.1	2.3	5.1	2.5
300	11.5	11.5	4.6	9.2	4.0
600	20.6	19.1	8.1	15.9	6.9

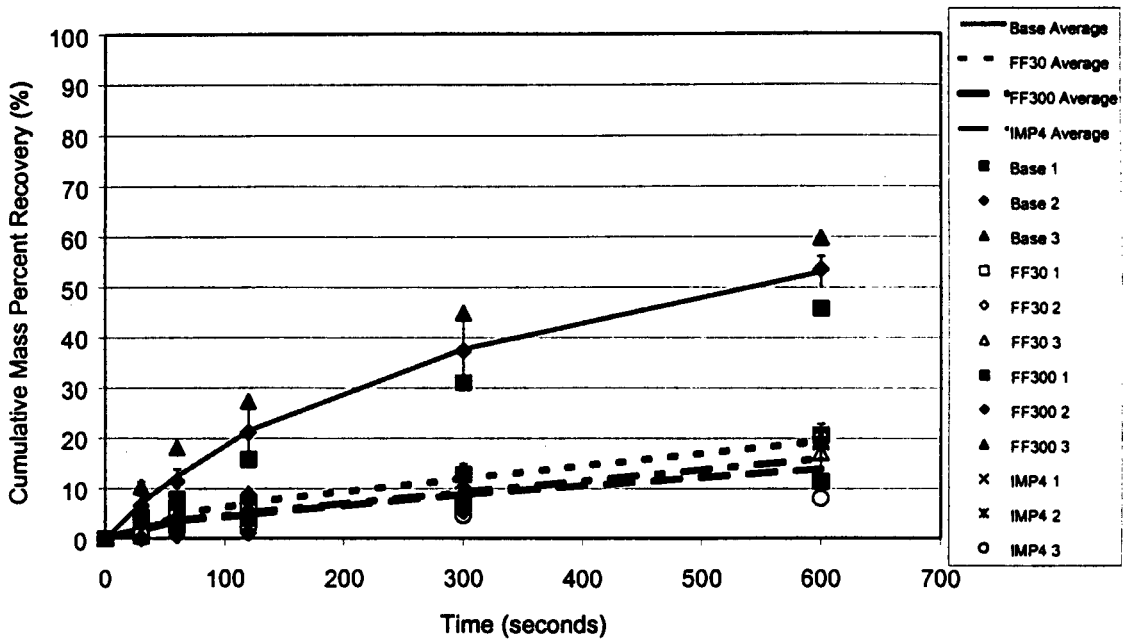

Figure 19: Example of flotation results to demonstrate reproducibility: the flotation of talc with time at a system ionic strength of 10^{-2} with magnesium and depressant addition of FF30 and FF300 at 60 mg/l and IMP4 at 40 mg/l

5.2.3.2 Influence of ions on the natural flotation of talc

Microflotation tests on talc with no depressant addition were carried out at two ionic strengths (10^{-3} - referred to as low, and 10^{-2} - referred to as high).

The flotation of talc with time was found to follow first order kinetics and therefore, all the floats done were modeled according to Equation 11 (section 4.3).

Figure 20 shows the effect of ionic type and concentration on the cumulative mass percent recovery of talc at 10 minutes. Figure 21 shows the effect of ionic type and concentration on the first order flotation rate constant.

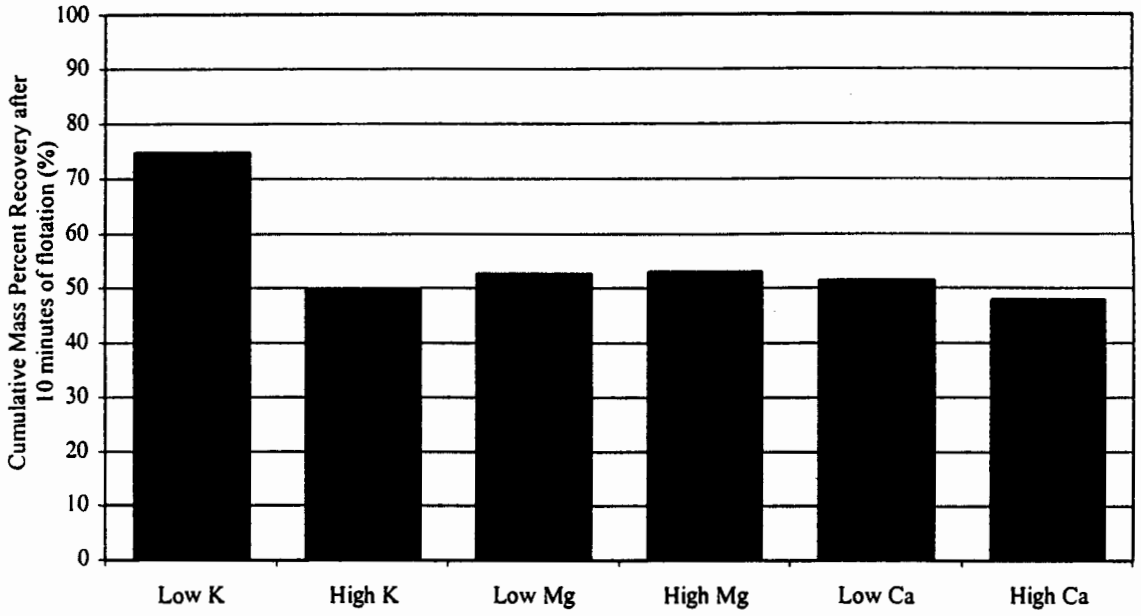

Figure 20: The cumulative mass percent recovery of talc after 10 minutes under various ionic conditions with no depressants added

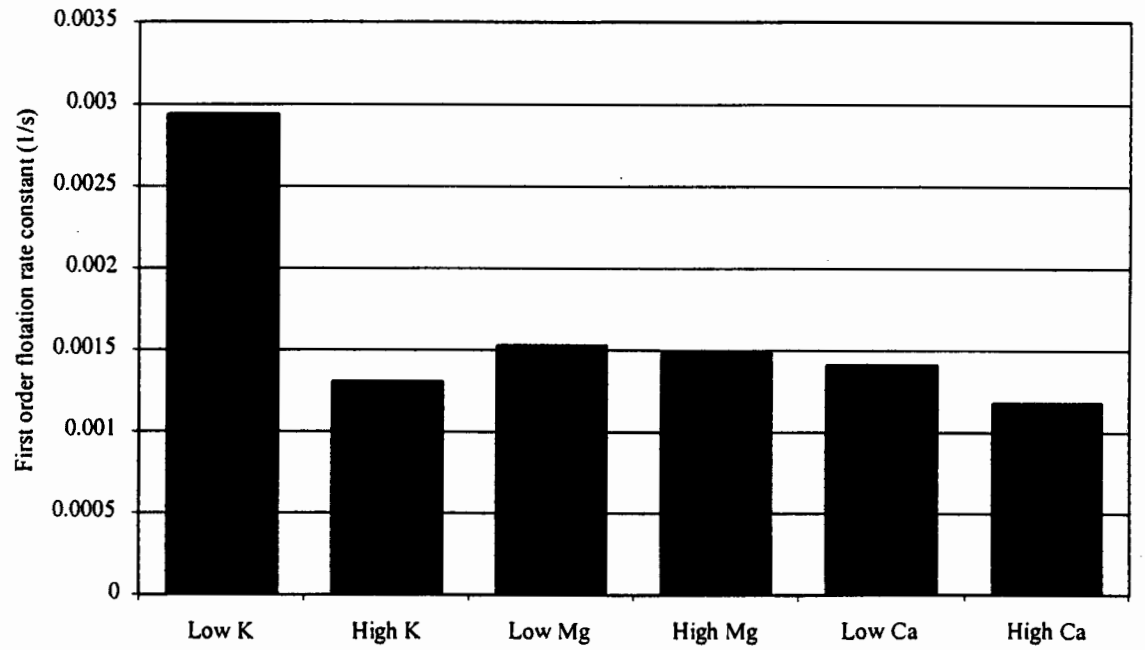

Figure 21: The first order flotation rate constant of talc under various ionic conditions with no depressants added

It can be seen that increasing the ionic strength from 10^{-3} to 10^{-2} using the monovalent cation, potassium, led to a reduction in the cumulative mass percent recovery of talc after 10 minutes and a reduction in the flotation rate. At an ionic strength of 10^{-3}, when the ion type used to modify the ionic strength was changed from the monovalent cation potassium to the divalent cation magnesium or calcium, the cumulative mass percent recovery of talc at 10 minutes and the flotation rate were reduced. At an ionic strength of 10^{-2}, no further reduction in the cumulative mass percent recovery of talc at 10 minutes and the flotation rate was obtained when the ion type used to modify the ionic strength was changed from the monovalent cation potassium to the divalent cation magnesium or calcium.

The fact that increasing the ionic strength from 10^{-3} to 10^{-2} using KNO_3 caused a drop in natural talc flotation indicates that an interaction occurs between K^+ ions and the talc surface. It is known that the talc has a highly negative zeta potential at a pH of 9 (Morris, 1996; Steenberg, 1982; Dalvie, 2001), which is attributed to the water layer surrounding the planes of the talc. It is possible that the K^+ ions adsorb onto the talc planar surface, thus reducing the surface hydrophobicity.

The addition of the divalent ions Mg^{2+} and Ca^{2+} caused a stronger depression of the talc at an ionic strength of 10^{-3} than the monovalent cation K^+. This indicates that a greater degree of adsorption of the divalent ions onto the talc surface occurs.

The program MINTEQA2 was used to investigate the speciation of magnesium nitrate and calcium nitrate in solution as a function of pH. The results of this are shown in Figure 23 and Figure 24. At a pH of 9, the predominant form of the magnesium and calcium ions

in solution is Mg^{2+} and Ca^{2+} respectively, with less than 1 % of these species being in the form $MgOH^{+}$ and $CaOH^{+}$.

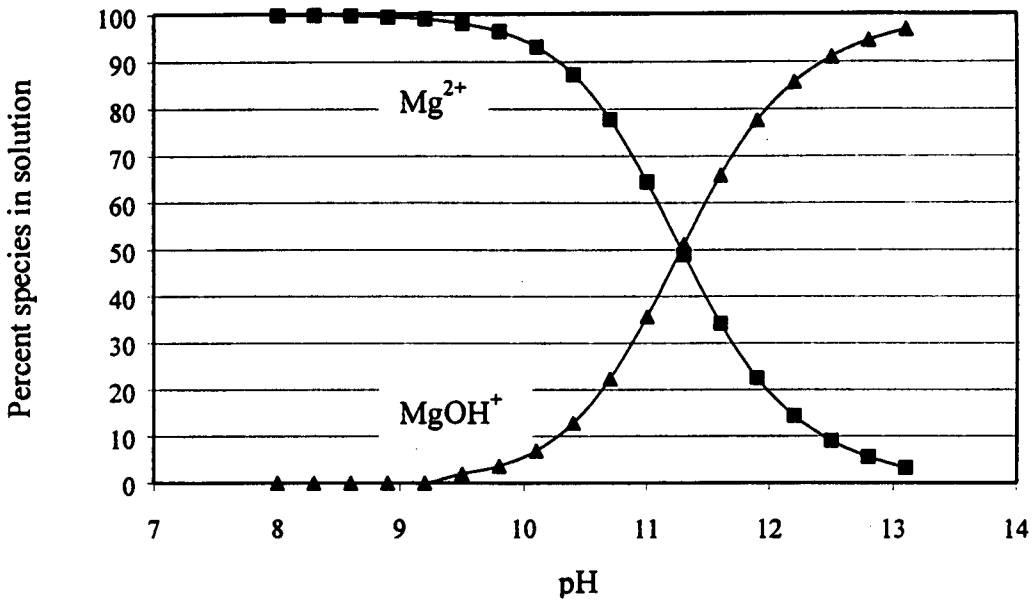

Figure 22: The percent of magnesium of the salt $Mg(NO_3)_2$ present in Mg^{2+} (solid squares) and $MgOH^{+}$ (solid triangles) at various pH values

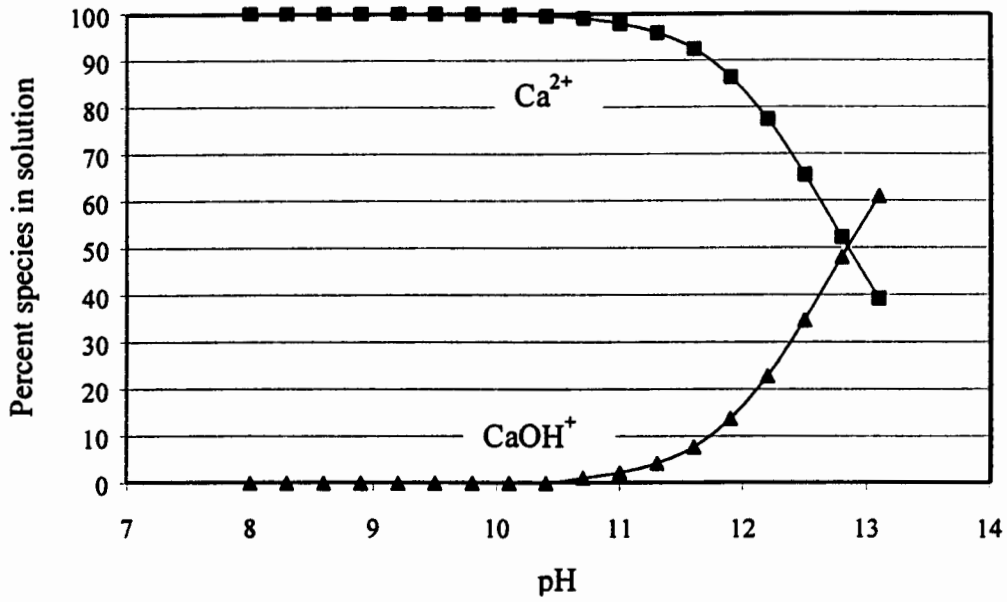

Figure 23: The percent of calcium of the salt $Ca(NO_3)_2$ present in Ca^{2+} (solid squares) and $CaOH^{+}$ (solid triangles) at various pH values

Figure 24 shows the log of the molal concentrations of the ions Mg^{2+} and $MgOH^{+}$ compared to that of Ca^{2+} and $CaOH^{+}$ at various pH values. This diagram shows that at a pH of 9, the concentrations of the $MgOH^{+}$ and $CaOH^{+}$ species is very small compared to the concentrations of Mg^{2+} and Ca^{2+}. It is therefore unlikely that these hydrated monovalent ions play any significant role in adsorption at the talc surface at the pH values used in this work.

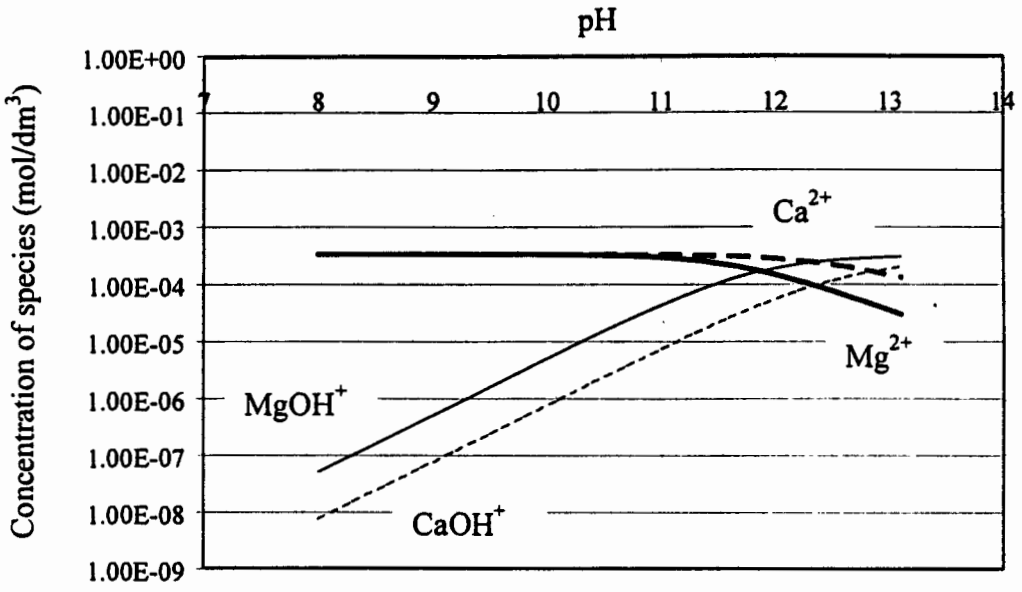

Figure 24: The molal concentrations of Mg^{2+} (solid thick line) and $MgOH^{+}$ (solid thin line), when the salt $Mg(NO_3)_2$ is placed in solutions of various pH values, compared with the molal concentrations of Ca^{2+} (dashed thick line) and $CaOH^{+}$ (dashed thin line) when the salt $Ca(NO_3)_2$ is placed in solutions of various pH values

Increasing the concentration of magnesium and calcium ions in solution tenfold did not result in a significant reduction in the natural floatability of the talc. It is possible that a sufficient adsorption of these ions on the talc surface is already obtained at the lower concentration and increasing the ions in the system does not therefore result in further adsorption. It is recommended that in further studies, the adsorption of K^{+} should be confirmed.

5.2.3.3 Influence of ions on the effectiveness of the CMC depressants

Figure 26 shows the change in talc recovery with FF30 added after 10 minutes of flotation under differing ionic conditions. Figure 27 shows the first order rate constant for talc flotation with FF30 added under differing ionic conditions.

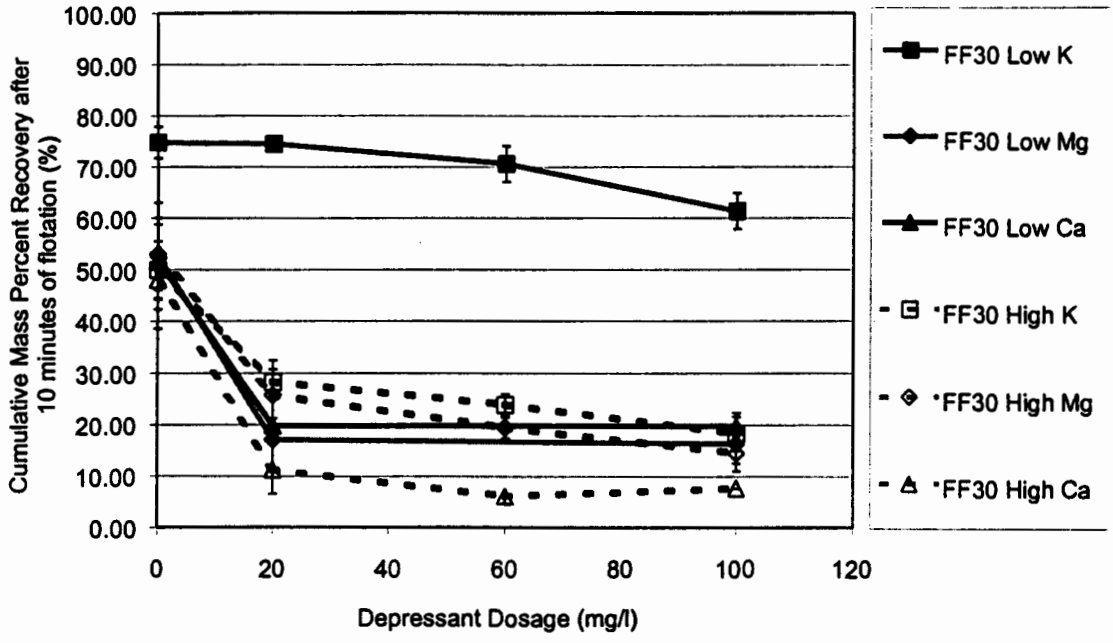

Figure 25: The flotation of talc after ten minutes using FF30 for various ionic strengths and ion types

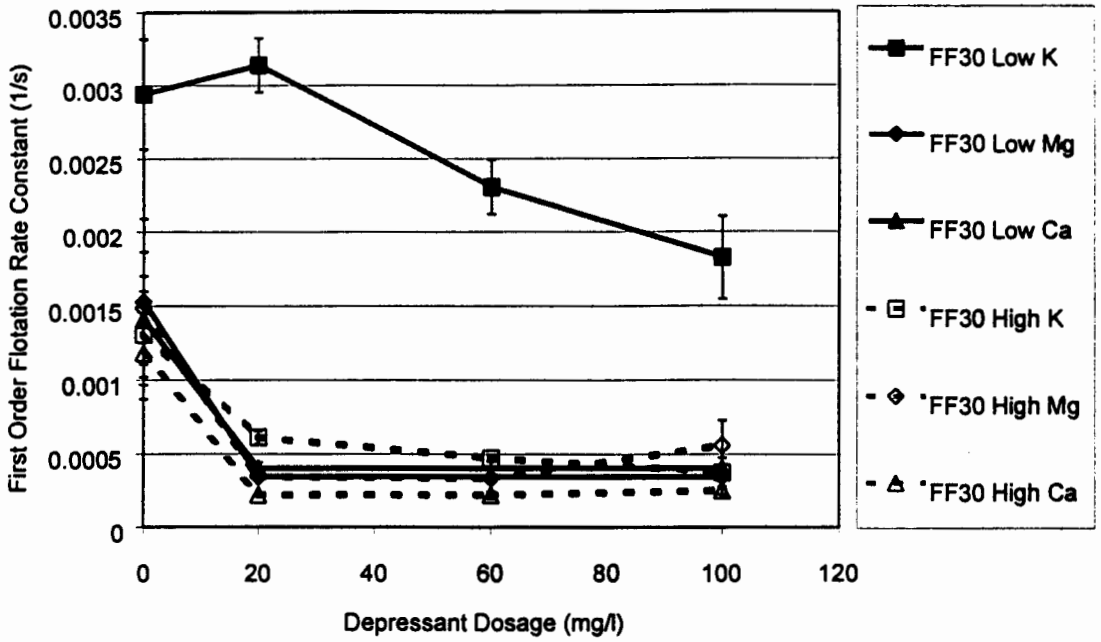

Figure 26: The first order flotation rate constant of talc using FF30 for various ionic strengths and ion types

Increasing the ionic strength from 10^{-3} to 10^{-2} using the monovalent cation potassium and the depressant FF30 resulted in a large reduction of the recovery after 10 minutes (R_{10min}) and the first order flotation rate constant (k) for all dosages of CMCs studied.

At the same ionic strength of 10^{-3}, a large reduction in R_{10min} and k was seen when the ion used to modify the ionic strength was changed from the monovalent cation, potassium to the divalent cation magnesium or calcium. At an ionic strength of 10^{-2}, R_{10min} and k were decreased when the ion used was changed from potassium to calcium.

Increasing the ionic strength from 10^{-3} to 10^{-2} using the divalent cation magnesium did not cause any noticeable change in the R_{10min} and k for talc over the dosage range investigated.

Changing the ionic strength from 10^{-3} to 10^{-2} using the divalent cation calcium resulted in a drop in R_{10min} and k over the dosage range studied.

Figure 28 shows the change in talc flotation with FF300 added after 10 minutes under differing ionic conditions. Figure 29 shows the first order rate constant for natural talc flotation with FF300 added under differing ionic conditions.

R_{10min} and k for talc were reduced over the entire dosage range of FF300 additions when the ionic strength was increased from 10^{-3} to 10^{-2} using the monovalent cation potassium. At the ionic strength of 10^{-2}, R_{10min} and k were reduced when the ion used was changed from potassium to magnesium and further reduced when the ion was changed from magnesium to calcium.

At a pH of 9, talc is known to exhibit a strongly negative zeta potential (Steenberg, 1982, Morris, 1996, Dalvie, 2001). The increase in depressant efficiency observed when the concentration of K^+ ions in solution was increased, could indicate that the adsorption of these ions reduce the negative charge of the talc particles, thereby reducing the electrostatic repulsion with the negatively charged CMC depressants. The effect of ionic strength on conformation of the CMC has already been demonstrated from viscosity measurements. It is probable that similar phenomena occur at the talc surface and thus influence the microflotation response. However, these mechanisms have not been confirmed, the observed effects could be due to a change in surface or solution properties or both.

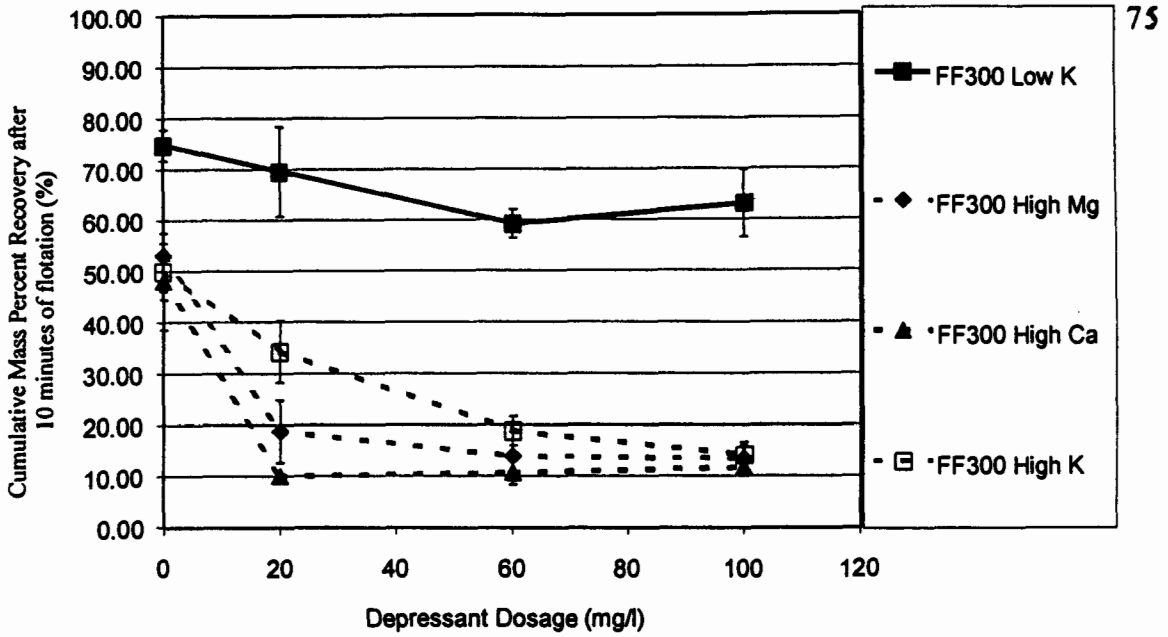

Figure 27: The flotation of talc after ten minutes using FF300 for various ionic strengths and ion types

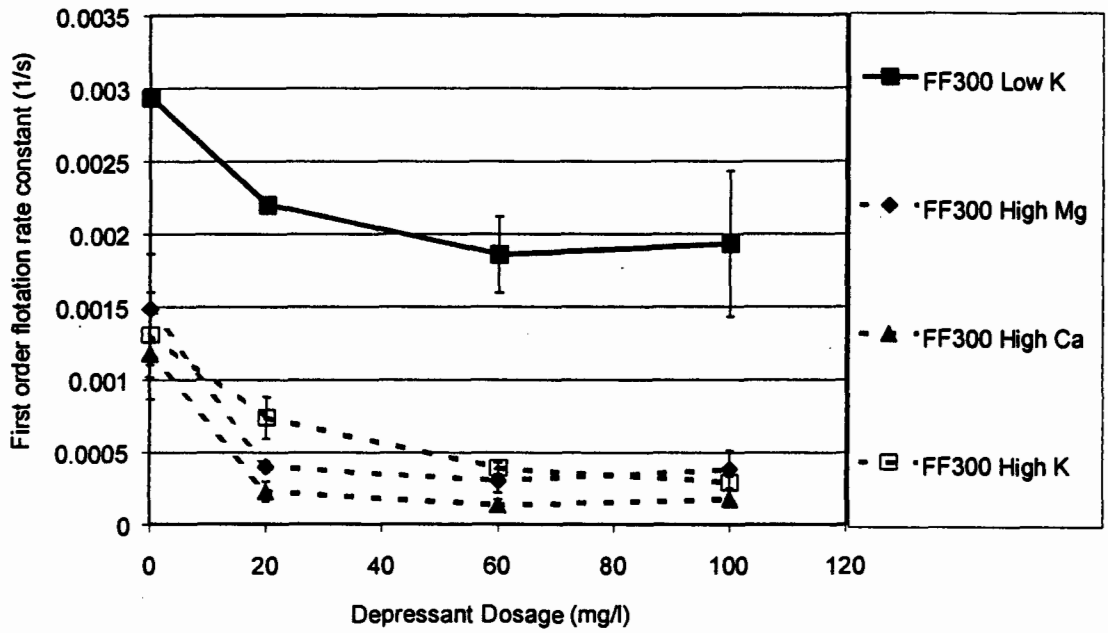

Figure 28: The first order flotation rate constant of talc using FF300 for various ionic strengths and ion types

The divalent cations, magnesium and calcium, were seen to be more effective in improving depressant performance than the potassium ions. This could be due to the

higher concentration of these ions at the talc surface or a stronger adsorption of these ions on the talc surface (as was seen in the greater reduction in natural floatability of the talc with the divalent cations as compared to the monovalent cation at the higher concentration).

The reductions in R_{10min} and k for all of these cases, except at a low ionic strength using potassium, were most marked at the lower dosage (20mg/l) of FF30 and FF300, with the curve flattening off at higher dosages (60mg/l and 100mg/l). This suggests that sufficient coverage has already occurred at the lowest dosage, after which CMC molecules are kept away from the surface by steric or electrostatic hindrances. At the higher ionic strength the amount of depressant adsorbing onto the surface may be larger due to the tighter coiling caused by these conditions as well as a reduction in surface charge along the CMC molecules.

It was observed that the presence of calcium ions reduced the flotation of talc with CMC depressants to a greater extent than magnesium ions. This could indicate that greater or stronger adsorption of calcium ions occurs on the talc surface compared to the adsorption of magnesium ions on the talc surface. It is recommended that the adsorption or complexation of Mg^{2+} and Ca^{2+} with CMC carboxylate groups be considered in further studies in this field as this may explain why calcium has a greater effect.

Although viscometry tests showed that the molecular weight of FF300 is significantly higher than that of FF30, no significant distinctions in the flotation performance of talc were seen between the tests using FF30 and FF300 under the conditions investigated.

However, the rate constants observed for the flotation of talc with FF300 were in all cases lower than the rate constants obtained for FF30.

5.2.3.4 Influence of ions on the effectiveness of a modified guar depressant (IMP4)

Due to the significant depression observed at 10^{-3} M KNO_3 for IMP4, only this and the ionic strength of 10^{-2} using magnesium as the ionic strength modifier condition were investigated.

Figure 29 shows the change in talc flotation recovery after ten minutes (R_{10min}) when IMP4 was used as the depressant under different ionic conditions. Figure 30 shows the first order rate constant for natural talc flotation with IMP4 added under differing ionic conditions.

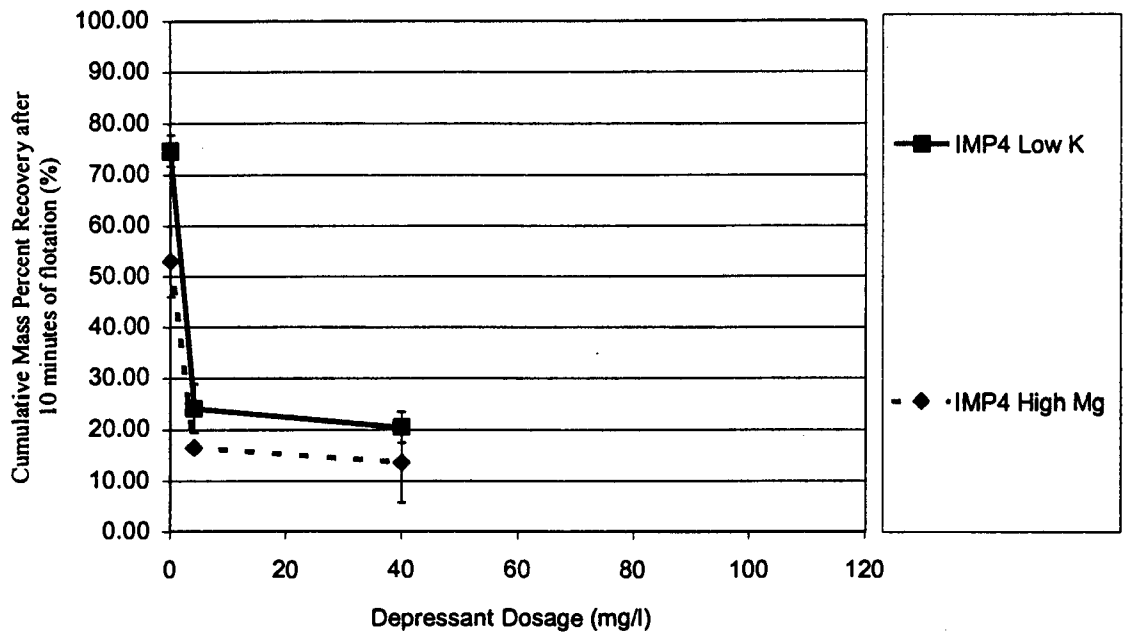

Figure 29: The flotation of talc after ten minutes using IMP4 for various ionic strengths and ion types

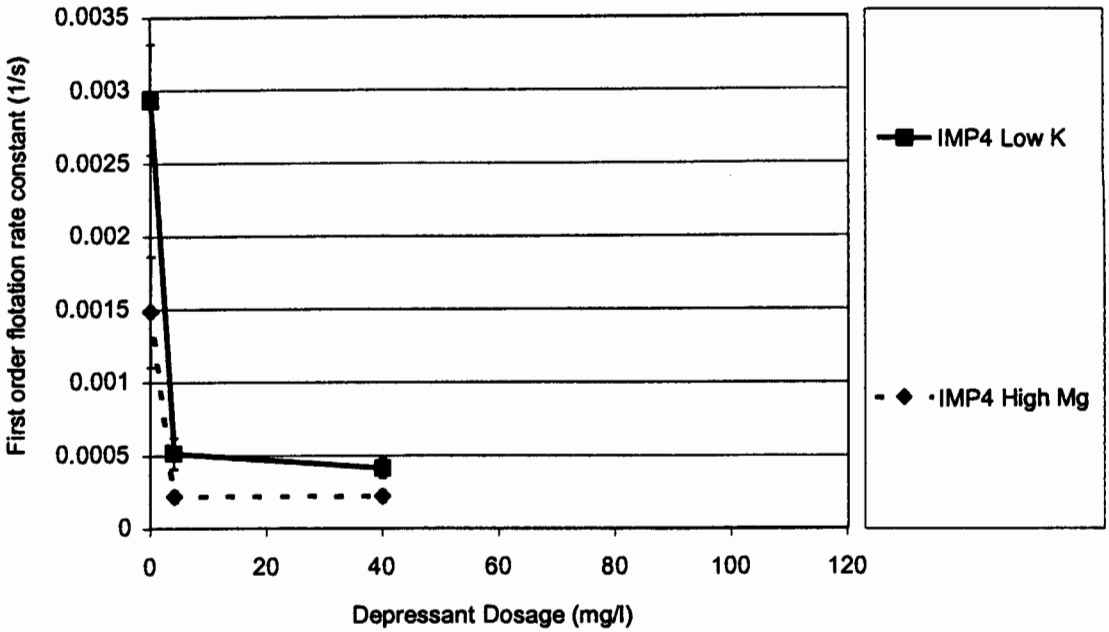

Figure 30: The first order flotation rate constant of talc using IMP4 for various ionic strengths and ion types

It was found that changing the ionic strength from 10^{-3} using potassium to 10^{-2} using magnesium resulted in a decrease in both R_{10min} and k for talc over the whole range of dosages studied using IMP4 as a depressant. However, the flotation of talc in the absence of any depressants was also reduced at the higher ionic strength and therefore it is likely that the lower flotation observed is due to this natural reduction and not improved guar depression due to the ions present. However, interactions between guar depressants and divalent cations such as magnesium cannot be neglected at this stage.

Guar depressants have a low charge and therefore, changes in the zeta potential of the talc are unlikely to affect the guar adsorption characteristics onto talc as strongly as they affect the adsorption obtained with the highly charged CMCs.

5.2.4 Key findings from microflotation tests

The following key findings were drawn from the microflotation test work.

1. The technique used in the microflotation tests needs to ensure an environment of constant equilibrium depressant concentration as the adsorption of the depressant appears reversible.

2. At low ionic strength (10^{-3} KNO_3) in a microflotation system, guars were much more effective depressants of talc than the CMC samples tested.

3. At low ionic strength (10^{-3} KNO_3) in a microflotation system, at a low dosage, increasing the molecular weight of the guar depressants (SM4060, IMP4 and SM4560) led to an enhanced overall depression of talc in the system. However, as the dosage was increased, the effect of the molecular weight of the guars on talc depression was diminished.

4. At low ionic strength (10^{-3} KNO_3) in a microflotation system, the CMC's (FF10, FF30, FF150 and FF300) showed no change in talc depression as the molecular weight of the system was increased.

5. At low ionic strength (10^{-3} KNO_3) in a microflotation system, at a very low dosage, the CMC depressants enhanced talc flotation - possibly due to a surface cleaning effect.

6. Speciation diagrams of magnesium and calcium showed that at pH = 9, these ions are predominantly in the form Mg^{2+} and Ca^{2+}.

7. Increasing the ionic strength from 10^{-3} to 10^{-2} using the monovalent cation potassium resulted in a reduction in the natural floatability of talc. It is postulated that the K^+ ions adsorb onto the talc surface and reduce its hydrophobicity. It is recommended that in further studies, the adsorption of K^+ should be confirmed.

8. The divalent cations, magnesium and calcium, caused a greater reduction in the natural flotation of talc than the monovalent cation potassium. This indicates that a greater degree of adsorption of these cations onto talc takes place.

9. Increasing the ionic strength from 10^{-3} to 10^{-2} using potassium caused an increase in the depressing behaviour of both CMC depressants (FF30 and FF300). This increase in depression was attributed to the adsorption of the K^+ ions causing a reduction in the zeta potential of the talc thus reducing the electrostatic repulsion between the talc surface and CMC molecules and resulting in an increase in CMC adsorption onto the talc.

10. At an ionic strength of 10^{-3}, changing the ionic strength modifier from the monovalent ion potassium to the divalent ion, calcium or magnesium, resulted in an increase in the efficiency of CMC depressants. This was attributed to the greater adsorption of the divalent cations on the talc surface as well as possible linkages formed between the talc surface and CMC molecules through these ions and a reduction in electrostatic repulsion between CMC molecules through the ions reducing the charge along these molecules.

11. Calcium ions reduced the flotation of talc with CMC depressants to a greater extent than magnesium ions indicating that greater or stronger adsorption of calcium ions

occurs on the talc surface compared to the adsorption of magnesium ions on the talc surface. It is recommended that IR spectroscopy studies be used in further studies to confirm the adsorption or complexation of Mg^{2+} and Ca^{2+} with CMC carboxylate groups.

12. In cases where the depression of talc was obtained with the CMCs, sufficient coverage of the talc surface seems to occur at low dosages, above which increasing the dosage of the CMC did not significantly reduce talc flotation recovery.

13. No significant differences were observed between the performance obtained with the FF30 and the FF300, although a reduction in the talc first order flotation rate constants was observed when FF300 was used as opposed to FF30.

14. The guar studied (IMP4) showed an increase in talc depression when the ionic strength was increased from 10^{-3} using potassium to 10^{-2} using magnesium but this increase was less than the reduction in natural talc floatability observed when these ions alone were used. This suggests that the guar performance was not affected by the ions in solution.

5.3 Batch Flotation tests

These batch flotation tests were done to support the microflotation results as a preliminary investigation so singular tests were conducted to determine the effect of depressant molecular weight and dosage on performance.

5.3.1 Reproducibility

The repeatability of the batch flotation tests was tested by comparing them with the results of a parallel investigation using a similar ore (Bacus, 2000). Overall, the common results for copper and nickel percent grade and percent recovery were within 2 standard deviations of each other and the results are therefore considered repeatable to within a 95% degree of significance.

5.3.2 CMC depressant results

To compare the performance of the different depressants at a fixed dosage when variable mass pulls and water recoveries are obtained, the cumulative mass and water relationship is examined. Since, in these tests, the concentrate consists mainly of gangue, the mass of solids recovered as a function of the water recovered gives an indication of the effectiveness of the reagent as a gangue depressant. However, such an analysis does not show how the depressant affects the recovery of valuable minerals. This can only be established from the grade-recovery curves and the kinetics of flotation of the valuable minerals (in this case, nickel and copper sulphides).

Figure 31 shows the cumulative mass percent recovery of ore with time, Figure 32 shows the cumulative water recovery with time and Figure 33 shows the cumulative mass

recovery to cumulative water recovery for the PGM ore with the addition of CMC depressants of varying molecular weight, at two different dosages (40mg/l and 100mg/l).

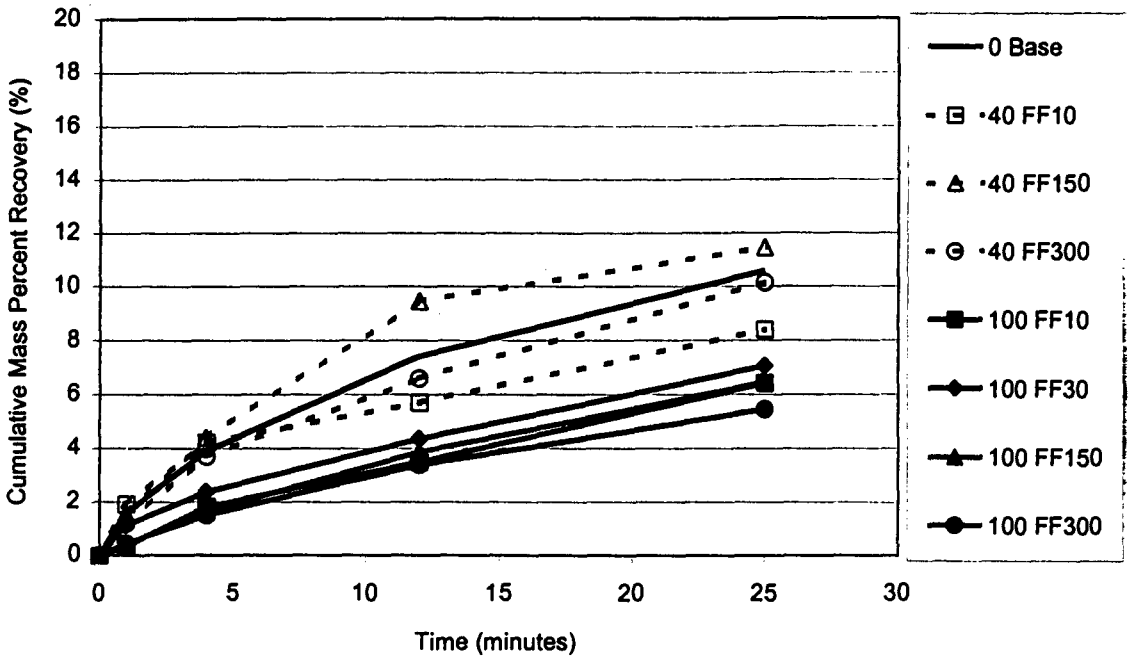

Figure 31: Cumulative mass percent recovery of PGM ore with time for CMC depressants of varying molecular weight at two dosages (40 mg/l and 100 mg/l)

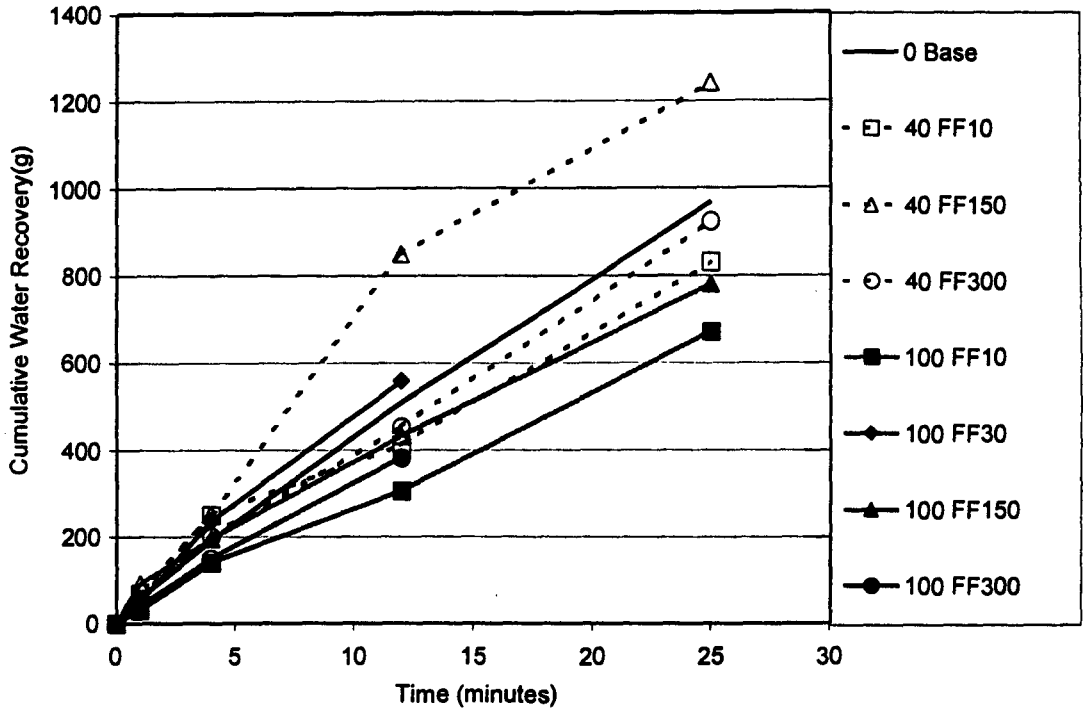

Figure 32: Cumulative water recovery of PGM ore with time for CMC depressants of varying molecular weight at two dosages (40 mg/l and 100 mg/l)

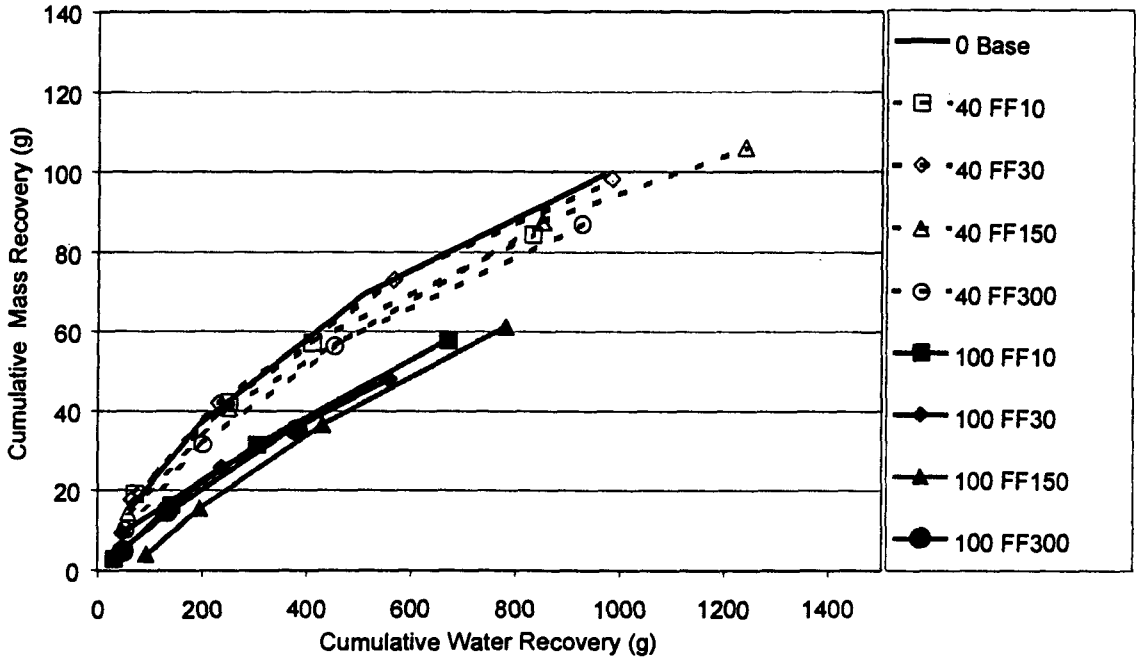

Figure 33: Cumulative mass recovery vs cumulative water recovery of PGM ore for CMC depressants of varying molecular weight at two dosages (40 mg/l and 100 mg/l)

It can be seen from Figure 34 that there does not seem to be a marked difference in the mass – water relationship of the ore as the molecular weight of the CMC depressant was varied from FF10 (the smallest depressant - M_w = 164,100) to FF300 (the largest depressant - M_w = 411,400).

However, an increase in dosage from 40 mg/l to 100 mg/l for all the CMC depressants led to a reduced amount of ore floated with time. The slope of the mass – water curve in Figure 34 was lower, indicating that the amount of water relative to the mass in the concentrate was higher.

Figure 32 and Figure 33 also show that the total amount of water that was recovered was lower when the CMC dosage was increased. This indicates a reduction of froth stability. Nickel and copper assays were performed on the concentrates in order to ascertain whether the drop in mass pull was for all minerals or whether it was due to the selective depression of the gangue. Figure 34 and Figure 35 show the resultant grade - recovery curves for the nickel and copper in the system as the depressant addition was changed.

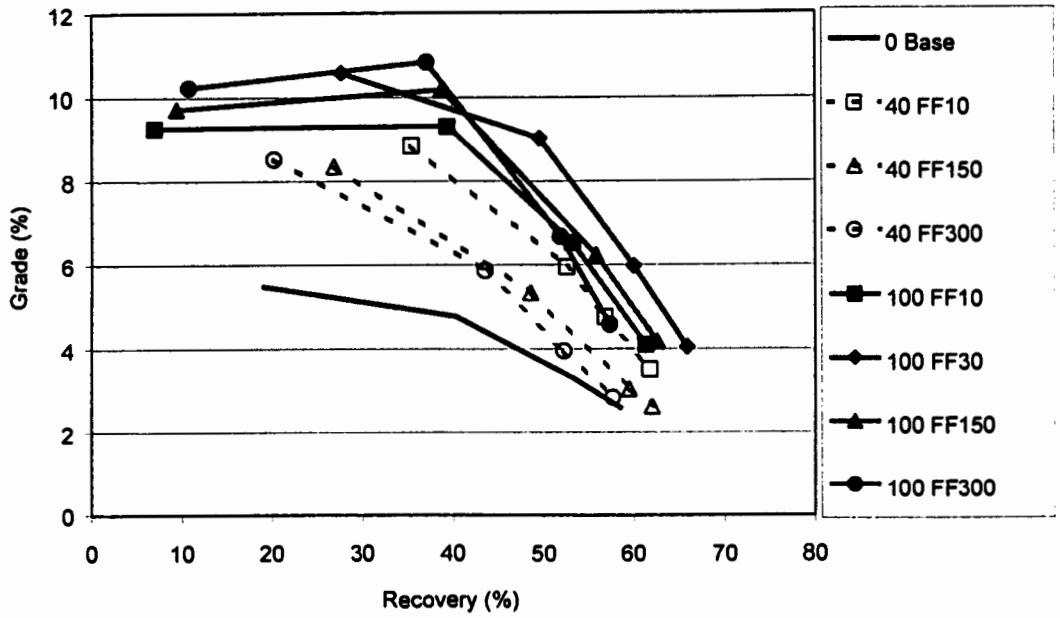

Figure 34: Nickel grade versus nickel recovery for PGM ore with the addition of CMC depressants of varying molecular weight at two dosages (40 mg/l and 100 mg/l) (Note, the 40 mg/l FF30 could not be included due to missing assay data)

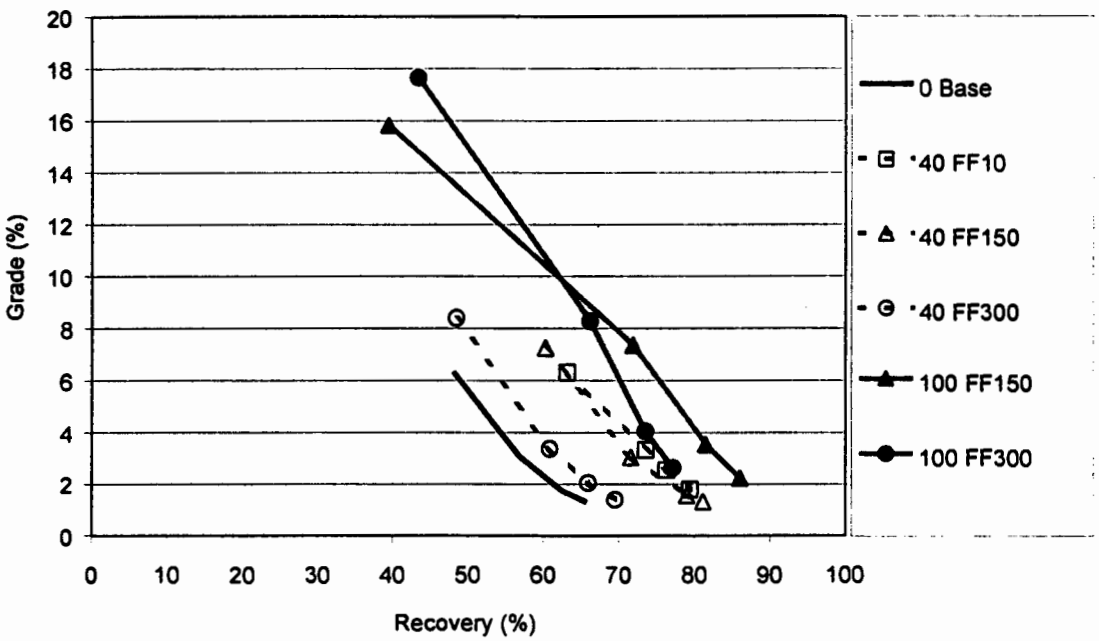

Figure 35: Copper grade versus copper recovery for PGM ore with the addition of CMC depressants of varying molecular weight at two dosages (40 mg/l and 100 mg/l) (Note, the FF30 and 100 mg/l FF10 curves could not be included due to lost assay data)

Figure 34 and Figure 35 show that the reduction in the overall mass flotation is due to the depression of gangue in the system as the grade of the nickel and the grade and recovery of the copper were enhanced upon the addition of depressant.

At the lower dosage (40 mg/l) not much change in the overall mass and water recovery was seen compared to the float where no depressant was added at all, yet the nickel grade was improved. Figure 34 shows that the same amount of nickel was recovered but because less gangue was floated, the overall nickel grade of the concentrate was higher.

The overall recovery and grade of the copper was improved with the addition of depressant. The overall mass flotation remained fairly constant irrespective of CMC depressant molecular weight, but dependent on depressant dosage. The low dosage of depressant increased copper recovery and suggests that the CMC performed a cleaning function on the surface of the copper and nickel sulphides within the ore body as well as depressing the gangue. Work done by Dalvie (2001) with the same ore as was used in these tests showed that the dispersion of gangue was increased when a CMC depressant was added. In particular, he showed that the addition of FF30 to talc increased the dispersion characteristics of the system at a dosage of 50 mg/l FF30 and further increased the dispersion characteristics of the system at a dosage of 100 mg/l FF30.

The higher dosage (100 mg/l) of depressant led to a clear increase in the nickel grade of the concentrate. This indicates that the dosage of the depressant has a marked influence on the amount of gangue that is depressed.

The nickel grade-recovery curves showed that at low depressant dosages (40 mg/l) the smaller depressant had the best grade-recovery relationship. This suggests that at low

concentrations, the depressant with a smaller molecular mass could have a higher slime cleaning action. At higher dosages (100 mg/l) this trend was no longer apparent.

5.3.3 Guar depressant results

Figure 36 shows the cumulative mass percent recovery of ore with time, Figure 37 shows the cumulative water recovery with time and Figure 38 shows the cumulative mass recovery to cumulative water recovery for the PGM ore with the addition of guar depressants of varying molecular weight, at two different dosages (40mg/l and 100mg/l). Figure 39 and Figure 40 show the grade - recovery curves for the nickel and copper in the system as the depressant addition was changed.

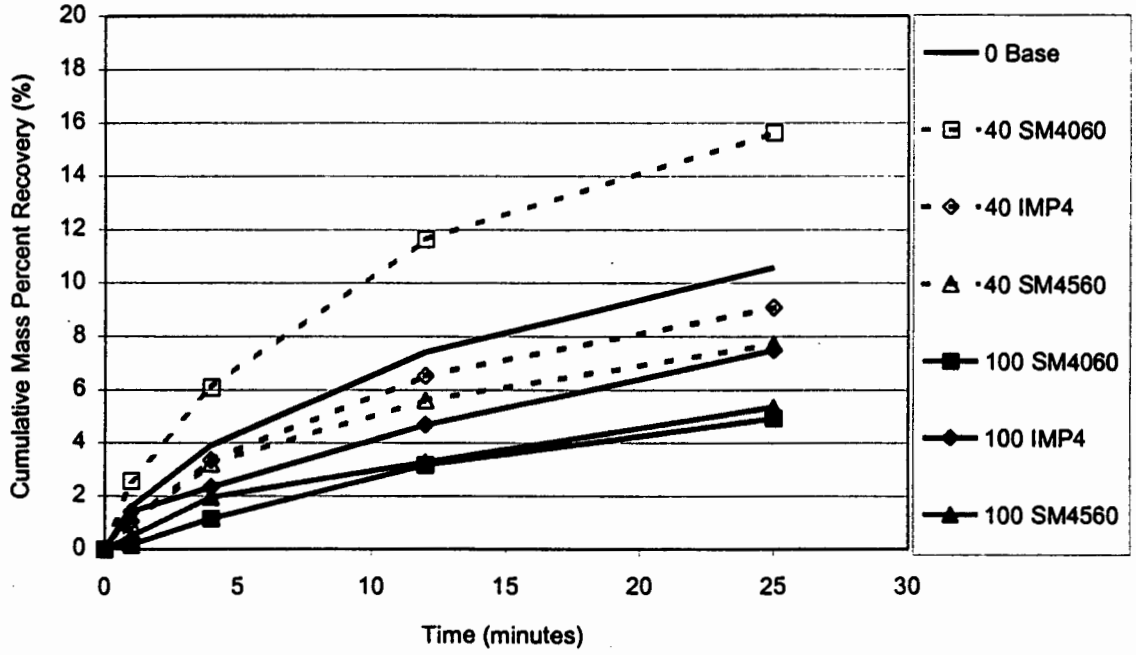

Figure 36: Cumulative mass percent recovery of PGM ore with time for guar depressants of varying molecular weight at two dosages (40 mg/l and 100 mg/l)

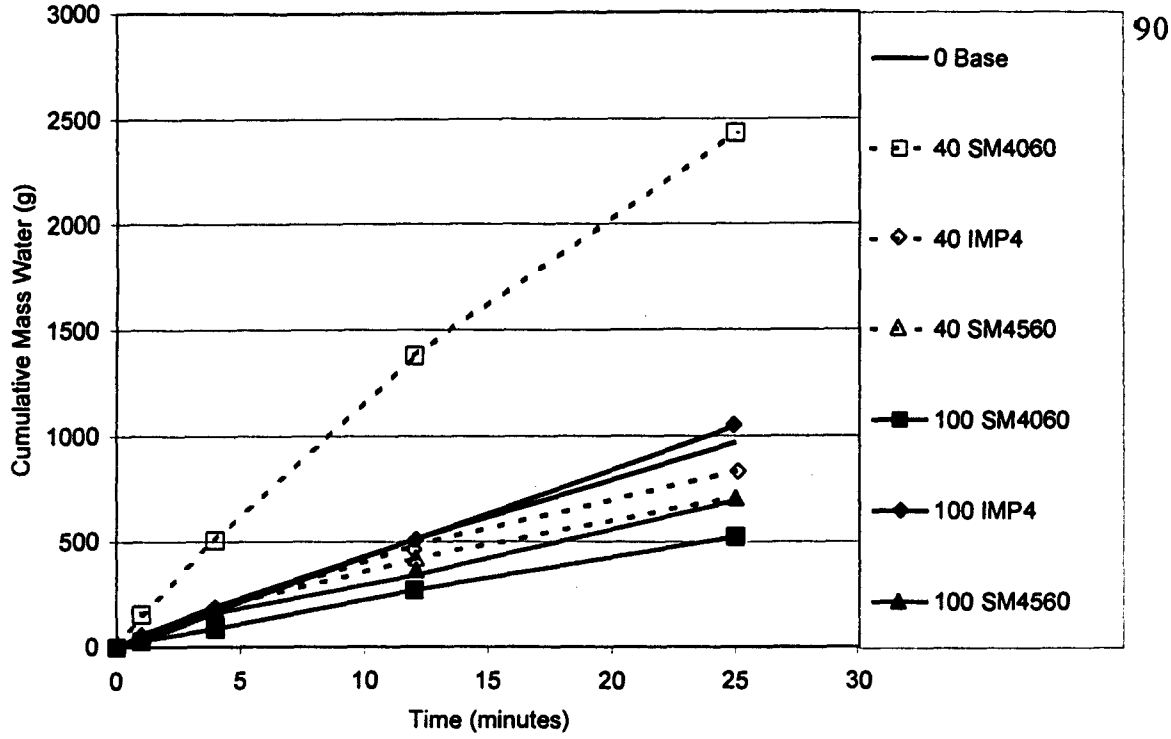

Figure 37: Cumulative water recovery of PGM ore with time for guar depressants of varying molecular weight at two dosages (40 mg/l and 100 mg/l)

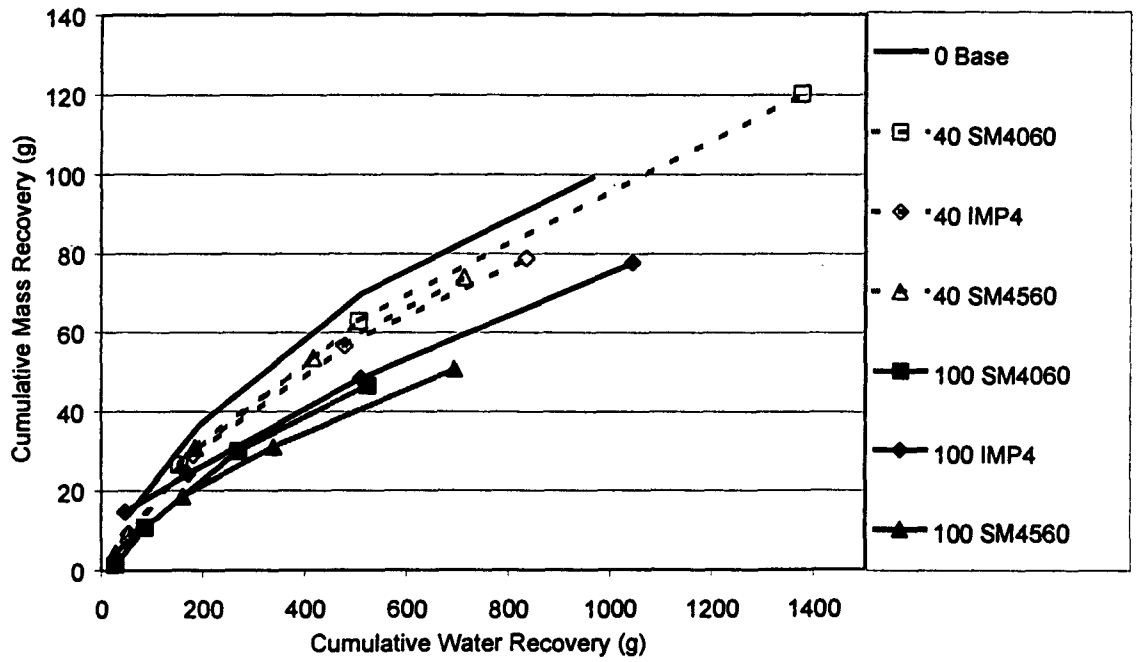

Figure 38: Cumulative mass recovery vs cumulative water recovery of PGM ore for guar depressants of varying molecular weight at two dosages (40 mg/l and 100 mg/l)

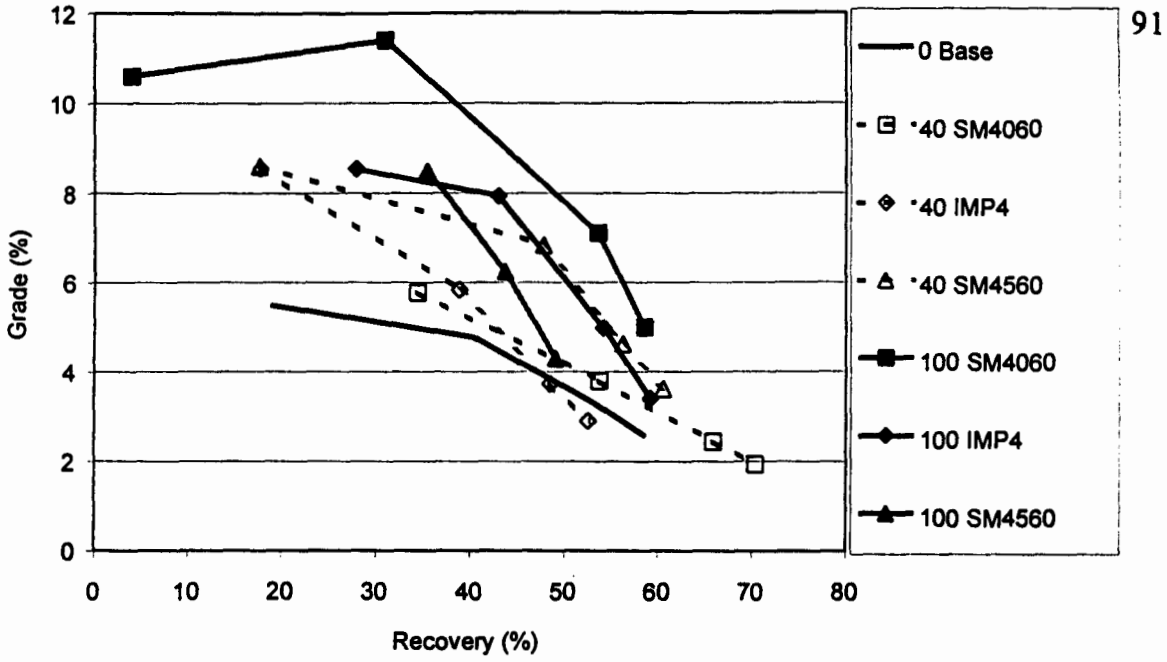

Figure 39: Nickel grade versus nickel recovery for PGM ore with the addition of guar depressants of varying molecular weight at two dosages (40 mg/l and 100 mg/l)

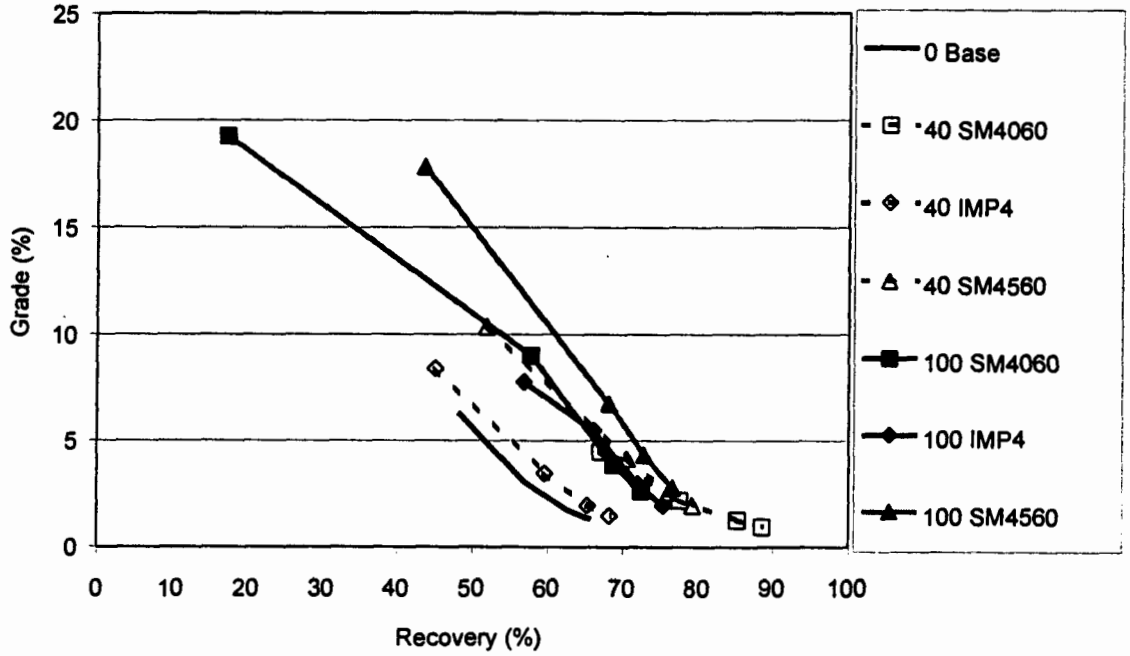

Figure 40: Copper grade versus copper recovery for PGM ore with the addition of guar depressants of varying molecular weight at two dosages (40 mg/l and 100 mg/l)

It appears that at low dosages of depressant (40 mg/l) that the mass recovery with time is affected by the size of the depressant used. Figure 36 and Figure 37 show that the

smallest depressant (SM4060 - M_w = 67,920) results in a larger mass and water recoveries than the larger depressant (IMP4 - M_w = 180,700) which in turn has a higher mass and water pulls with time than the largest guar depressant used in these tests (SM4560 - M_w = 290,800). At the higher dosage (100 mg/l), this trend is no longer apparent.

The increase in the overall mass flotation by the smallest guar, SM4060, was accompanied by an increase in the overall recovery of both nickel and copper minerals in the concentrate. The marked increase in water recovery associated with this float indicates that the increase in mass recovery is likely due to increased froth stability. Overall, the grade of the nickel and the copper was not changed with the addition of this reagent, suggesting only weak depression at a dosage of 40mg/l SM4060.

At the low dosage (40 mg/l) of the IMP4, the grade recovery curve for both the nickel and the copper did not appear to be improved.

At the low dosage (40 mg/l) of the SM4560, the nickel grade of the concentrate was markedly improved, although it did not appear that the overall nickel recovery was greatly changed. This indicated that the largest guar at this low dosage is performing a gangue depression role - thereby enhancing the concentrate nickel grade without increasing the overall mass floated. However, the overall recovery of the copper sulphides was also increased at the low dosage of SM4560, indicating that it could also be performing a cleaning role on the sulphide surfaces.

At the higher dosage, the IMP4 depressant improves the grade of the nickel concentrate - indicating that it selectively depresses the gangue and not the nickel. It also improves the

overall recovery of the copper indicating that it plays a role in cleaning the surface of the copper, thereby improving its overall recovery.

At the higher dosage, the largest depressant (SM4560) exhibited reduced overall mass and water recoveries similar to those exhibited at the lower dosage. Its overall copper grade and recovery remains the same indicating that it continues to perform a cleaning function on the copper sulphides in the ore. The nickel grade remains approximately the same as it was at the lower dosage but the overall nickel recovery is reduced. This suggests that at the higher dosage, the largest guar depressant is depressing the nickel sulphides in the pulp.

5.3.4 Comparing CMC and guar depression

Figure 41 shows the mass recovery versus water recovery for the system at two different dosages, with the CMCs and guars placed on the same set of axes.

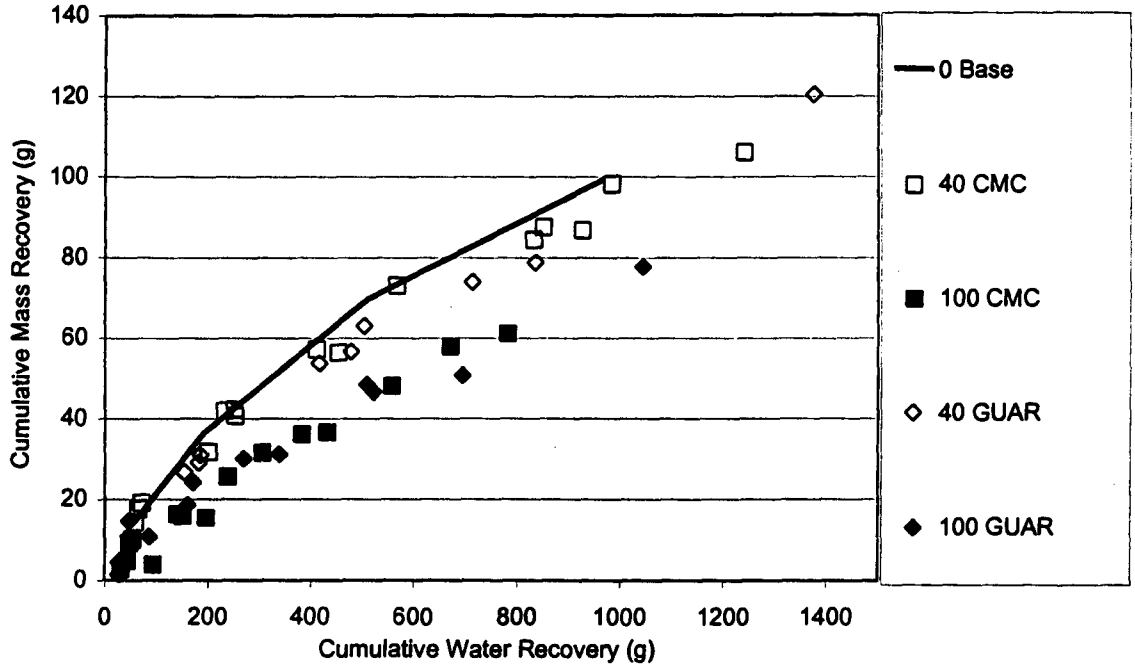

Figure 41: Cumulative mass recovery vs cumulative water recovery for CMC's and guars at two dosages (40 mg/l and 100 mg/l)

Figure 41 shows that the effect of dosage is stronger than the effect of depressant type with regard to the mass-water recovery ratio. Figure 33 and Figure 34 show the grade-recovery curves for nickel and copper respectively at two different dosages with both CMCs and guars on the same set of axes.

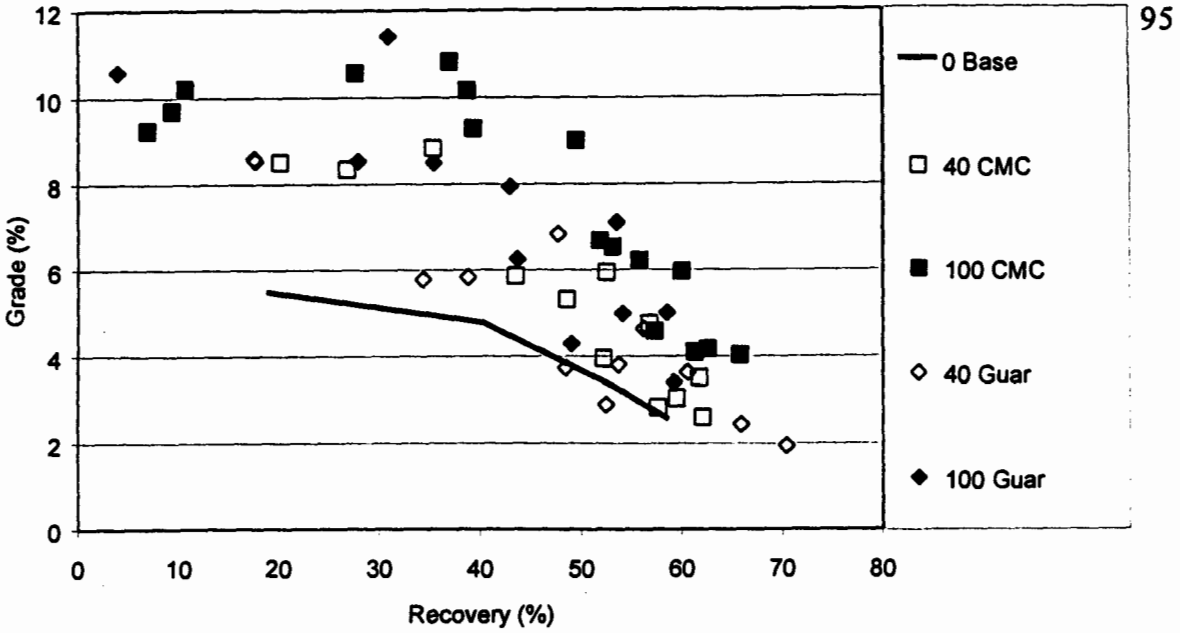

Figure 42: Nickel grade - recovery of pgm ore for CMCs and guars at two different dosages (40 mg/l and 100 mg/l)

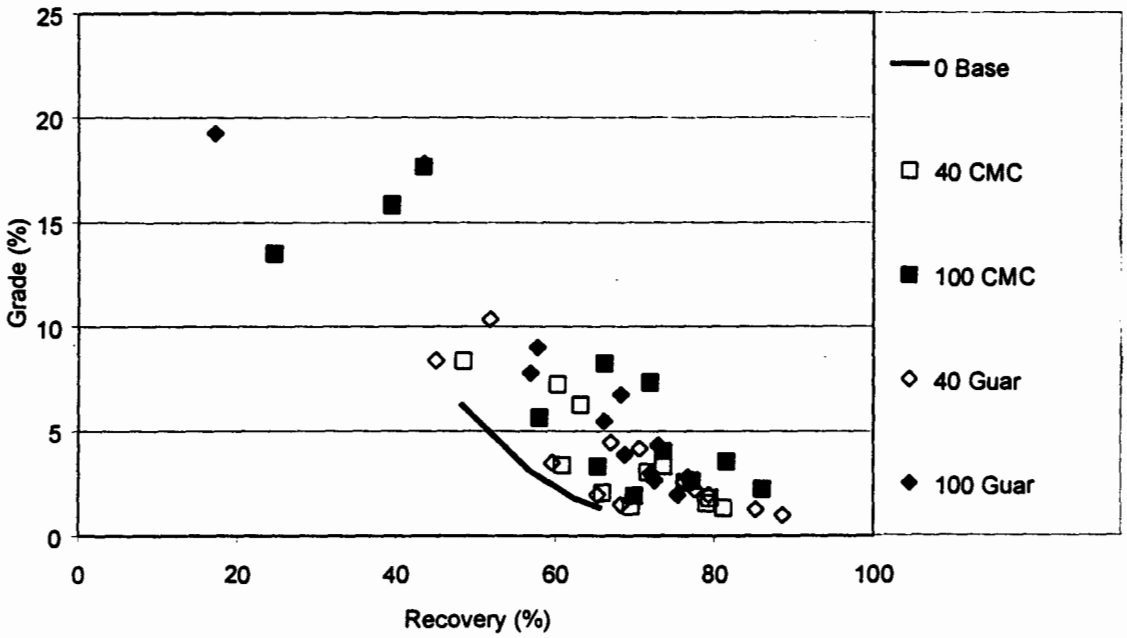

Figure 43: Copper grade - recovery of pgm ore for CMCs and guars at two different dosages (40 mg/l and 100 mg/l)

Overall, no marked differences between the performance of the CMC as opposed to the guar depressants that were chosen for this study are apparent. One could suggest that the guar line in Figure 41 for both dosages lies slightly below the CMC curves for the corresponding dosages. However, as previously mentioned, these tests were a preliminary study and further investigation would be required should one wish to firmly establish the existence of such differences.

5.3.5 Key findings from batch flotation tests

The following key findings were drawn from the batch flotation testwork

1. No clear differences in flotation performance of a PGM ore were noted when CMC's were used as depressants as opposed to guars.

2. The dosage of the depressant appears to be an important factor in determining performance of the depressant. A higher dosage leads to a lower mass – water ratio as well as reduced overall water and mass recoveries – indicating changed froth characteristics. It also leads to increased copper recoveries and increased nickel grades.

3. The largest guar depressant (SM4560) appeared to depress the nickel sulphide mineral at high dosages. This could suggest that for optimum performance, smaller guars at higher dosages would be preferable.

4. Sulphide recoveries were affected by the addition of depressants, which indicated that in addition to a gangue depression role, the depressants could also be performing a slime cleaning function, resulting in higher grades and a froth stabilisation function, resulting in higher mass pulls.

6 Final conclusions

This work has investigated the difference in depressant behaviour of guars and CMCs at varying molecular weights and it has shown that although similar results can be achieved, the depressants are influenced by different factors. In the microflotation tests, ionic conditions were found to be a pivotal factor in the performance of the CMC depressants in reducing the flotation of talc, while in the batch flotation tests, dosage was found to be a key factor.

Viscometry tests indicated that the ionic conditions of the system could affect the conformation and interactions of CMCs. This was confirmed clearly later where the depressant performance in microflotation of the CMCs were markedly different when the ionic character of the system was varied. Guars did not appear to be affected by varied ionic conditions in either the viscosity or the microflotation tests.

It was also noted that talc itself has a lower level of flotation when the system has a high ionic strength. It was suggested that at higher ionic conditions, adsorption of the ions onto the talc planes occurs – reducing the overall hydrophobicity of talc as well as creating positive sites which could attract the charged CMC molecules. The ionic content of mineral processing plants is known to be high and therefore, this factor has to be taken into consideration when attempting to examine these systems in a laboratory setting.

Overall, it appears that the addition of ions to the talc – CMC system leads both to the neutralisation of charges along the CMC chain as well as the creation of charged sites along the talc planar surfaces. At low CMC dosages and at low ionic strengths, an

increase in talc flotation was seen – indicating possible slime cleaning effects, which were also apparent during batch flotation tests.

The valency of the cation added appeared to be a factor in the system – divalent cations (Mg^{2+} and Ca^{2+}) were more effective talc depressants at lower ionic strengths than the monovalent cation K^{+}. The divalent cations also appeared to improve the efficiency of the CMC depressants to a greater degree – perhaps due to the formation of linkages between charged CMC molecules and the talc surface. The Ca^{2+} ion was generally more effective than Mg^{2+} in reducing talc flotation, which suggests that these ions adsorb more strongly onto the talc surface.

The importance of keeping the depressant equilibrium concentration constant during the microflotation process indicates that the adsorption of the depressants onto talc is physical and reversible – confirming the findings of previous authors who suggested physical adsorption such as hydrogen bonding and hydrophobic adsorption forces were predominant in interactions between talc and depressants.

The batch flotation tests showed very little differentiation between the depressant performance of CMCs and guars. This compares favourably with the microflotation findings where at higher ionic strengths, guars and CMCs exhibited similar depressant strengths. It is likely that the batch floats have a higher ionic strength, due to the release of ions into the pulp during the milling process. It is interesting that at very low ionic conditions, guars exhibited much better depressing ability than CMCs.

In the batch floats done, dosage appeared to be an important factor in affecting the overall water and mass recoveries while in the microflotation system, the guars and CMCs both

appeared to reach the sufficient surface coverage to cause depression on the talc at fairly low dosages (< 40 mg/l), after which, increasing the dosage did not appear to improve the performance of the depressants. This is attributed to the different solids density in the two systems. The overall solids to liquid ratio in the batch floats is 35% as opposed to the 1% solids to liquid ratio of the microfloats. This indicates that in the batch flotation system, the depressant added is taken up by other materials apart from the talc – leading to a situation where the actual amount of depressant interacting directly with the talc in a batch system is much less than in a microflotation system.

Both guars and CMCs appeared to interact with the copper and nickel minerals in the system. The smaller CMC and guar depressants appeared to perform a cleaning function on these minerals (enhancing their grade) as well as a froth stabilisation function (increasing the overall mass and water pulls), and the largest guar at high dosages appeared to depress the nickel sulphide minerals. All this indicates that in a batch flotation system, the depressants do not interact only with the talc but also with the other minerals present.

Overall, molecular weight did not appear to have a large effect on the depression of talc – particularly in the microflotation system. However, at high dosages in the batch system it appeared that a smaller guar depressant would be preferable to the larger guar depressant due to the larger guar depressing nickel sulphide minerals.

7 Recommendations

Based on the final conclusions, the following recommendations are made:

1. Work should be done at lower depressant dosages in the microflotation system in order to simulate the equilibrium depressant concentration that is experienced in the batch flotation system

2. K^+ adsorption should be confirmed

3. Various dosages of depressant should be used in a microflotation system with nickel and copper sulphides as well as some gangue materials common in Merensky ore to examine the effect of depressants on these minerals

4. The standard microflotation technique which involves filling the launder in between concentrates with deionised water at the correct pH should be revised when conditions involving weak, reversible, physical adsorption are involved. In such a case, the chemical which adsorbs onto the solid via weak, reversible, physical adsorption should be included at the correct solution concentration in between concentrates to avoid desorption occurring as the concentration of solution is steadily reduced through the float

5. The singular batch floats done in this work should be repeated to consolidate these findings

6. Adsorption tests should be done to ascertain whether the differences in microflotation arise from differences in adsorption

7. IR spectroscopy studies should be used in further studies to confirm the adsorption or complexation of Mg^{2+} and Ca^{2+} with CMC carboxylate groups

BIBLIOGRAPHY

5. Allain R. J., "Water soluble polymers - the future?", *in "Reagents for Better Metallurgy"*, Makutla P. S. Ed., Society for Mining, Metallurgy and Exploration, inc., Littleton, Colorado, 264 - 267, (1994)

6. Aspinall G. O., "Polysaccharides", Pergamon Press, Oxford, (1970)

7. Bacus I., "The Role of Nitrogen on the Flotation Performance of a Complex Sulphice Ore", Masters Thesis, Faculty of Engineering and the Built Environment, University of Cape Town, Cape Town, South Africa (2000)

8. Ball B. and Fuerstenau D. W., "A review of the measurement of streaming potentials", *Miner. Sci. Engng*, **5**, (4), 267 – 277, (October 1973)

9. Bradshaw D. J. and O'Connor C. T., "Measurement of the sub - process of bubble loading in flotation", *Minerals Engineering*, **9**, (4), 443, (1996)

10. Bremmell K. E., Biggs S. & Jameson G. J., "Polyelectrolyte/surfactant interactions in particulate flotation", *in "Polymers in the mineral processing industry"*, Laskowski J. S. Ed., MetSoc, Canada, 497 - 506, (1999)

11. Cheng Z., Lu W., Tang J. and Sun B., "Study on the separation of silicate minerals from quartz with collector mixture ", *Proceedings of the XIX International Mineral Processing Congress*, **3**, 263 – 266, (1997)

12. Crawford R. & Ralston J., "The influence of particle size and contact angle in mineral flotation", *International Journal of Mineral Processing*, **23**, 1 - 24, (1988)

13. Cullum D. C., "Introduction to surfactant analysis", Blackie Academic and Professional, Glasgow, (1994)

14. Dai Z. and Lu S., "Hydrophobic interaction in flocculation and flotation. 2. Interaction between non-polar oil drop and hydrophobic mineral particle", *Colloids and surfaces*, **57**, 61 - 72, (1991)

15. Dalvie M. A., "The Effect of Polysaccharides and Inorganic Dispersants on the Surface Characteristics of Talc and the Effect on the Flotation Performance of a Merensky ore", Masters Thesis, Faculty of Engineering and the Built Environment, University of Cape Town, Cape Town, South Africa (2001)

16. Djuve J. & Pugh R. J., "The influence of polymeric flocculant/surfactant interactions on foam stability", *in "Polymers in the mineral processing industry"*, Laskowski J. S. Ed., MetSoc, Canada, 507 - 521, (1999)

17. Frisch H. L. & Simha R., "The viscosity of colloidal suspensions and macromolecular solutions", *in "Rheology"*, F.R. Eirich Ed., Academic Press Inc. Publishers, New York, **1**, 557 (1956)

18. Fuerstenau D. W., "Where we are in flotation chemistry after 70 years of research", *Proceedings of the XIX International Mineral Processing Congress*, **3**, 3 – 17, (1997)

19. Fuerstenau D.W. and Fuerstenau M. C., "The flotation of oxide and silicate minerals", *in "Principles of Flotation"*, R. P. King Ed., S.A.I.M.M., Johannesburg, 109 – 158, (1982)

20. Fuerstenau M. C., "Role of Metal Ion Hydrolysis in Oxide and Silicate Flotation Systems", *AICHLhE, symposium series no. 150*, **71**, pp 16 – 23

21. Fuerstenau M. C., Lopez-Valdivieso A. & Fuerstenau D. W., "Role of hydrolysed cations in the natural hydrophobicity of talc", *International Journal of Mineral Processing*, **23**, 161 - 170, (1988)

22. Gigowski B., Vogg A., Wierer K. and Dobias B., "Effect of Fe-lattice ions on adsorption, electrokinetic, calorimetric and flotation properties of sphalerite", *International Journal of Mineral Processing*, 33, 103 – 120, (1991)

23. Gong W., Jenkins P., Ralston J. & Schumann, "Poly(acrylamides) at the talc-aqueous solution interface", *in "Polymers in the mineral processing industry"*, Laskowski J. S. Ed., MetSoc, Canada, 203 - 216, (1999)

24. Grimshaw R. W., "The Chemistry and Physics of Clays and allied ceramic materials", 4th edition, Ernest Benn Ltd., London. (1971)

25. Guthrie R. D. and Honeyman, J., "An introduction to the chemistry of carbohydrates", Third edition, Clarendon Press, Oxford, (1968)

26. Harris P. J., Mapasa K., Canham A. & Bradshaw D., "The effects of power input on the efficiency of guar depressants in flotation", *in "Polymers in the mineral processing industry"*, Laskowski J. S. Ed., MetSoc, Canada, 51 - 61, (1999)

27. Huang H.H., Calara, J. V., Bauer, D. L. and Miller, J. D., "Adsorption Reactions in the Depression of Coal by Organic Colloids", In: *Recent Developments in Separation Science*, CRC Press, Florida, vol. 4, pp. 115-133 (1978)

28. Hiemenz P. C. and Rajagopalan R. Principles of colloid and surface chemistry. 3rd Edn., Marcell Dekker, New York (1997)

29. Hogg R., "Polymer adsorption and flocculation", *in "Polymers in the mineral processing industry"*, Laskowski J. S. Ed., MetSoc, Canada, 3 - 17, (1999)

30. Israelachvili J. N., "Intermolecular and surface forces", 2nd Edition, Academic Press, London, Chapter 8, (1992)

31. Jenkins P. and Ralston J., "The adsorption of a polysaccharide at the talc-aqueous solution interface", *Colloids and surfaces* (accepted October 1997)

32. Kato A. and Nakai S., "Hydrophobicity determined by a flourescence probe method and its correlation with surface properties of proteins", *Biochimica et Biophysica Acta*, **624**, 13 - 20, (1980)

33. King R. P. Ed. "Principles of flotation", *SAIMM*, Johannesburg, (1982)

34. Kitchener J. A., "Discussion of surface forces in flotation", *Minerals Sci. Engng*, **6**, (4), 245 - 246, (October 1974)

35. Klimpel R. R., "Froth flotation: The kinetic approach", The Dow Chemical Company Midland, Michigan 48640

36. Kurata M. & Tsunashima Y., "Viscosity – Molecular Weight Relationships and Unperturbed Domensions of Linear Molecules", *in "Polymer Handbook"*, Brandrup J. & Immergut E. H. Ed., 3rd Edn, John Wiley & Sons, New York, **VII**, 1-6 (1989)

37. Laskowski J. S., "Surface processes course manual", University of Cape Town, (1996)

38. Laskowski J. S., "The relationship between floatability and hydrophobicity", Advances in Mineral Processing, Chapter 11, (1986)

39. Liu Q. & Laskowski J. S., "Adsorption of polysaccharides onto sulphides and their use in sulphide flotation", *in "Polymers in the mineral processing industry"*, Laskowski J. S. Ed., MetSoc, Canada, 71 - 88, (1999)

40. Liu Q. & Laskowski J. S., "On the adsorption mechanism of carboxymethylcellulose", *in "Polymers in the mineral processing industry"*, Laskowski J. S. Ed., MetSoc, Canada, 357 - 372, (1999)

41. Lu S, "Hydrophobic interaction in flocculation and flotation. 3. Role of hydrophobic interaction in particle-bubble attachment", *Colloids and surfaces*, **57**, 73 - 81, (1991)

42. Lu S. and Song S., "Hydrophobic interaction in flocculation and flotation. 1. Hydrophobic flocculation of fine mineral particles in aqueous solution", *Colloids and surfaces*, **57**, 49 - 60, (1991)

43. Mackenzie J. M. W., "Zeta-potential studies in mineral processing: measurement, techniques and applications", *Minerals Sci. Engng*, **6**, (1), 25 – 43, (January 1974)

44. Mackenzie J. M., "Guar-Based Reagents", Engineering and Mining Journal, McGraw-Hill, (October 1980)

45. Mangalam V. and Khangaonkar P. R., "Zeta - Potential and Adsorption studied of the chalcopyrite - sodium diethyl dithiocarbamate system", *International Journal of Mineral Processing*, **15**, 269 – 280, (1985)

46. Mao M., Fornasiero D., Ralston J. & Sobieraj S., "Use of depressants in the separation of zircon from rutile and ilmenite", *in "Polymers in the mineral processing industry"*, Laskowski J. S. Ed., MetSoc, Canada, 219 - 229, (1999)

47. Marshall C. E., "The colloid chemistry of the silicate minerals", Academic press inc., New York, (1949)

48. Masakona M. R. and Tshepe T. E., "The effect of ions on the role of depressants in the flotation of sulphide minerals - a literature survey", U.C.T. undergraduate project, (1997)

49. Mehrotra S. and Kapur P. C., "The effects of aeration rate, particle size and pulp density on the flotation rate distributions", Powder technology, 9, 213 - 219, (1974)

50. Mellgren O., Gochen R. J., Shergold H. L. and Kitchener J. A., "Thermochemical measurements in flotation research", *10th International Minerals Processing Congress*, London, Jones M. J., Ed., 451 – 472, (1973)

51. Michelmore A., Gong W., Jenkins P., Ralston J. & Schumann R., "The influence of polyphosphates in modifying the surface behaviour and interactions of metal oxide

particles", *in "Polymers in the mineral processing industry"*, Laskowski J. S. Ed., MetSoc, Canada, 231 - 245, (1999)

52. Miller, J D., Laskowski, J. S. and Chang, S. S., "Dextrin Adsorption by Oxidised Coal", *Colloids and Surfaces*, **8**, pp. 137-151 (1983)

53. Morris G. E. "The adsorption characteristics of polymeric depressants at the talc water interface", PhD thesis, School of Chemical Technology, Faculty of Applied Science and Technology, University of South Australia, Adelaide, Australia (1996)

54. Morris G. E., Fornasiero D., Ralston J., "Low molecular weight polyacrylamide depressant adsorption by silane modified talc", *in "Polymers in the mineral processing industry"*, Laskowski J. S. Ed., MetSoc, Canada, 171 - 183, (1999)

55. Morris, G. E., Fornasiero D. and Ralston J.," The surface properties of depressants at the talc-water interface", *Proceedings of the XIX International Mineral Processing Congress*, **3**, 43 – 48, (1997)

56. Nagaraj D. R., "Recent developments in new sulphide and precious metals collectors and mineral surface analysis", Cytec Industries

57. Napier-Munn T. J., "An introduction to Comparative Statistics and Experimental Design for Minerals Engineers", JKMRC, University of Queensland, Course Notes, Second Edition, Version 2, (1996)

58. Napier-Munn T., "Detecting performance improvements in trials with time-varying mineral processes - three case studies", *Minerals Engineering*, **8**, (8), 843 - 858, (1995)

59. Oliviera J. F. & Gomes L. M. B., "Organic macromolecular depressants for talc associated with sulphide minerals", *in "Processing of hydrophobic minerals and fine coal"*, Laskowski J. S. and Poling G. W., Ed., Canadian institute of mining, metallurgy and petroleum, Montreal, Quebec, Canada, 341 - 354, (1995)

60. Ouyang J., Lu S. and Wu L., "Dispersion and aggregation of fine talc particles in aqueous solution", *in "Processing of hydrophobic minerals and fine coal"*, Laskowski J. S. and Poling G. W. Ed., Canadian institute of mining, metallurgy and petroleum, Montreal, Quebec, Canada, 356 - 361, (1995)

61. Person I., "Review: Adsorption of ions and molecules to solid surface in connection with flotation of sulphide minerals", Journal of coordination chemistry, **32(4)**, 261 - 341, (1994)

62. Porter M. R., "Handbook of Surfactants", Second Edition, Blackie Academic and Professional, Glasgow, (1994)

63. Prabhanjan H., Gharia M. M. & Srivastava H. C., "Guar Gum Derivatives. Part 1: Preparation and Properties", Carbohydrate Polymers, **11**, 279 - 292, (1989)

64. Rao S. R., "Surface forces in flotation", *Minerals Sci. Engng*, **6**, (1), 45 – 53, (January 1974)

65. Rath R. K. & Subramanian S., "Studies on adsorption of guar gum onto biotite mica", *Minerals Engineering*, **19**, (12), 1405 - 1420, (1997)

66. Rath R. K., Subrahmanian S. & Laskowski J. S., "Interaction of guar gum with hydrophobic solids", *in "Polymers in the mineral processing industry"*, Laskowski J. S. Ed., MetSoc, Canada, 185 - 201, (1999)

67. Rath R. K., Subramanian S. & Laskowski J. S., "Adsorption of guar gum onto talc", *in "Processing of hydrophobic minerals and fine coal"*, Laskowski J. S. and Poling G. W. Ed., Canadian institute of mining, metallurgy and petroleum, Montreal, Quebec, Canada, 105 - 119, (1995)

68. Rath R. K., Subramanian S. and Laskowski J. S., "Adsorption of dextrin and guar gum onto talc, a comparitive study", Langmuir, **13**, 6260-6266, (1997)

69. Rosen M. J. Ed., "Surfactants and interfacial phenomena", John Wiley & Sons, New York, 1 - 76, (1978)

70. Scatena, L. F., Brown, M. G. and Richmond, G. L., "Water at Hydrophobic Surfaces: Weak Hydrogen Bonding and Strong Orientation Effects", Science, **292**, p. 90, (4 May 2001)

71. Schulze H. J., "Physico - chemical elementary processes in flotation", *Developments in Mineral Processing*, **4**, 14 - 25

72. Snyder L. R., "Interactions responsible for the selective adsorption of nonionic organic compounds on alumina. Comparisons with adsorption on silica", *The Journal of Pysical Chemistry*, **72**, (2), (February 1968)

73. Steenberg E. and Harris P. J., "Adsorption of carbomethoxycellulose, guar gum and starch onto talc, sulphides, oxides and salt-type minerals", *South African Journal of Chem.*, **37**, (3), 85 – 90, (1984)

74. Steenberg E., "The depression of the natural floatability of talc: The mechanism involved in the adsorption of organic reagents of high molecular mass", PhD thesis (Industrial Chemistry), Faculty of Science, University of Potchefstroom, Johannesburg, South Africa (1982)

75. Subramanian S., Natarajan K.A. and Sathyanarayana D. N., "FTIR spectroscopic studies on the adsorption of an oxidised starch on some oxide minerals", *Minerals and Metallurgical processing*, 152 - 158, (August, 1989)

76. Townsend A.A. and Nakai S., "Relationships between hydrophobicity and foaming characteristics of food proteins", *Journal of food science*, **48** , 588 - 594, (1983)

77. Van Lierde A., "Effects of acrylate polymers on the sulphidization of copper, lead and zinc oxide ores associated with a carbonate gangue", *Transactions of the Institution of Mining and Metallurgy*, Section C, **81**, 793, C204 – C212, (December 1972)

78. Van Olphen, H "An Introduction to Clay Colloid Chemistry', 2nd edition, Wiley - Interscience, New York, pp. 36-38, (1977)

79. Vaughn D. J., Becker U. and Wright K., "Sulphide mineral surfaces: Theory and Experiment", Invited Contribution for *International Journal of Mineral Processing*, (1996)

80. Whistler R. L., "INDUSTRIAL GUMS - Polysaccharides and their derivates", Second Edition, Academic Press, New York, (1973)

81. Wie, J. M. and Fuerstenau, D. W., "The effect of Dextrin on Surface Properties and the flotation of Molybdenite", *International Journal of Mineral Processing*, 1, 17, (1974)

82. Woods R., "Electrochemistry of sulphide flotation", Principles of Mineral Flotation, 91 - 115

83. Xu Z. and Finch J. A., "Direct method for studying collector adsorption on minerals in mixed-mineral system", Technical notes C197 - C199

APPENDIX 1 – XRD ANALYSES ON TALC

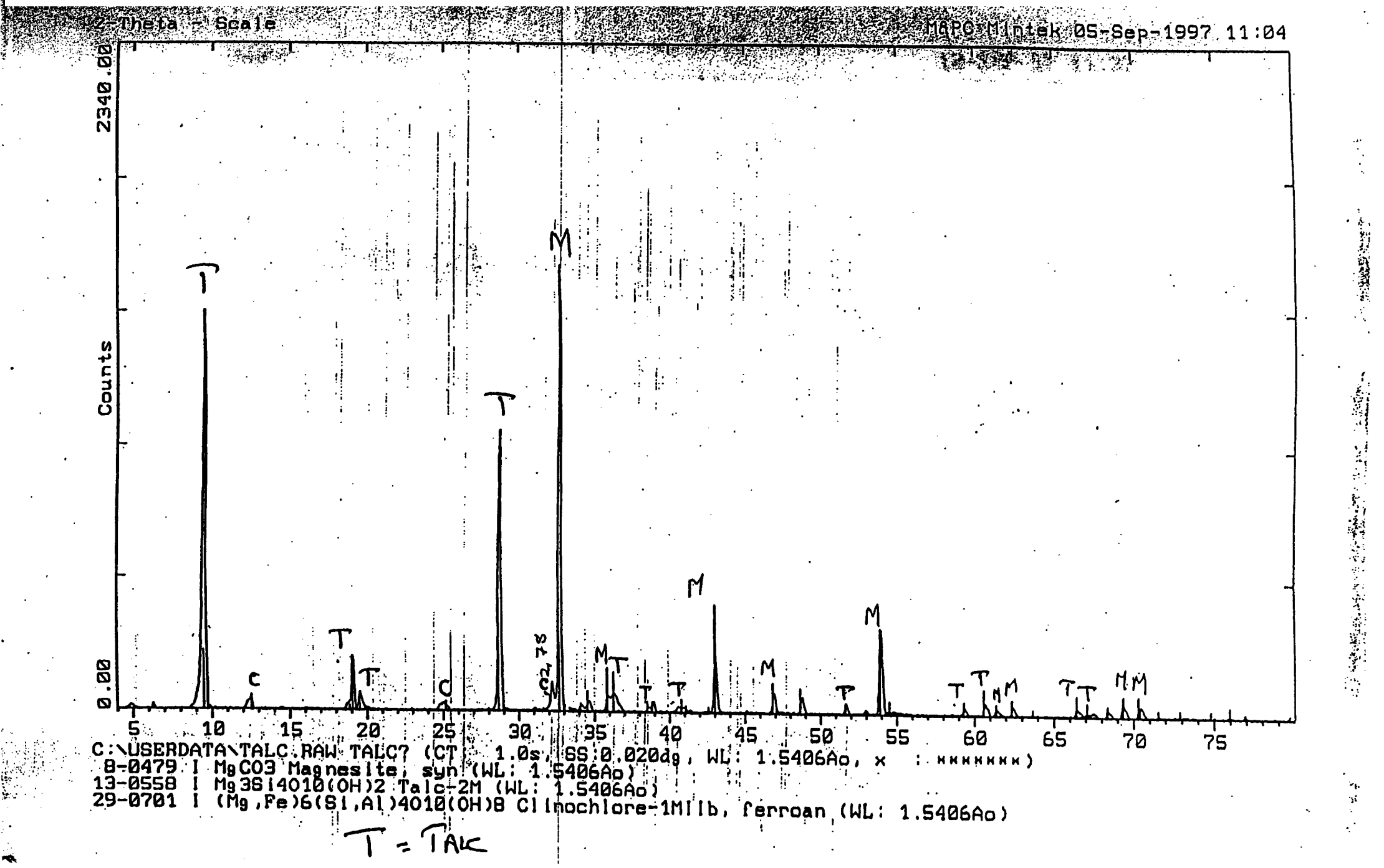
02-Theta - Scale
MAPC Minlek 05-Sep-1997 11:04
2340.00
Counts
0.00
5
10
15
20
25
30
35
40
45
50
55
60
65
70
75
T
C
M
C2,78
C:\USERDATA\TALC.RAW TALC? (CT: 1.0s, SS:0.020dg, WL: 1.5406Ao, x : ннннннн)
8-0479 | MgCO3 Magnesite, syn (WL: 1.5406Ao)
13-0558 | Mg3Si4O10(OH)2 Talc-2M (WL: 1.5406Ao)
29-0701 | (Mg,Fe)6(Si,Al)4O10(OH)8 Clinochlore-1MIIb, ferroan (WL: 1.5406Ao)
T = TALC

APPENDIX 2 – XRF ANALYSES ON TALC

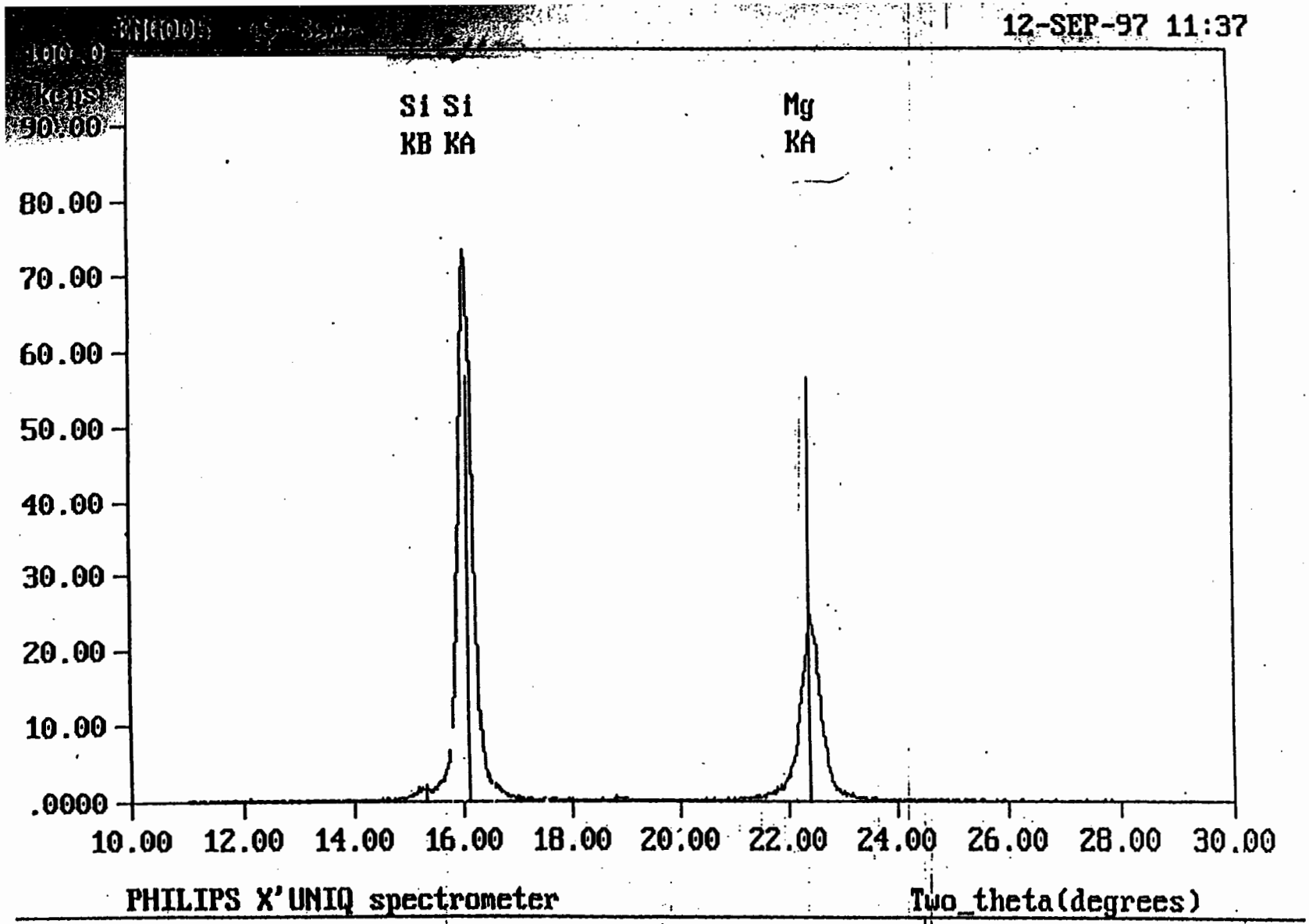
12-SEP-97 11:37
kcps
Si Si
KB KA
Mg
KA
90.00
80.00
70.00
60.00
50.00
40.00
30.00
20.00
10.00
.0000
10.00
12.00
14.00
16.00
18.00
20.00
22.00
24.00
26.00
28.00
30.00
PHILIPS X'UNIQ spectrometer
Two_theta(degrees)

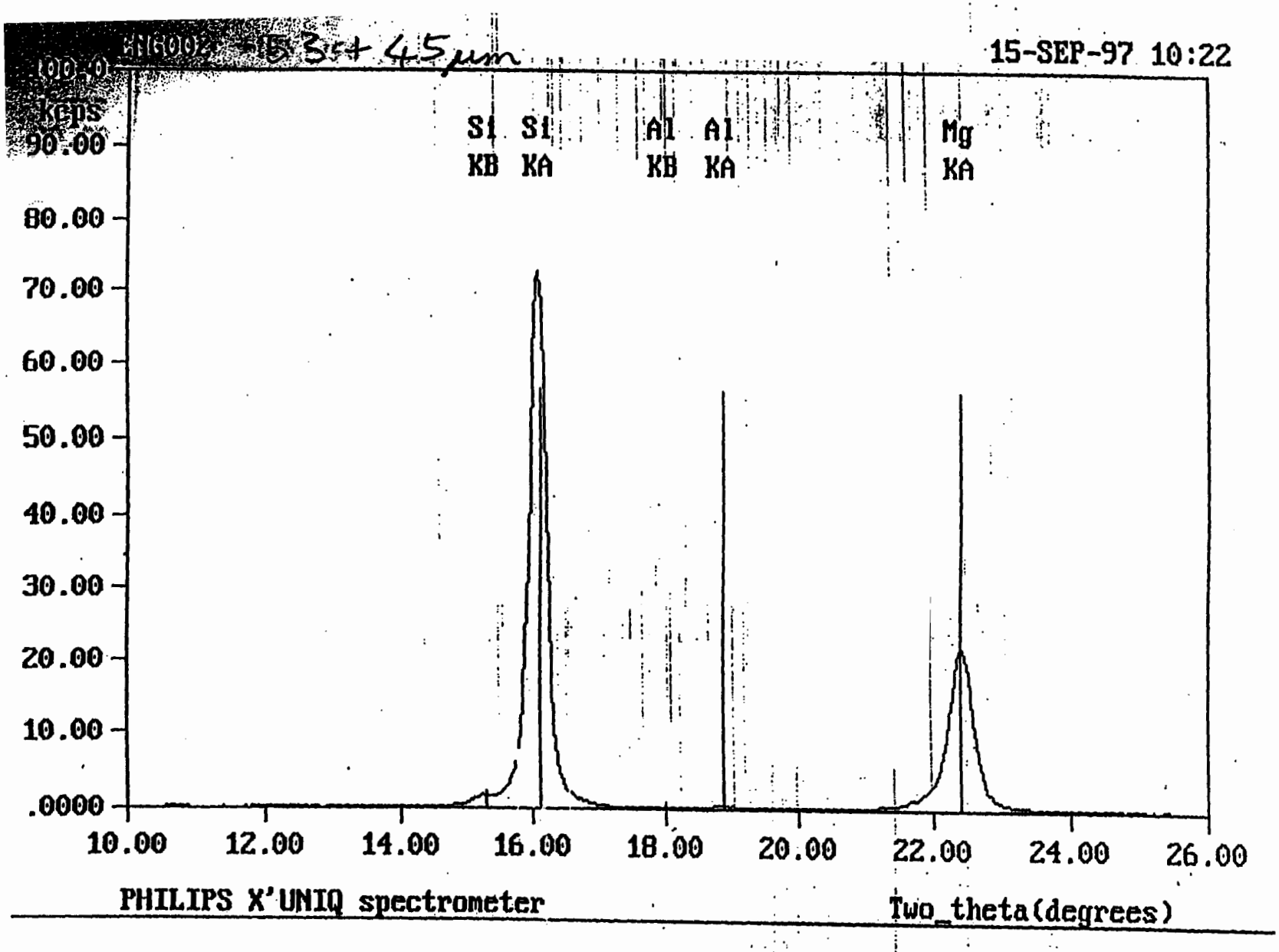
EN6002 -15 3+4 5µm
15-SEP-97 10:22
100.0
Kcps
90.00
80.00
70.00
60.00
50.00
40.00
30.00
20.00
10.00
.0000
Si KB
Si KA
Al KB
Al KA
Mg KA
10.00
12.00
14.00
16.00
18.00
20.00
22.00
24.00
26.00
PHILIPS X'UNIQ spectrometer
Two_theta(degrees)

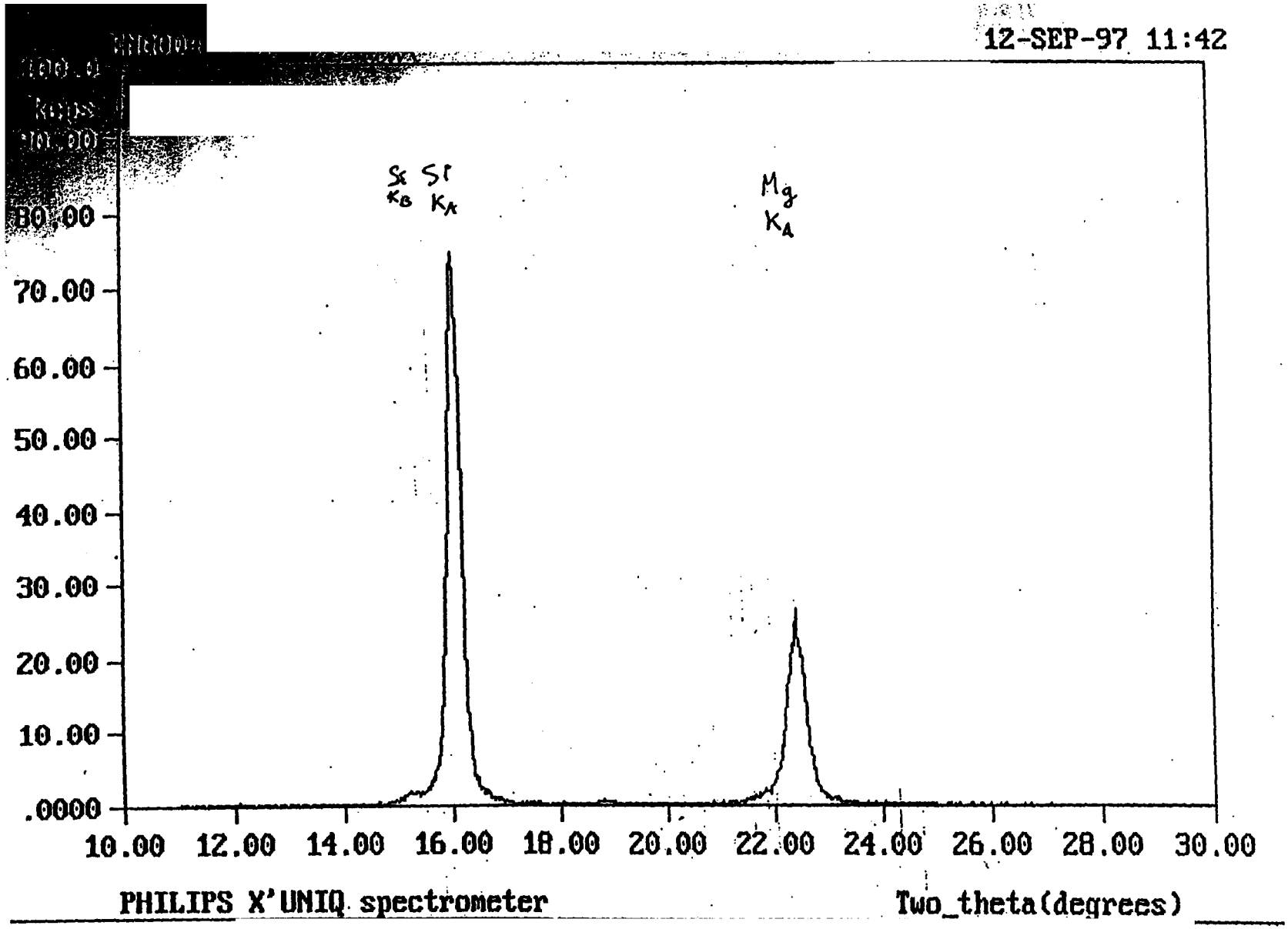
12-SEP-97 11:42
Sr Kβ
Sr KA
Mg KA
80.00
70.00
60.00
50.00
40.00
30.00
20.00
10.00
.0000
10.00 12.00 14.00 16.00 18.00 20.00 22.00 24.00 26.00 28.00 30.00
PHILIPS X'UNIQ spectrometer
Two_theta(degrees)

APPENDIX 3 – SUMMARY B.E.T. REPORT OF TALC

UCT Chemical Engineering

ASAP 2000 V3.01 B PAG

SAMPLE DIRECTORY/NUMBER: MINP /3 START 10:21:13 06/
SAMPLE ID: -38 PGS COMPL 13:16:05 06/
SUBMITTER: MA DALVEY REPRT 13:29:21 06/
OPERATOR: A.RAMPLIN SAMPLE WT: 0.93
UNIT NUMBER: 1 FREE SPACE: 62.39
ANALYSIS GAS: Nitrogen EQUIL INTRVL: 1

-38 μm

BET SURFACE AREA REPORT

BET SURFACE AREA:	3.6285	+/- 0.0442	sq. m/g
SLOPE:	1.168980	+/- 0.014482	
Y-INTERCEPT:	0.030730	+/- 0.002044	
C:	39.040909		
VM:	0.833535	cc/g STP	

CORRELATION COEFFICIENT: 9.99770E-01

RELATIVE PRESSURE	VOL ADSORBED (cc/g STP)	1/ [VA(Po/P - 1)]
0.0679	0.6702	0.108704
0.0998	0.7478	0.148297
0.1399	0.8302	0.195892
0.1598	0.8744	0.217516
0.1998	0.9487	0.263184

UCT Chemical Engineering

ASAP 2000 V3.01 B

SAMPLE DIRECTORY/NUMBER: MINP /5
SAMPLE ID: 106=75MICROMETER
SUBMITTER: MA DALVEY
OPERATOR: AUDREY
UNIT NUMBER: 1
ANALYSIS GAS: Nitrogen

START 10:53:31 06/
COMPL 13:1_:09 06/
REPRT 13:38:26 06/
SAMPLE WT: 1.0
FREE SPACE: 44.1
EQUIL INTRVL: 1

SUMMARY REPORT

106+75μm (group of four

AREA

BET SURFACE AREA:	1.5125	sq
SINGLE POINT SURFACE AREA AT P/Po 0.1997:	1.3342	sq
BJH CUMULATIVE ADSORPTION SURFACE AREA OF PORES BETWEEN 17.0000 AND 3000.0000 A DIAMETER:	1.7871	sq
BJH CUMULATIVE DESORPTION SURFACE AREA OF PORES BETWEEN 17.0000 AND 3000.0000 A DIAMETER:	1.9821	sq.
MICROPORE AREA:	-0.5373	sq.

VOLUME

SINGLE POINT TOTAL PORE VOLUME OF PORES LESS THAN 380.6421 A DIAMETER AT P/Po 0.9922:	0.004031	cc/
BJH CUMULATIVE ADSORPTION PORE VOLUME OF PORES BETWEEN 17.0000 AND 3000.0000 A DIAMETER:	0.004106	cc/
BJH CUMULATIVE DESORPTION PORE VOLUME OF PORES BETWEEN 17.0000 AND 3000.0000 A DIAMETER:	0.003046	cc/
MICROPORE VOLUME:	-0.000306	cc/

PORE SIZE

AVERAGE PORE DIAMETER (4V/A BY BET):	106.6009	A
BJH ADSORPTION AVERAGE PORE DIAMETER (4V/A):	91.9033	A
BJH DESORPTION AVERAGE PORE DIAMETER (4V/A):	61.4696	A

APPENDIX 4 – DETAILED VISCOMETRY TEST RESULTS

CMC VISCOMETRY MEASUREMENTS								
Measured Data								
Mass Percent Concentration	**FF10 (10^{-3})**	**FF10 (10^{-2})**	**FF30 (10^{-3})**	**FF150 (10^{-3})**	**FF300 (10^{-3})**	**FF30 (10^{-2})**	**FF150 (10^{-2})**	**FF300 (10^{-2})**
2.0	36.5	18.4	127.0	220.0	1,200.0	101.0	243.0	1,100.0
1.5			69.8	114.0	474.0	55.2	72.4	394.0
1.0	22.1	13.6	39.4	65.6	167.0	31.8	51.6	128.0
0.5			19.0	26.9	50.6	14.6	19.7	34.0
0.2			11.1	12.9	19.3	9.2	11.2	13.7
0.0	6.5	6.5	6.5	6.5	6.5	6.5	6.5	6.5
Corrected Data								
	FF10 (10^{-3})	**FF10 (10^{-2})**	**FF30 (10^{-3})**	**FF150 (10^{-3})**	**FF300 (10^{-3})**	**FF30 (10^{-2})**	**FF150 (10^{-2})**	**FF300 (10^{-2})**
2.0	5.6	2.8	19.4	33.7	183.8	15.5	37.2	168.5
1.5			10.7	17.5	72.6	8.5	11.1	60.3
1.0	3.4	2.1	6.0	10.0	25.6	4.9	7.9	19.6
0.5			2.9	4.1	7.7	2.2	3.0	5.2
0.2			1.7	2.0	3.0	1.4	1.7	2.1
0.0	1.0	1.0	1.0	1.0	1.0	1.0	1.0	1.0
[n] data								
	FF10 (10^{-3})	**FF10 (10^{-2})**	**FF30 (10^{-3})**	**FF150 (10^{-3})**	**FF300 (10^{-3})**	**FF30 (10^{-2})**	**FF150 (10^{-2})**	**FF300 (10^{-2})**
2.0	229.5	922.4	1,634.5	9,138.4	90.9	723.4	1,810.6	8,372.7
1.5		645.9	1,097.2	4,772.5		496.9	672.5	3,955.8
1.0	238.4	503.4	904.6	2,457.4	108.3	387.0	690.2	1,860.2
0.5		381.9	623.9	1,349.8		247.2	403.4	841.3
0.2		349.9	487.7	977.8		200.6	357.6	549.0
Intrinsic Viscosities								
	FF10 (10^{-3})	**FF10 (10^{-2})**	**FF30 (10^{-3})**	**FF150 (10^{-3})**	**FF300 (10^{-3})**	**FF30 (10^{-2})**	**FF150 (10^{-2})**	**FF300 (10^{-2})**
	247.8	**299.8**	**443.7**	**768.5**	**129.0**	**177.0**	**278.4**	**399.1**

GUAR VISCOMETRY MEASUREMENTS						
Measured Data						
Mass Percent Concentration	**SM4060 (10^{-2})**	**IMP4 (10^{-2})**	**SM4560 (10^{-2})**	**SM4060 (10^{-1})**	**IMP4 (10^{-1})**	**SM4560 (10^{-1})**
2.0	34.0	75.4	148.0	36.3	69.2	151.0
1.5	23.2	42.8	69.4	24.0	41.4	70.4
1.0	13.9	24.0	36.8	14.9	23.6	33.0
0.5	9.2	13.1	16.0	9.5	12.1	15.2
0.2	7.6	8.5	9.3	7.6	8.5	9.2
0.0	6.5	6.5	6.5	6.5	6.5	6.5
Corrected Data						
	SM4060 (10^{-2})	**IMP4 (10^{-2})**	**SM4560 (10^{-2})**	**SM4060 (10^{-1})**	**IMP4 (10^{-1})**	**SM4560 (10^{-1})**
2.0	5.2	11.5	22.7	5.6	10.6	23.1
1.5	3.6	6.6	10.6	3.7	6.3	10.8
1.0	2.1	3.7	5.6	2.3	3.6	5.1
0.5	1.4	2.0	2.5	1.5	1.9	2.3
0.2	1.2	1.3	1.4	1.2	1.3	1.4
0.0	1.0	1.0	1.0	1.0	1.0	1.0
[n] data						
	SM4060 (10^{-2})	**IMP4 (10^{-2})**	**SM4560 (10^{-2})**	**SM4060 (10^{-1})**	**IMP4 (10^{-1})**	**SM4560 (10^{-1})**
2.0	210.3	527.3		227.9	479.9	
1.5	170.2	370.3	641.9	178.4	356.0	652.1
1.0	112.9	267.5	463.6	128.2	261.4	405.4
0.5	80.2	201.2	290.0	90.0	170.6	265.5
0.2		147.0	210.6		147.0	200.6
Intrinsic Viscosities						
	SM4060 (10^{-2})	**IMP4 (10^{-2})**	**SM4560 (10^{-2})**	**SM4060 (10^{-1})**	**IMP4 (10^{-1})**	**SM4560 (10^{-1})**
	133.2	**91.1**	**31.5**	**105.4**	**88.7**	**40.2**

APPENDIX 5.1 – EXAMPLE OF MICROFLOTATION TEST SHEET

Microflotation Data Sheet

Date : ~~Jan~~ 28 Jan 1999	Float Test : 28
Sample Mass : 2.0028	Depressant Addition : 0
Salt concentration : 3.33 x10^{-3}M	Salt Used: $Mg(NO_3)_2 \cdot 6H_2O$

Sample Preparation

pH at start of float :	pH at end of float :

Time	Sample #	Paper mass	Paper + sample	Sample mass
30 sec		1,72	1,80	
1 min		1,75	1,82	
2 min		1,74	1,89	
5 min		1,75	2,04	
10 min		1,80	2,08	
Tails		1,77	2,80	
Blank		1,82	1,82	

Comments

~~Add in KCl~~

Seems 2 B some depression.

APPENDIX 5.2 – SAMPLE OF THE MICROFLOTATION TEST RESULTS

Test #	Sample mass	Depressant	pH start	pH end	Times	Paper mass	Paper + sample	Sample	Percent	Cumulative percent
1	2.0023	0 mg/l	10.07		30 sec	1.88	2.05	0.27	13.48%	13.48%
					1 min	1.87	2	0.23	11.49%	24.97%
					2 min	1.83	1.98	0.25	12.49%	37.46%
					5 min	1.85	2.13	0.38	18.98%	56.44%
					10 min	1.91	2.04	0.23	11.49%	67.92%
					Blank	2.04	1.94	-0.1		
Test #	Sample mass	Depressant	pH start	pH end	Times	Paper mass	Paper + sample	Sample	Percent	Cumulative percent
2	2.0004	0 mg/l	9.56		30 sec	1.88	2.05	0.27	13.50%	13.50%
					1 min	1.87	2	0.23	11.50%	25.00%
					2 min	1.83	1.98	0.25	12.50%	37.49%
					5 min	1.85	2.13	0.38	19.00%	56.49%
					10 min	1.91	2.04	0.23	11.50%	67.99%
					Blank	2.04	1.94	-0.1		
Test #	Sample mass	Depressant	pH start	pH end	Times	Paper mass	Paper + sample	Sample	Percent	Cumulative percent
3	2.0037	0 mg/l			30 sec	1.94	2.05	0.22	10.98%	10.98%
					1 min	1.95	2.04	0.2	9.98%	20.96%
					2 min	1.98	2.2	0.33	16.47%	37.43%
					5 min	2.04	2.34	0.41	20.46%	57.89%
					10 min	1.97	2.1	0.24	11.98%	69.87%
					Blank	1.95	1.84	-0.11		
Test #	Sample mass	Depressant	pH start	pH end	Times	Paper mass	Paper + sample	Sample	Percent	Cumulative percent
4	2.0000	40 mg/l FF10	9.44	9.11	30 sec	1.81	1.88	0.17	8.50%	8.50%
					1 min	1.84	1.96	0.22	11.00%	19.50%
					2 min	1.74	1.85	0.21	10.50%	30.00%
					5 min	1.84	2.19	0.45	22.50%	52.50%
					10 min	1.88	2.07	0.29	14.50%	67.00%
					Blank	1.89	1.79	-0.1		
Test #	Sample mass	Depressant	pH start	pH end	Times	Paper mass	Paper + sample	Sample	Percent	Cumulative percent
5	2.0000	40 mg/l FF10	9.32	9.23	30 sec	1.87	1.93	0.14	7.00%	7.00%
					1 min	1.96	1.98	0.1	5.00%	12.00%
					2 min	1.97	2.05	0.16	8.00%	20.00%
					5 min	1.95	2.25	0.38	19.00%	39.00%
					10 min	1.97	2.12	0.23	11.50%	50.50%
					Blank	1.85	1.77	-0.08		
Test #	Sample mass	Depressant	pH start	pH end	Times	Paper mass	Paper + sample	Sample	Percent	Cumulative percent
6	2.0000	40 mg/l FF10	9.23	9.1	30 sec	1.8	1.99	0.29	14.50%	14.50%
					1 min	1.72	1.82	0.2	10.00%	24.50%
					2 min	1.76	1.91	0.25	12.50%	37.00%
					5 min				0.00%	37.00%
					10 min	1.75	2.25	0.6	30.00%	67.00%
					Blank	1.84	1.74	-0.1		
Test #	Sample mass	Depressant	pH start	pH end	Times	Paper mass	Paper + sample	Sample	Percent	Cumulative percent
7	2.0000	4 mg/l FF10			30 sec	1.88	1.98	0.21	10.50%	10.50%
					1 min	1.77	1.85	0.19	9.50%	20.00%
					2 min	1.87	2.01	0.25	12.50%	32.50%
					5 min	1.99	2.28	0.4	20.00%	52.50%
					10 min	2.01	2.14	0.24	12.00%	64.50%
					Blank	2.03	1.92	-0.11		
Test #	Sample mass	Depressant	pH start	pH end	Times	Paper mass	Paper + sample	Sample	Percent	Cumulative percent
8	2.0000	4 mg/l FF10	9.36		30 sec	2.01	2.15	0.24	12.00%	12.00%
					1 min	2	2.15	0.25	12.50%	24.50%
					2 min	1.92	2.09	0.27	13.50%	38.00%
					5 min	1.87	2.2	0.43	21.50%	59.50%
					10 min	1.88	2.04	0.26	13.00%	72.50%
					Blank	1.85	1.75	-0.1		
Test #	Sample mass	Depressant	pH start	pH end	Times	Paper mass	Paper + sample	Sample	Percent	Cumulative percent
9	2.0000	4 mg/l FF10	9.33	9.02	30 sec	1.86	1.95	0.19	9.50%	9.50%
					1 min	1.88	2	0.22	11.00%	20.50%
					2 min	1.79	1.99	0.3	15.00%	35.50%
					5 min	1.79	2.07	0.38	19.00%	54.50%
					10 min	1.82	2.01	0.29	14.50%	69.00%
					Blank	1.77	1.67	-0.1		
Test #	Sample mass	Depressant	pH start	pH end	Times	Paper mass	Paper + sample	Sample	Percent	Cumulative percent
10	2.0000	60 mg/l FF10		7.11	30 sec	1.79	1.85	0.18	9.00%	9.00%
					1 min	1.81	1.87	0.18	9.00%	18.00%
					2 min	1.86	1.98	0.24	12.00%	30.00%
					5 min	1.79	2.06	0.39	19.50%	49.50%
					10 min	1.78	1.97	0.31	15.50%	65.00%
					Blank	1.84	1.72	-0.12		

Test #	Sample mass	Depressant	pH start	pH end	Times	Paper mass	Paper + sample	Sample	Percent	Cumulative percent
11	2.0067	60 mg/l FF10	9.23	7.45	30 sec	1.8	1.86	0.15	7.47%	7.47%
					1 min	1.79	1.83	0.13	6.48%	13.95%
					2 min	1.76	1.93	0.26	12.96%	26.91%
					5 min	1.78	2.12	0.43	21.43%	48.34%
					10 min	1.79	1.99	0.29	14.45%	62.79%
					Blank	1.78	1.69	-0.09		
Test #	Sample mass	Depressant	pH start	pH end	Times	Paper mass	Paper + sample	Sample	Percent	Cumulative percent
12	2.0042	60 mg/l FF10	9.06	8.62	30 sec	1.79	1.82	0.13	6.49%	6.49%
					1 min	1.79	1.78	0.09	4.49%	10.98%
					2 min	1.8	1.92	0.22	10.98%	21.95%
					5 min	1.84	2.15	0.41	20.46%	42.41%
					10 min	1.94	2.15	0.31	15.47%	57.88%
					Blank	1.94	1.84	-0.1		
Test #	Sample mass	Depressant	pH start	pH end	Times	Paper mass	Paper + sample	Sample	Percent	Cumulative percent
13	2.0025	100 mg/l FF10	9.17		30 sec	1.96	2.02	0.15	7.49%	7.49%
					1 min	1.93	1.96	0.12	5.99%	13.48%
					2 min	1.99	2.09	0.19	9.49%	22.97%
					5 min	1.99	2.25	0.35	17.48%	40.45%
					10 min	2.04	2.24	0.29	14.48%	54.93%
					Blank	2.01	1.92	-0.09		
Test #	Sample mass	Depressant	pH start	pH end	Times	Paper mass	Paper + sample	Sample	Percent	Cumulative percent
14	2.0072	100 mg/l FF10	9.01	8.02	30 sec	2.02	2.1	0.17	8.47%	8.47%
					1 min	2.05	2.11	0.15	7.47%	15.94%
					2 min	1.91	2.05	0.23	11.46%	27.40%
					5 min	1.91	2.23	0.41	20.43%	47.83%
					10 min	1.93	2.14	0.3	14.95%	62.77%
					Blank	1.92	1.83	-0.09		
Test #	Sample mass	Depressant	pH start	pH end	Times	Paper mass	Paper + sample	Sample	Percent	Cumulative percent
15	1.9998	100 mg/l FF10	9.11	8.62	30 sec	1.98	2	0.11	5.50%	5.50%
					1 min	1.95	1.98	0.12	6.00%	11.50%
					2 min	1.93	2.03	0.19	9.50%	21.00%
					5 min	1.96	2.22	0.35	17.50%	38.50%
					10 min	1.93	2.13	0.29	14.50%	53.01%
					Blank	1.95	1.86	-0.09		
Test #	Sample mass	Depressant	pH start	pH end	Times	Paper mass	Paper + sample	Sample	Percent	Cumulative percent
16	2.0024	200 mg/l FF10	9.33	8.41	30 sec	1.9	1.93	0.11	5.49%	5.49%
					1 min	1.9	1.93	0.11	5.49%	10.99%
					2 min	1.9	2.01	0.19	9.49%	20.48%
					5 min	1.91	2.22	0.39	19.48%	39.95%
					10 min	1.94	2.15	0.29	14.48%	54.43%
					Blank	1.88	1.8	-0.08		
Test #	Sample mass	Depressant	pH start	pH end	Times	Paper mass	Paper + sample	Sample	Percent	Cumulative percent
17	2.0034	200 mg/l FF10	9.23	8.18	30 sec	1.92	1.9	0.06	2.99%	2.99%
					1 min	1.92	1.92	0.08	3.99%	6.99%
					2 min	1.91	2	0.17	8.49%	15.47%
					5 min	1.94	2.22	0.36	17.97%	33.44%
					10 min	1.75	1.96	0.29	14.48%	47.92%
					Blank	1.76	1.68	-0.08		
Test #	Sample mass	Depressant	pH start	pH end	Times	Paper mass	Paper + sample	Sample	Percent	Cumulative percent
18	2.0082	200 mg/l FF10	9.16	7.71	30 sec	1.73	1.85	0.2	9.96%	9.96%
					1 min	1.75	1.82	0.15	7.47%	17.43%
					2 min	1.75	1.88	0.21	10.46%	27.89%
					5 min	1.79	1.71	0	0.00%	27.89%
					10 min	1.8	2.36	0.64	31.87%	59.76%
					Blank	1.75	1.67	-0.08		
Test #	Sample mass	Depressant	pH start	pH end	Times	Paper mass	Paper + sample	Sample	Percent	Cumulative percent
19	2.0035	4 mg/l FF300	9.23	8.41	30 sec	1.72	1.86	0.25	12.48%	12.48%
					1 min	1.76	1.83	0.18	8.98%	21.46%
					2 min	1.97	2.13	0.27	13.48%	34.94%
					5 min	2.01	2.31	0.41	20.46%	55.40%
					10 min	2	2.12	0.23	11.48%	66.88%
					Blank	2.02	1.91	-0.11		
Test #	Sample mass	Depressant	pH start	pH end	Times	Paper mass	Paper + sample	Sample	Percent	Cumulative percent
20	2.0008	4 mg/l FF300	9.41	8.49	30 sec	2.09	2.18	0.22	11.00%	11.00%
					1 min	2.1	2.15	0.18	9.00%	19.99%
					2 min	2.14	2.24	0.23	11.50%	31.49%
					5 min	2.12	2.34	0.35	17.49%	48.98%
					10 min	2.13	2.21	0.21	10.50%	59.48%
					Blank	2.14	2.01	-0.13		

Test #	Sample mass	Depressant	pH start	pH end	Times	Paper mass	Paper + sample	Sample	Percent	Cumulative percent
21	2.0041	4 mg/l FF300	9.51	8.92	30 sec	1.93	2.06	0.19	9.48%	9.48%
					1 min	1.88	2.01	0.19	9.48%	18.96%
					2 min	1.87	2.09	0.28	13.97%	32.93%
					5 min	1.87	2.19	0.38	18.96%	51.89%
					10 min	1.9	1.99	0.15	7.48%	59.38%
					Blank	1.78	1.72	-0.06		
Test #	Sample mass	Depressant	pH start	pH end	Times	Paper mass	Paper + sample	Sample	Percent	Cumulative percent
22	2.0008	40 mg/l FF300	9.32	8.4	30 sec	1.8	1.9	0.21	10.50%	10.50%
					1 min	1.86	1.92	0.17	8.50%	18.99%
					2 min	1.79	1.94	0.26	12.99%	31.99%
					5 min	1.86	2.24	0.49	24.49%	56.48%
					10 min	1.87	1.99	0.23	11.50%	67.97%
					Blank	1.84	1.73	-0.11		
Test #	Sample mass	Depressant	pH start	pH end	Times	Paper mass	Paper + sample	Sample	Percent	Cumulative percent
23	2.0051	40 mg/l FF300	9.58	8.9	30 sec	1.92	2	0.19	9.48%	9.48%
					1 min	1.87	1.94	0.18	8.98%	18.45%
					2 min	1.89	2	0.22	10.97%	29.42%
					5 min	1.85	2.13	0.39	19.45%	48.88%
					10 min	1.87	2.02	0.26	12.97%	61.84%
					Blank	1.86	1.75	-0.11		
Test #	Sample mass	Depressant	pH start	pH end	Times	Paper mass	Paper + sample	Sample	Percent	Cumulative percent
24	2.0053	40 mg/l FF300	8.9	8.35	30 sec	1.79	1.89	0.19	9.47%	9.47%
					1 min	1.79	1.84	0.14	6.98%	16.46%
					2 min	1.86	1.97	0.2	9.97%	26.43%
					5 min	1.87	2.15	0.37	18.45%	44.88%
					10 min	1.85	2.04	0.28	13.96%	58.84%
					Blank	1.84	1.75	-0.09		
Test #	Sample mass	Depressant	pH start	pH end	Times	Paper mass	Paper + sample	Sample	Percent	Cumulative percent
25	2.0000	60 mg/l FF300	9.47	8.83	30 sec	1.84	1.92	0.18	9.00%	9.00%
					1 min	1.89	1.97	0.18	9.00%	18.00%
					2 min	1.87	2.03	0.26	13.00%	31.00%
					5 min	1.93	2.12	0.29	14.50%	45.50%
					10 min	1.92	2.21	0.39	19.50%	65.00%
					Blank	1.97	1.87	-0.1		
Test #	Sample mass	Depressant	pH start	pH end	Times	Paper mass	Paper + sample	Sample	Percent	Cumulative percent
26	2.0027	60 mg/l FF300	9.06	8.43	30 sec	1.93	1.96	0.12	5.99%	5.99%
					1 min	1.98	2.03	0.14	6.99%	12.98%
					2 min	1.96	1.96	0.09	4.49%	17.48%
					5 min	1.95	2.35	0.49	24.47%	41.94%
					10 min	1.93	2.15	0.31	15.48%	57.42%
					Blank	1.73	1.64	-0.09		
Test #	Sample mass	Depressant	pH start	pH end	Times	Paper mass	Paper + sample	Sample	Percent	Cumulative percent
27	2.0021	60 mg/l FF300	9.3	8.51	30 sec	1.74	1.79	0.13	6.49%	6.49%
					1 min	1.73	1.81	0.16	7.99%	14.48%
					2 min	1.75	1.87	0.2	9.99%	24.47%
					5 min	1.75	2.07	0.4	19.98%	44.45%
					10 min	1.74	1.99	0.33	16.48%	60.94%
					Blank	1.69	1.61	-0.08		
Test #	Sample mass	Depressant	pH start	pH end	Times	Paper mass	Paper + sample	Sample	Percent	Cumulative percent
28	2.0017	100 mg/l FF300	9.06		30 sec	1.72	1.74	0.12	5.99%	5.99%
					1 min	1.75	1.79	0.14	6.99%	12.99%
					2 min	1.78	1.86	0.18	8.99%	21.98%
					5 min	1.77	2.05	0.38	18.98%	40.97%
					10 min	1.74	1.94	0.3	14.99%	55.95%
					Blank	1.74	1.64	-0.1		
Test #	Sample mass	Depressant	pH start	pH end	Times	Paper mass	Paper + sample	Sample	Percent	Cumulative percent
29	2.0004	100 mg/l FF300	8.9	8.38	30 sec	1.75	1.79	0.14	7.00%	7.00%
					1 min	1.7	1.75	0.15	7.50%	14.50%
					2 min	1.75	1.86	0.21	10.50%	25.00%
					5 min	1.7	2.07	0.47	23.50%	48.49%
					10 min	1.85	2.03	0.28	14.00%	62.49%
					Blank	1.84	1.74	-0.1		
Test #	Sample mass	Depressant	pH start	pH end	Times	Paper mass	Paper + sample	Sample	Percent	Cumulative percent
30	2.0003	100 mg/l FF300	9.34	8.74	30 sec	1.73	1.76	0.14	7.00%	7.00%
					1 min	1.75	1.75	0.11	5.50%	12.50%
					2 min	1.72	1.84	0.23	11.50%	24.00%
					5 min	1.75	2.08	0.44	22.00%	45.99%
					10 min	1.8	1.98	0.29	14.50%	60.49%

APPENDIX 6 – DETAILED BATCH FLOTATION TEST RESULTS

1 - Base Float

Concentrate Type	Mass Recovery			Water recovery	Sample Mass for Assays	Nickel						Copper					
	Mass (g)	Cum Mass (g)	Cum mass %	Mass (g)		AA Reading (ppm)	Ratio	Mass (g)	Cum Mass (g)	Cum recovery (%)	Cum grade (%)	AA Reading (ppm)	Ratio	Mass (g)	Cum Mass (g)	Cum recovery (%)	Cum grade (%)
Feed	30.97				0.51	8.96	0.00	0.14		0.0%		3.82	0.00	0.06		0.0%	
1 minute	54.60	54.60	5.3%		0.11	17.79	0.04	2.31	2.31	53.6%	4.2%	9.48	0.02	1.23	1.23	72.6%	2.3%
4 minutes	12.22	66.82	6.5%	107.64	0.10	8.95	0.02	0.27	2.58	59.8%	3.9%	3.84	0.01	0.11	1.34	79.4%	2.0%
12 minutes	20.51	87.33	8.5%	232.41	0.10	6.06	0.01	0.30	2.88	66.8%	3.3%	1.94	0.00	0.10	1.44	85.1%	1.7%
25 minutes	17.32	104.65	10.2%	288.61	0.11	3.96	0.01	0.16	3.03	70.4%	2.9%	1.26	0.00	0.05	1.49	88.0%	1.4%
TOTAL	1,026.15				0.51	8.96	0.00	4.55		0.0%		3.82	0.00	1.94		0.0%	

2 - 40 mg/l FF10

Concentrate Type	Mass Recovery			Water recovery	Sample Mass for Assays	Nickel						Copper					
	Mass (g)	Cum Mass (g)	Cum mass %	Mass (g)		AA Reading (ppm)	Ratio	Mass (g)	Cum Mass (g)	Cum recovery (%)	Cum grade (%)	AA Reading (ppm)	Ratio	Mass (g)	Cum Mass (g)	Cum recovery (%)	Cum grade (%)
Feed	17.54				0.50	9.59	0.00	0.08		0.0%		3.84	0.00	0.03		0.0%	
1 minute	19.17	19.17	1.9%	70.98	0.11	37.32	0.09	1.69	1.69	39.3%	8.8%	26.65	0.06	1.21	1.21	71.4%	6.3%
4 minutes	23.14	42.31	4.2%	179.59	0.10	14.45	0.04	0.82	2.51	58.4%	5.9%	3.53	0.01	0.20	1.41	83.2%	3.3%
12 minutes	14.94	57.25	5.7%	160.60	0.10	5.66	0.01	0.20	2.72	63.1%	4.7%	1.44	0.00	0.05	1.46	86.3%	2.6%
25 minutes	27.14	84.39	8.4%	419.91	0.10	3.63	0.01	0.24	2.95	68.6%	3.5%	0.92	0.00	0.06	1.52	89.8%	1.8%
TOTAL	1,005.36				0.50	9.59	0.00	4.79		0.0%		3.84	0.00	1.92		0.0%	

4 - 100 mg/l FF10

Concentrate Type	Mass Recovery			Water recovery	Sample Mass for Assays	Nickel						Copper					
	Mass (g)	Cum Mass (g)	Cum mass %	Mass (g)		AA Reading (ppm)	Ratio	Mass (g)	Cum Mass (g)	Cum recovery (%)	Cum grade (%)	AA Reading (ppm)	Ratio	Mass (g)	Cum Mass (g)	Cum recovery (%)	Cum grade (%)
Feed	12.10				0.50	8.64	0.00	0.05		0.0%		3.55	0.00	0.02		0.0%	
1 minute	2.90	2.90	0.3%	31.34	0.12	43.17	0.09	0.27	0.27	6.2%	9.3%	63.13	0.14	0.39	0.39	23.2%	13.5%
4 minutes	13.49	16.39	1.8%	108.83	0.11	41.85	0.09	1.25	1.52	35.4%	9.3%	17.66	0.04	0.53	0.92	54.4%	5.6%
12 minutes	15.12	31.51	3.5%	165.09	0.11	14.99	0.04	0.53	2.06	47.8%	6.5%	3.26	0.01	0.12	1.04	61.3%	3.3%
25 minutes	26.44	57.95	6.4%	365.42	0.11	5.16	0.01	0.31	2.37	55.0%	4.1%	1.20	0.00	0.07	1.11	65.6%	1.9%
TOTAL	903.90				0.50	8.64	0.00	3.87		0.0%		3.55	0.00	1.59		0.0%	

5 - 100 mg/l FF30																	
Concentrate Type	Mass Recovery			Water recovery	Sample Mass for Assays	Nickel						Copper					
	Mass (g)	Cum Mass (g)	Cum mass %	Mass (g)		AA Reading (ppm)	Ratio	Mass (g)	Cum Mass (g)	Cum recovery (%)	Cum grade (%)	AA Reading (ppm)	Ratio	Mass (g)	Cum Mass (g)	Cum recovery (%)	Cum grade (%)
Feed	19.23				0.50	8.69	0.00	0.08		0.0%		0.36	0.00	0.00		0.0%	
1 minute	9.37	9.37	1.1%	47.11	0.11	48.10	0.11	0.99	0.99	23.0%	10.6%	48.95	0.11	1.01	1.01	59.5%	10.8%
4 minutes	10.31	19.68	2.4%		0.11	34.36	0.08	0.78	1.77	41.2%	9.0%	9.78	0.02	0.22	1.23	72.7%	6.3%
12 minutes	16.34	36.02	4.3%	190.38	0.11	9.65	0.02	0.38	2.15	49.9%	6.0%	2.07	0.00	0.08	1.31	77.4%	3.6%
25 minutes	22.40	58.42	7.1%	320.24	0.11	4.05	0.01	0.21	2.36	54.7%	4.0%	0.93	0.00	0.05	1.36	80.2%	2.3%
TOTAL	828.55				0.50	8.69	0.00	3.58		0.0%		0.36	0.00	0.15		0.0%	

6 - 100 mg/l IMP4																	
Concentrate Type	Mass Recovery			Water recovery	Sample Mass for Assays	Nickel						Copper					
	Mass (g)	Cum Mass (g)	Cum mass %	Mass (g)		AA Reading (ppm)	Ratio	Mass (g)	Cum Mass (g)	Cum recovery (%)	Cum grade (%)	AA Reading (ppm)	Ratio	Mass (g)	Cum Mass (g)	Cum recovery (%)	Cum grade (%)
Feed	29.36				0.51	8.66	0.00	0.13		0.0%		3.89	0.00	0.06		0.0%	
1 minute	14.58	14.58	1.4%	46.98	0.10	34.73	0.09	1.24	1.24	28.9%	8.5%	31.67	0.08	1.13	1.13	66.9%	7.8%
4 minutes	9.53	24.11	2.3%	123.88	0.11	30.11	0.07	0.67	1.91	44.4%	7.9%	8.35	0.02	0.19	1.32	77.9%	5.5%
12 minutes	24.30	48.41	4.7%	338.09	0.10	8.43	0.02	0.50	2.41	55.9%	5.0%	2.01	0.00	0.12	1.44	84.9%	3.0%
25 minutes	29.26	77.67	7.5%	535.16	0.10	3.19	0.01	0.22	2.63	61.1%	3.4%	0.96	0.00	0.07	1.50	88.8%	1.9%
TOTAL	1,037.44				0.51	8.66	0.00	4.44		0.0%		3.89	0.00	2.00		0.0%	

7 - 40 mg/l FF150																	
Concentrate Type	Mass Recovery			Water recovery	Sample Mass for Assays	Nickel						Copper					
	Mass (g)	Cum Mass (g)	Cum mass %	Mass (g)		AA Reading (ppm)	Ratio	Mass (g)	Cum Mass (g)	Cum recovery (%)	Cum grade (%)	AA Reading (ppm)	Ratio	Mass (g)	Cum Mass (g)	Cum recovery (%)	Cum grade (%)
Feed	35.89				0.51	9.80	0.00	0.17		0.0%		3.80	0.00	0.07		0.0%	
1 minute	14.36	14.36	1.6%	58.87	0.11	36.20	0.08	1.20	1.20	27.8%	8.3%	31.48	0.07	1.04	1.04	61.5%	7.3%
4 minutes	26.34	40.70	4.4%	192.86	0.11	15.47	0.04	0.97	2.17	50.3%	5.3%	3.13	0.01	0.20	1.24	73.1%	3.0%
12 minutes	46.83	87.53	9.4%	598.97	0.11	4.56	0.01	0.49	2.65	61.6%	3.0%	1.20	0.00	0.13	1.37	80.6%	1.6%
25 minutes	18.49	106.02	11.4%	390.54	0.10	2.46	0.01	0.11	2.76	64.2%	2.6%	0.81	0.00	0.04	1.40	82.8%	1.3%
TOTAL	926.38				0.51	9.80	0.00	4.46		0.0%		3.80	0.00	1.73		0.0%	

8 - 40 mg/l FF300																	
Concentrate Type	Mass Recovery			Water recovery	Sample Mass for Assays	Nickel						Copper					
	Mass (g)	Cum Mass (g)	Cum mass %	Mass (g)		AA Reading (ppm)	Ratio	Mass (g)	Cum Mass (g)	Cum recovery (%)	Cum grade (%)	AA Reading (ppm)	Ratio	Mass (g)	Cum Mass (g)	Cum recovery (%)	Cum grade (%)
Feed	30.45				0.50	9.98	0.00	0.15		0.0%		4.11	0.00	0.06		0.0%	
1 minute	10.15	10.15	1.2%	52.94	0.10	34.83	0.09	0.86	0.86	20.1%	8.5%	34.33	0.08	0.85	0.85	50.3%	8.4%
4 minutes	21.54	31.69	3.7%	147.57	0.10	18.63	0.05	0.99	1.86	43.1%	5.9%	4.06	0.01	0.22	1.07	63.0%	3.4%
12 minutes	24.81	56.50	6.6%	253.15	0.10	5.97	0.01	0.37	2.23	51.7%	3.9%	1.44	0.00	0.09	1.16	68.3%	2.0%
25 minutes	30.50	87.00	10.1%	472.13	0.10	3.09	0.01	0.23	2.46	57.1%	2.8%	0.84	0.00	0.06	1.22	72.0%	1.4%
TOTAL	857.95				0.50	9.98	0.00	4.26		0.0%		4.11	0.00	1.76		0.0%	

9 - Base Float																	
Concentrate Type	Mass Recovery			Water recovery	Sample Mass for Assays	Nickel						Copper					
	Mass (g)	Cum Mass (g)	Cum mass %	Mass (g)		AA Reading (ppm)	Ratio	Mass (g)	Cum Mass (g)	Cum recovery (%)	Cum grade (%)	AA Reading (ppm)	Ratio	Mass (g)	Cum Mass (g)	Cum recovery (%)	Cum grade (%)
Feed	32.43				0.50	9.26	0.00	0.15		0.0%		4.20	0.00	0.07		0.0%	
1 minute	14.90	14.90	1.6%	59.57	0.10	22.26	0.05	0.82	0.82	19.0%	5.5%	25.67	0.06	0.94	0.94	55.7%	6.3%
4 minutes	21.61	36.51	3.9%	133.20	0.10	17.72	0.04	0.93	1.74	40.5%	4.8%	3.30	0.01	0.17	1.12	65.8%	3.1%
12 minutes	33.11	69.62	7.4%	316.24	0.10	6.81	0.02	0.56	2.30	53.4%	3.3%	1.34	0.00	0.11	1.22	72.3%	1.8%
25 minutes	29.82	99.44	10.6%	460.01	0.10	3.24	0.01	0.24	2.54	58.9%	2.6%	0.89	0.00	0.07	1.29	76.2%	1.3%
TOTAL	939.60				0.50	9.26	0.00	4.33		0.0%		4.20	0.00	1.96		0.0%	

10 - 100 mg/l FF150																	
Concentrate Type	Mass Recovery			Water recovery	Sample Mass for Assays	Nickel						Copper					
	Mass (g)	Cum Mass (g)	Cum mass %	Mass (g)		AA Reading (ppm)	Ratio	Mass (g)	Cum Mass (g)	Cum recovery (%)	Cum grade (%)	AA Reading (ppm)	Ratio	Mass (g)	Cum Mass (g)	Cum recovery (%)	Cum grade (%)
Feed	27.21				0.50	8.63	0.00	0.12		0.0%		3.36	0.00	0.05		0.0%	
1 minute	3.96	3.96	0.4%	92.78	0.10	39.20	0.10	0.38	0.38	8.9%	9.7%	63.86	0.16	0.63	0.63	37.0%	15.8%
4 minutes	11.58	15.54	1.6%	102.73	0.11	44.99	0.10	1.20	1.58	36.7%	10.2%	19.36	0.04	0.51	1.14	67.4%	7.3%
12 minutes	21.03	36.57	3.9%	236.06	0.11	13.88	0.03	0.69	2.28	52.8%	6.2%	3.04	0.01	0.15	1.29	76.4%	3.5%
25 minutes	24.71	61.28	6.5%	348.91	0.11	4.83	0.01	0.28	2.55	59.2%	4.2%	1.26	0.00	0.07	1.37	80.6%	2.2%
TOTAL	948.19				0.50	8.63	0.00	4.08		0.0%		3.36	0.00	1.59		0.0%	

11 - 100 mg/l FF300																	
Concentrate Type	Mass Recovery			Water recovery	Sample Mass for Assays	Nickel						Copper					
	Mass (g)	Cum Mass (g)	Cum mass %	Mass (g)		AA Reading (ppm)	Ratio	Mass (g)	Cum Mass (g)	Cum recovery (%)	Cum grade (%)	AA Reading (ppm)	Ratio	Mass (g)	Cum Mass (g)	Cum recovery (%)	Cum grade (%)
Feed	37.33				0.51	8.84	0.00	0.16		0.0%		3.78	0.00	0.07		0.0%	
1 minute	4.90	4.90	0.5%	42.81	0.11	43.56	0.10	0.50	0.50	11.6%	10.2%	75.17	0.18	0.86	0.86	51.0%	17.6%
4 minutes	11.04	15.94	1.5%	108.03	0.11	47.72	0.11	1.23	1.73	40.1%	10.8%	17.67	0.04	0.45	1.32	77.8%	8.3%
12 minutes	20.28	36.22	3.4%	231.35	0.11	14.44	0.03	0.69	2.42	56.1%	6.7%	3.06	0.01	0.15	1.46	86.5%	4.0%
25 minutes	22.17	58.39	5.4%		0.10	4.63	0.01	0.25	2.67	62.0%	4.6%	1.29	0.00	0.07	1.54	90.6%	2.6%
TOTAL	1,072.54				0.51	8.84	0.00	4.66		0.0%		3.78	0.00	1.99		0.0%	

12 - 40 mg/l SM4060																	
Concentrate Type	Mass Recovery			Water recovery	Sample Mass for Assays	Nickel						Copper					
	Mass (g)	Cum Mass (g)	Cum mass %	Mass (g)		AA Reading (ppm)	Ratio	Mass (g)	Cum Mass (g)	Cum recovery (%)	Cum grade (%)	AA Reading (ppm)	Ratio	Mass (g)	Cum Mass (g)	Cum recovery (%)	Cum grade (%)
Feed	34.04				0.51	8.75	0.00	0.15		0.0%		3.49	0.00	0.06		0.0%	
1 minute	26.54	26.54	2.6%	154.17	0.10	23.23	0.06	1.53	1.53	35.5%	5.8%	18.02	0.04	1.19	1.19	70.1%	4.5%
4 minutes	36.42	62.96	6.1%	350.55	0.10	9.49	0.02	0.86	2.39	55.4%	3.8%	2.07	0.01	0.19	1.37	81.1%	2.2%
12 minutes	57.29	120.25	11.6%	872.15	0.10	3.85	0.01	0.54	2.93	68.0%	2.4%	0.97	0.00	0.14	1.51	89.1%	1.3%
25 minutes	41.33	161.58	15.6%	1,052.83	0.11	2.15	0.00	0.20	3.12	72.6%	1.9%	0.64	0.00	0.06	1.57	92.6%	1.0%
TOTAL	1,033.98				0.51	8.75	0.00	4.44		0.0%		3.49	0.00	1.77		0.0%	

13 - 40 mg/l IMP4																	
Concentrate Type	Mass Recovery			Water recovery	Sample Mass for Assays	Nickel						Copper					
	Mass (g)	Cum Mass (g)	Cum mass %	Mass (g)		AA Reading (ppm)	Ratio	Mass (g)	Cum Mass (g)	Cum recovery (%)	Cum grade (%)	AA Reading (ppm)	Ratio	Mass (g)	Cum Mass (g)	Cum recovery (%)	Cum grade (%)
Feed	25.95				0.50	10.01	0.00	0.13		0.0%		3.89	0.00	0.05		0.0%	
1 minute	9.05	9.05	1.0%	54.50	0.10	35.45	0.09	0.77	0.77	17.9%	8.5%	34.86	0.08	0.76	0.76	44.9%	8.4%
4 minutes	19.91	28.96	3.3%	127.11	0.10	19.03	0.05	0.91	1.69	39.2%	5.8%	5.09	0.01	0.24	1.00	59.3%	3.5%
12 minutes	27.67	56.63	6.5%	296.99	0.11	6.85	0.02	0.42	2.10	48.9%	3.7%	1.58	0.00	0.10	1.10	65.0%	1.9%
25 minutes	22.14	78.77	9.1%	356.12	0.11	3.31	0.01	0.17	2.28	52.9%	2.9%	0.95	0.00	0.05	1.15	67.9%	1.5%
TOTAL	867.94				0.50	10.01	0.00	4.34		0.0%		3.89	0.00	1.69		0.0%	

14 - 40 mg/l SM4560

Concentrate Type	Mass Recovery			Water recovery	Sample Mass for Assays	Nickel						Copper					
	Mass (g)	Cum Mass (g)	Cum mass %	Mass (g)		AA Reading (ppm)	Ratio	Mass (g)	Cum Mass (g)	Cum recovery (%)	Cum grade (%)	AA Reading (ppm)	Ratio	Mass (g)	Cum Mass (g)	Cum recovery (%)	Cum grade (%)
Feed	29.08				0.51	9.32	0.00	0.13		0.0%		3.83	0.00	0.05		0.0%	
1 minute	9.07	9.07	0.9%	52.52	0.11	37.14	0.09	0.78	0.78	18.1%	8.6%	44.70	0.10	0.94	0.94	55.4%	10.3%
4 minutes	21.77	30.84	3.2%	132.34	0.11	27.48	0.06	1.33	2.11	48.9%	6.8%	7.03	0.02	0.34	1.28	75.4%	4.1%
12 minutes	22.84	53.68	5.6%	232.06	0.10	6.65	0.02	0.37	2.48	57.6%	4.6%	1.80	0.00	0.10	1.38	81.4%	2.6%
25 minutes	20.26	73.94	7.7%	296.56	0.11	4.01	0.01	0.19	2.67	62.0%	3.6%	1.19	0.00	0.06	1.44	84.7%	1.9%
TOTAL	958.48				0.51	9.32	0.00	4.41		0.0%		3.83	0.00	1.81		0.0%	

15 - 100 mg/l SM4060

Concentrate Type	Mass Recovery			Water recovery	Sample Mass for Assays	Nickel						Copper					
	Mass (g)	Cum Mass (g)	Cum mass %	Mass (g)		AA Reading (ppm)	Ratio	Mass (g)	Cum Mass (g)	Cum recovery (%)	Cum grade (%)	AA Reading (ppm)	Ratio	Mass (g)	Cum Mass (g)	Cum recovery (%)	Cum grade (%)
Feed	30.34				0.51	8.50	0.00	0.13		0.0%		3.61	0.00	0.05		0.0%	
1 minute	1.51	1.51	0.2%	27.52	0.10	43.21	0.11	0.16	0.16	3.7%	10.6%	78.45	0.19	0.29	0.29	17.2%	19.2%
4 minutes	9.27	10.78	1.1%	58.31	0.10	47.63	0.12	1.07	1.23	28.5%	11.4%	30.36	0.07	0.68	0.97	57.4%	9.0%
12 minutes	19.14	29.92	3.2%	182.86	0.11	19.78	0.05	0.90	2.12	49.3%	7.1%	4.09	0.01	0.19	1.16	68.3%	3.9%
25 minutes	16.61	46.53	4.9%	253.49	0.11	5.00	0.01	0.20	2.32	53.9%	5.0%	1.60	0.00	0.06	1.22	72.0%	2.6%
TOTAL	946.47				0.51	8.50	0.00	3.97		0.0%		3.61	0.00	1.68		0.0%	

16 - 100 mg/l SM4560

Concentrate Type	Mass Recovery			Water recovery	Sample Mass for Assays	Nickel						Copper					
	Mass (g)	Cum Mass (g)	Cum mass %	Mass (g)		AA Reading (ppm)	Ratio	Mass (g)	Cum Mass (g)	Cum recovery (%)	Cum grade (%)	AA Reading (ppm)	Ratio	Mass (g)	Cum Mass (g)	Cum recovery (%)	Cum grade (%)
Feed	24.52				0.51	9.50	0.00	0.11		0.0%		3.94	0.00	0.05		0.0%	
1 minute	4.49	4.49	0.5%	27.29	0.10	0.00	0.00	0.00	0.00	0.0%	0.0%	72.92	0.18	0.80	0.80	47.2%	17.8%
4 minutes	14.03	18.52	1.9%	132.72	0.11	50.05	0.11	1.57	1.57	36.5%	8.5%	14.39	0.03	0.45	1.25	73.9%	6.8%
12 minutes	12.52	31.04	3.3%	178.67	0.10	12.21	0.03	0.37	1.94	45.0%	6.2%	2.92	0.01	0.09	1.34	79.0%	4.3%
25 minutes	19.70	50.74	5.3%	354.89	0.11	5.06	0.01	0.24	2.17	50.5%	4.3%	1.47	0.00	0.07	1.41	83.1%	2.8%
TOTAL	951.66				0.51	9.50	0.00	4.43				3.94	0.00	1.84			

APPENDIX 7 – DEPRESSANT RESEARCH FACILITY (DRF) DEPRESSANT CHARACTERISATION METHODS

Updated Dec 2001, Prepared by Dr Lesley Parolis & Prof Peter Harris

Moisture

Weigh 3 to 5g of the "as received" sample into a 100mL beaker. Dry overnight in an oven at 105°C. Remove from the oven and place in a dessicator for 30 minutes until cool. Weigh.

Calculate:

$$\text{Moisture} = \frac{(A-B)x100}{A}$$

A = mass of "as received" sample

B = mass of dry sample

Purity

Weigh 4g of the "as received" sample into a 400mL beaker. Add 150mL of 80% ethanol that has been heated to 60-65°C and then immerse the beaker into a water bath that is at 60-65°C. Cover with a foil lid as much as possible and stir for 10 minutes with an overhead stirrer. Stop stirring and allow the solid to settle. Decant the supernatant liquid through a fritted glass filtering crucible. Add another 150mL of 80% ethanol at 60-65°C and repeat the procedure.

Transfer the solid into the filtering crucible using 80% ethanol that is at 60-65°C. Be careful to scrape all solid from the beaker and the stirrer. Usually about 250mL of 80%

ethanol is required to complete the transfer and to wash the solid in the crucible. Wash the residue in the crucible with 50mL of 95% ethanol then dry the solid as much as possible using the suction. Place the crucible in an oven at 105°C and dry overnight.

Remove crucible and place in a dessicator for 30 minutes until cool. Weigh.

$$Purity = \frac{(Ax10000)}{(Bx(100-C))}$$

A = mass of purified sample

B = mass of "as received" sample

C = moisture of sample

Degree of Substitution

Weigh approximately 0.5g of purified sample into a metal crucible. Ignite the sample over a Bunsen burner flame until the sample becomes charred. Place in an oven at 650°C for 45 minutes. The remaining ash should be greyish white. Grind the ash with a pestle until no lumps remain. Dissolve the ash in a small amount of water, add methyl red indicator and titrate using 0.1N H_2SO_4. Calculate:

$$DS = \frac{(0.162xB)}{(1-0.080xB)}$$

$B = 0.1x\,{}^{b}/_{G}$ = milliequivalents Na/g of pure CMC

b = consumption of 0.1N H_2SO_4, mL

G = weight of pure CMC, g

NB: Guar depressants are not characterized for degree of substitution

pH

Make up a 1% solution of the guar or CMC in deionised water. Measure the pH using a pH meter.

Viscosity

Make up a solution of a concentration equal to that of the highest concentration required using deionised water. Dilute this solution to give the other concentrations required, using deionised water. Add 16mL of each solution to be tested into the Brookfield heat jacketed vessel. Attach it to the viscometer and turn the motor on. Allow to temperature equilibrate for about 10 minutes. Record all of the readings.

% Insoluble Material

Weigh approximately 1g of sample accurately and dissolve it in approximately 100mL of deionised water. Stir for two hours. Weigh centrifuge tubes. Centrifuge the sample for 10 minutes. Decant the clear liquid off and add more water to the centrifuge tube, breaking up the gel. Centrifuge again for 10 minutes. Repeat. Decant the clear liquid off and dry the tubes in an oven at 105°C. Weigh the tubes and calculate.

NB: Very viscous samples may require extra washing and centrifuging.

$$\%Insol.Material = \frac{(A-B)}{C} x100$$

A = mass of tube and insoluble material

B = mass of tube

C = mass of dry sample

Size exclusion chromatography

Sample preparation

Add 60 mg purified polymer slowly to 20 mL 0.2 M $NaNO_3$ in a beaker and stir until dissolved (1.5 –2 h). Centrifuge at 5000 rpm for 20 min. Decant supernatant, filter (0.45 μm) and inject ~2 mL into chromatograph and start recording file. Sample loop is 100 μL and should be overfilled at least 5 times. $NaNO_3$ eluent must be filtered (0.45 um filter) and degassed before use.

Chromatographic system

Waters Ultrahydrogel Linear column (0.78 x 30 cm) and guard column. Waters 510 solvent delivery system, eluent 0.2 M $NaNO_3$ at a flow rate of 0.6 mL/min, column temperature 45 °C. Waters R401 detector (35 °C), attenuation x 4. Rheodyne injector with 100 μL sample loop. Data capture using A/D data logger with REFLOG3 program (EW Randall, UCT). One point per second recorded and every 2 points averaged to give one data point per 2 seconds. Data from file is transferred to MS Excel and analysed on a template spreadsheet containing sample information, the linear regression equation from the calibration curve, and calculations of M_w, M_n and DP.

Calibration curve

Record the chromatograms for the 7 polyethylene oxide standards. Plot a graph of the elution volume at the peak *vs* log of the molecular weight (given by manufacturer).

Calculate the equation of the linear regression line (a straight line with y = mx + c). To obtain the molecular weight of an unknown polymer, multiply the measured elution volume by the slope and add the intercept and then take the antilog.

Calculation of molecular weight averages

Weight average molecular weight (M_w) is calculated as follows:

$$M_w = \frac{\Sigma (\text{detector response}_I \times Mw_i)}{\Sigma (\text{detector response}_I)}$$

Number average molecular weight (Mn) is calculated as follows:

$$M_n = \frac{\Sigma (\text{detector response}_I)}{\Sigma (\text{detector response}_I / Mw_i)}$$

Polydispersity (PD) is defined as M_w/M_n